

CELLULAR DIAGONALS OF PERMUTAHEDRA

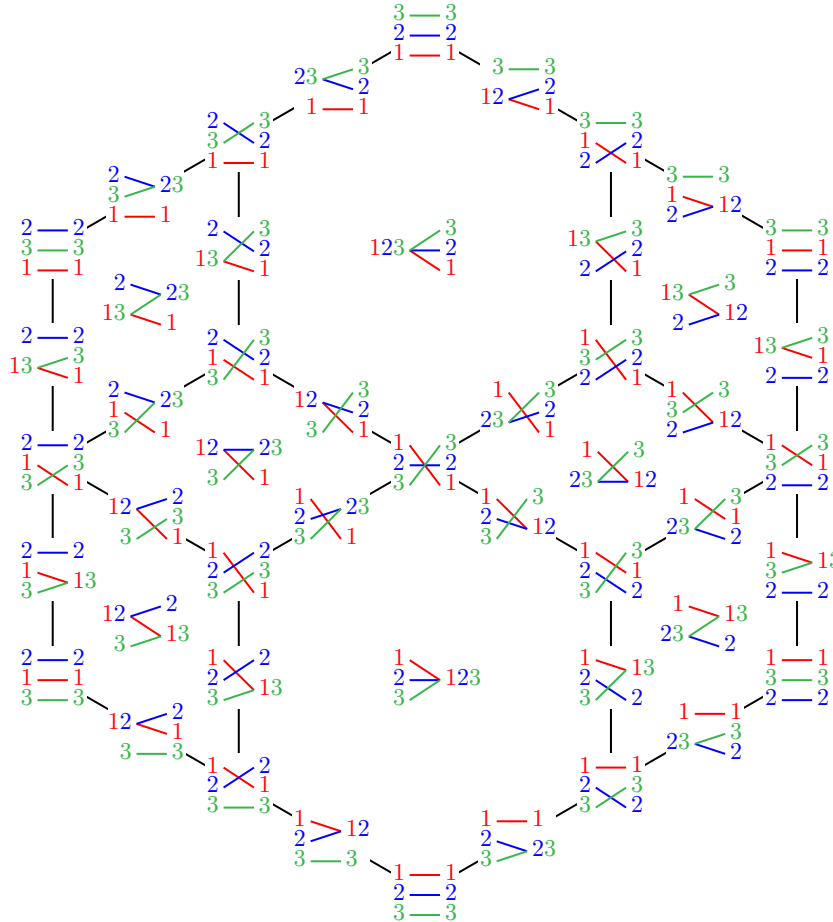
BÉRÉNICE DELCROIX-OGER, GUILLAUME LAPLANTE-ANFOSSI, VINCENT PILAUD,
AND KURT STOECKL

ABSTRACT. We provide a systematic enumerative and combinatorial study of geometric cellular diagonals on the permutahedra.

In the first part of the paper, we study the combinatorics of certain hyperplane arrangements obtained as the union of ℓ generically translated copies of the classical braid arrangement. Based on Zaslavsky's theory, we derive enumerative results on the faces of these arrangements involving combinatorial objects named partition forests and rainbow forests. This yields in particular nice formulas for the number of regions and bounded regions in terms of exponentials of generating functions of Fuss-Catalan numbers. By duality, the specialization of these results to the case $\ell = 2$ gives the enumeration of any geometric diagonal of the permutahedron.

In the second part of the paper, we study diagonals which respect the operadic structure on the family of permutahedra. We show that there are exactly two such diagonals, which are moreover isomorphic. We describe their facets by a simple rule on paths in partition trees, and their vertices as pattern-avoiding pairs of permutations. We show that one of these diagonals is a topological enhancement of the Sanbeblidze–Umble diagonal, and unravel a natural lattice structure on their sets of facets.

In the third part of the paper, we use the preceding results to show that there are precisely two isomorphic topological cellular operadic structures on the families of operahedra and multipihedra, and exactly two infinity-isomorphic geometric universal tensor products of homotopy operads and A-infinity morphisms.



BDO was partially supported by the French ANR grants ALCOHOL (ANR-19-CE40-0006), CARPLO (ANR-20-CE40-0007), HighAGT (ANR-20-CE40-0016) and S3 (ANR-20-CE48-0010). GLA and KS were supported by the Australian Research Council Future Fellowship FT210100256. KS was supported by an Australian Government Research Training Program (RTP) Scholarship. VP was partially supported by the French ANR grant CHARMS (ANR-19-CE40-0017) and by the French–Austrian project PAGCAP (ANR-21-CE48-0020 & FWF I 5788).

CONTENTS

Introduction	3
Part I. Combinatorics of multiple braid arrangements	4
Part II. Diagonals of permutahedra	5
Part III. Higher algebraic structures	7
Acknowledgements	7
PART I. COMBINATORICS OF MULTIPLE BRAID ARRANGEMENTS	8
1. Recollection on hyperplane arrangements and braid arrangements	8
1.1. Hyperplane arrangements	8
1.2. The braid arrangement	9
1.3. The (ℓ, n) -braid arrangement	12
2. Flat poset and enumeration of \mathcal{B}_n^ℓ	14
2.1. Partition forests	14
2.2. Möbius polynomial	15
2.3. Rainbow forests	18
2.4. Enumeration of vertices of \mathcal{B}_n^ℓ	21
2.5. Enumeration of regions and bounded regions of \mathcal{B}_n^ℓ	22
3. Face poset and combinatorial description of $\mathcal{B}_n^\ell(\mathbf{a})$	24
3.1. Ordered partition forests	24
3.2. From partition forests to ordered partition forests	25
3.3. A criterion for ordered partition forests	27
PART II. DIAGONALS OF PERMUTAHEDRA	29
4. Cellular diagonals	29
4.1. Cellular diagonals for polytopes	29
4.2. Cellular diagonals for the permutahedra	32
4.3. Enumerative results on cellular diagonals of the permutahedra	34
5. Operadic diagonals	36
5.1. The LA and SU diagonals	36
5.2. The operadic property	36
5.3. Isomorphisms between operadic diagonals	39
5.4. Facets of operadic diagonals	40
5.5. Vertices of operadic diagonals	41
5.6. Relation to the facial weak order	43
6. Shift lattices	44
6.1. Topological enhancement of the original SU diagonal	44
6.2. Shifts under the face poset isomorphism	51
6.3. Shift lattices	52
6.4. Cubical description	55
6.5. Matrix description	60
PART III. HIGHER ALGEBRAIC STRUCTURES	62
7. Higher tensor products	62
7.1. Topological operadic structures	62
7.2. Relating operadic structures	65
7.3. Tensor products	67
References	70

INTRODUCTION

The purpose of this article is to study *cellular diagonals* on the *permutahedra*, which are cellular maps homotopic to the usual *thin diagonal* $\Delta : P \rightarrow P \times P$, $x \mapsto (x, x)$ (Definitions 4.1 and 4.2). Such diagonals, and in particular coherent families that we call *operadic diagonals* (Definition 5.5), are of interest in algebraic geometry and topology: via the theory of Fulton–Sturmfels [FS97], they give explicit formulas for the cup product on Losev–Manin toric varieties [LM00]; they define universal tensor products of permutadic A_∞ -algebras [LR13, Mar20]; they define a coproduct on permutahedral sets, which are models of two-fold loop spaces [SU04], and their study is needed to pursue the work of H. J. Baues aiming at defining explicit combinatorial models for higher iterated loop spaces [Bau80]; using the canonical projections to the operahedra, associahedra and multiplihedra, they define universal tensor products of homotopy operads, A_∞ -algebras and A_∞ -morphisms, respectively [LA22, LAM23].

Cellular diagonals for face-coherent families of polytopes are a fundamental object in algebraic topology. The Alexander–Whitney diagonal for simplices [EM54], and the Serre map for cubes [Ser51], allow one to define the cup product in singular simplicial and cubical cohomology. These two diagonals are also needed in the study of iterated loop spaces [Bau80], while other diagonals are needed in the study of the homology of fibered spaces [San09, RS18, Pro11]. In another direction, cellular diagonals allow one to define universal tensor products in homotopical algebra. The seminal case of the *associahedra* has a rich history: the first algebraic diagonal was found by S. Saneblidze and R. Umble [SU04], followed by a second one by M. Markl and S. Shnider [MS06], which was conjectured to coincide with the first one. This has recently been shown to hold [SU22], while a topological enhancement of the *magical formula* of [MS06] was provided by N. Masuda, H. Thomas, A. Tonks and B. Vallette [MTTV21].

In [MTTV21], the authors re-introduced the powerful technique of Fulton–Sturmfels [FS97], which came from the theory of fiber polytopes of [BS92], to define a topological cellular diagonal of the associahedra. We shall call such a diagonal a *geometric diagonal* (Definition 4.5). There are two remarkable features of this diagonal (or more precisely this family of diagonals, one for the Loday associahedron in each dimension). First, it respects the operadic structure of the associahedra (in fact, forces a unique topological cellular operad structure on them!), that is, the fact that each face of an associahedron is isomorphic to a product of lower-dimensional associahedra. Second, it satisfies the *magical formula* of J.-L. Loday: the faces in the image of the diagonal are given by the pairs of faces which are comparable in the Tamari order (see Section 4 and Remark 4.9 for a precise statement). This magical formula for the associahedra recently lead to new enumerative results for Tamari intervals [BCP23].

Building on [MTTV21], a general theory of geometric diagonals was developed in [LA22]. In particular, a combinatorial formula describing the image of the diagonal of any polytope was given [LA22, Thm. 1.26]. The topological operad structure of [MTTV21] on the associahedra was generalized to the family of *operahedra*, which comprise the family of permutahedra, and encodes the notion of homotopy operad. Cellular diagonals of the operahedra do *not* satisfy the magical formula, and the combinatorial difficulty of describing their image is what prompted the development of the theory in [LA22]. In fact, there is an interesting dichotomy between the families of polytopes which satisfy the magical formula (simplices, cubes, freehedra, associahedra) and those who do not (permutahedra, multiplihedra, operahedra).

Since the operahedra are *generalized permutahedra* [Pos09], their operadic diagonals are completely determined by the operadic diagonals of permutahedra (see [LA22, Sect. 1.6]), which is the purpose of study of the present paper.

The first cellular diagonal of the permutahedra was obtained at the algebraic level by S. Saneblidze and R. Umble [SU04]. We shall call this diagonal the *original SU diagonal*. The first topological cellular diagonal of the permutahedra was defined in [LA22], we shall call it the *geometric LA diagonal*. Both of these families of diagonals are *operadic*, *i.e.* they respect the product structure on the faces of permutahedra (this property is called “comultiplicativity” in [SU04]). More precisely, the algebraic structure encoded by the permutahedra is that of permutadic A_∞ -algebra [LR13, Mar20].

The toric varieties associated with the permutahedra are called Losev–Manin varieties, introduced in [LM00]. At this level, the operadic structure is that of a reconnectad [DKL22]. The cohomology ring structure was studied by A. Losev and Y. Manin, and quite extensively since then, see for instance [BM14, Lin16]. Our current work brings a completely combinatorially explicit description of the cup product; it would be interesting to know if this new description can lead to new results, or how it can be used to recover existing ones.

The first part of the paper derives enumerative results for the iterations of any geometric diagonal of the permutahedra. According to the Fulton–Sturmfels formula [FS97] (see Proposition 4.7 and Remark 4.10), this amounts to the study of hyperplane arrangements made of generically translated copies of the braid arrangement. The second part studies in depth the combinatorics of operadic diagonals of the permutahedra, providing in particular a topological enhancement of the original SU diagonal, while the third part derives consequences of this combinatorial study in the field of homotopical algebra. We now proceed to introduce separately each part in more detail.

Part I. Combinatorics of multiple braid arrangements. As the dual of the permutahedron $\text{Perm}(n)$ is the classical braid arrangement \mathcal{B}_n , the dual of a diagonal of the permutahedron $\text{Perm}(n)$ is a hyperplane arrangement \mathcal{B}_n^2 made of 2 generically translated copies of the braid arrangement \mathcal{B}_n . In the first part of the paper, we therefore study the combinatorics of the (ℓ, n) -braid arrangement \mathcal{B}_n^ℓ , defined as the union of ℓ generically translated copies of the braid arrangement \mathcal{B}_n (Definition 1.14). We are mainly interested in the $\ell = 2$ case for the enumeration of the faces of the diagonals of the permutahedron $\text{Perm}(n)$, but the general ℓ case is not much harder and corresponds algebraically to the enumeration of the faces of cellular ℓ -gonals of the permutahedron $\text{Perm}(n)$.

Section 2 is dedicated to the combinatorial description of the flat poset of \mathcal{B}_n^ℓ and its enumerative consequences. We first observe that the flats of \mathcal{B}_n^ℓ are in bijection with (ℓ, n) -partition forests, defined as ℓ -tuples of (unordered) partitions of $[n]$ whose intersection hypergraph is a hyperforest (Definition 2.2). As this description is independent of the translations of the different copies (as long as these translations are generic), we obtain by T. Zaslavsky’s theory that the number of k -dimensional faces and of bounded faces of \mathcal{B}_n^ℓ only depends on k , ℓ , and n . In fact, we obtain the following formula for the Möbius polynomial of the (ℓ, n) -braid arrangement \mathcal{B}_n^ℓ in terms of pairs of (ℓ, n) -partition forests.

Theorem (Theorem 2.4). *The Möbius polynomial of the (ℓ, n) -braid arrangement \mathcal{B}_n^ℓ is given by*

$$\mu_{\mathcal{B}_n^\ell}(x, y) = x^{n-1-\ell n} y^{n-1-\ell n} \sum_{\mathbf{F} \leq \mathbf{G}} \prod_{i \in [\ell]} x^{\#F_i} y^{\#G_i} \prod_{p \in G_i} (-1)^{\#F_i[p]-1} (\#F_i[p] - 1)!,$$

where $\mathbf{F} \leq \mathbf{G}$ ranges over all intervals of the (ℓ, n) -partition forest poset, and $F_i[p]$ denotes the restriction of the partition F_i to the part p of G_i .

This formula is not particularly easy to handle, but it turns out to simplify to very elegant formulas for the number of vertices, regions, and bounded regions of the (ℓ, n) -braid arrangement \mathcal{B}_n^ℓ . Namely, using an alternative combinatorial description of the (ℓ, n) -partition forests in terms of (ℓ, n) -rainbow forests and a colored analogue of the classical Prüfer code for permutations, we first obtain the number of vertices of the (ℓ, n) -braid arrangement \mathcal{B}_n^ℓ .

Theorem (Theorem 2.18). *The number of vertices of the (ℓ, n) -braid arrangement \mathcal{B}_n^ℓ is*

$$f_0(\mathcal{B}_n^\ell) = \ell((\ell - 1)n + 1)^{n-2}.$$

This result can even be refined according to the dimension of the flats of the different copies intersected to obtain the vertices of the (ℓ, n) -braid arrangement \mathcal{B}_n^ℓ .

Theorem (Theorem 2.19). *For any k_1, \dots, k_ℓ such that $0 \leq k_i \leq n-1$ for $i \in [\ell]$ and $\sum_{i \in [\ell]} k_i = n-1$, the number of vertices v of the (ℓ, n) -braid arrangement \mathcal{B}_n^ℓ such that the smallest flat of the i^{th} copy of \mathcal{B}_n containing v has dimension $n - k_i - 1$ is given by*

$$n^{\ell-1} \binom{n-1}{k_1, \dots, k_\ell} \prod_{i \in [\ell]} (n - k_i)^{k_i-1}.$$

We then consider the regions of the (ℓ, n) -braid arrangement \mathcal{B}_n^ℓ . We first obtain a very simple exponential formula for its characteristic polynomial.

Theorem (Theorem 2.20). *The characteristic polynomial $\chi_{\mathcal{B}_n^\ell}(y)$ of the (ℓ, n) -braid arrangement \mathcal{B}_n^ℓ is given by*

$$\chi_{\mathcal{B}_n^\ell}(y) = \frac{(-1)^n n!}{y} [z^n] \exp\left(-\sum_{m \geq 1} \frac{F_{\ell, m} y z^m}{m}\right),$$

where $F_{\ell, m} := \frac{1}{(\ell-1)m+1} \binom{\ell m}{m}$ is the Fuss-Catalan number.

Evaluating the characteristic polynomial at $y = -1$ and $y = 1$ respectively, we obtain by T. Zaslavsky's theory the numbers of regions and bounded regions of the (ℓ, n) -braid arrangement \mathcal{B}_n^ℓ .

Theorem (Theorem 2.21). *The numbers of regions and of bounded regions of the (ℓ, n) -braid arrangement \mathcal{B}_n^ℓ are given by*

$$\begin{aligned} f_{n-1}(\mathcal{B}_n^\ell) &= n! [z^n] \exp\left(\sum_{m \geq 1} \frac{F_{\ell, m} z^m}{m}\right) \\ \text{and} \quad b_{n-1}(\mathcal{B}_n^\ell) &= (n-1)! [z^{n-1}] \exp\left((\ell-1) \sum_{m \geq 1} F_{\ell, m} z^m\right), \end{aligned}$$

where $F_{\ell, m} := \frac{1}{(\ell-1)m+1} \binom{\ell m}{m}$ is the Fuss-Catalan number.

Finally, Section 3 is dedicated to the combinatorial description of the face poset of \mathcal{B}_n^ℓ . We observe that the faces of \mathcal{B}_n^ℓ are in bijection with certain *ordered* (ℓ, n) -partition forests, defined as ℓ -tuples of ordered partitions of $[n]$ whose underlying unordered partitions form an (unordered) (ℓ, n) -partition forest (Definition 3.1). Here, which ordered (ℓ, n) -partition forests actually appear as faces of \mathcal{B}_n^ℓ depends on the choice of the translations of the different copies. We provide a combinatorial description of the possible orderings of a (ℓ, n) -partition forest compatible with some given translations in terms of certain paths in the forest (Propositions 3.3 and 3.5), and a combinatorial characterization of the ordered partition forests which appear for some given translations in terms of the circuits of a certain oriented graph (Proposition 3.7).

Part II. Diagonals of permutahedra. We present cellular diagonals, the Fulton–Sturmfels method, the magical formula and specialize the results of Part I to the permutahedra in Section 4. Then, we initiate in Section 5 the study of operadic diagonals (Definition 5.5). These are families of diagonals of the permutahedra which are compatible with the property that faces of permutahedra are product of lower-dimensional permutahedra.

Theorem (Theorems 5.13 and 5.15). *There are exactly four operadic geometric diagonals of the permutahedra, the geometric LA and SU diagonals and their opposites, and only the first two respect the weak order on permutations. Moreover, their cellular images are isomorphic as posets.*

It turns out that the facets and vertices of operadic diagonals admit elegant combinatorial descriptions. The following is a consequence of a general geometrical result, that holds for any diagonal (Proposition 3.3).

Theorem (Theorem 5.17). *A pair of ordered partitions (σ, τ) forming a partition tree is a facet of the LA (resp. SU) geometric diagonal if and only if the minimum (resp. maximum) of every directed path between two consecutive blocks of σ or τ is oriented from σ to τ (resp. from τ to σ).*

Vertices of operadic diagonals are pairs of permutations, and form a strict subset of intervals of the weak order. They admit an analogous description in terms of pattern-avoidance.

Theorem (Theorem 5.24). *A pair of permutations of $[n]$ is a vertex of the LA (resp. SU) diagonal if and only if for any $k \geq 1$ and for any $I = \{i_1, \dots, i_k\}, J = \{j_1, \dots, j_k\} \subset [k]$ such that $i_1 = 1$ (resp. $j_k = 2k$) it avoids the patterns*

$$(LA) \quad (j_1 i_1 j_2 i_2 \cdots j_k i_k, i_2 j_1 i_3 j_2 \cdots i_k j_{k-1} i_1 j_k),$$

$$(SU) \quad \text{resp. } (j_1 i_1 j_2 i_2 \cdots j_k i_k, i_1 j_k i_2 j_1 \cdots i_{k-1} j_{k-2} i_k j_{k-1}),$$

For each $k \geq 1$, there are $\binom{2k-1}{k-1,k}(k-1)k!$ such patterns, which are $(21, 12)$ for $k = 1$, and the following for $k = 2$

- LA avoids $(3142, 2314), (4132, 2413), (2143, 3214), (4123, 3412), (2134, 4213), (3124, 4312),$
- SU avoids $(1243, 2431), (1342, 3421), (2143, 1432), (2341, 3412), (3142, 1423), (3241, 2413).$

In Section 6, we introduce *shifts* that can be performed on the facets of operadic diagonals. These allow us to show that the geometric SU diagonal is a topological enhancement of the original SU diagonal.

Theorem (Theorem 6.24). *The original and geometric SU diagonals coincide.*

The proof of this result, quite technical, proceeds by showing the equivalence between 4 different descriptions of the diagonal: the original, 1-shift, m -shift and geometric SU diagonals (Section 6.1). This brings a positive answer to [LA22, Rem. 2.19], showing that the original SU diagonal can be recovered from a choice of chambers in the fundamental hyperplane arrangement of the permutahedron. Our formulas for the number of facets also agrees with the experimental count made in [Vej07]. Moreover, it provides a new proof that all known diagonals on the associahedra coincide [SU22]. Indeed, since the family of vectors inducing the geometric SU diagonal all have strictly decreasing coordinates, the diagonal induced on the associahedron is given by the magical formula [MTTV21, Thm. 2], see also [LA22, Prop. 3.8].

The above theorem also allows us to translate the different combinatorial descriptions of the facets of operadic diagonals from one to the other, compiled in the following table.

Description	SU diagonal	LA diagonal
Original	[SU04]	Definition 6.26
Geometric	Theorem 5.4	[LA22]
Path extrema	Theorem 5.17	Theorem 5.17
1-shifts	Definition 6.10	Definition 6.26
m -shifts	Definition 6.10	Definition 6.26
Lattice	Proposition 6.37	Proposition 6.37
Cubical	[SU04]	Theorem 6.51
Matrix	[SU04]	Section 6.5

In Section 6.3, we show that the facets of operadic diagonals are disjoint unions of lattices, that we call the *shift lattices*. These lattices are isomorphic to a product of chains, and are indexed by the permutations of $[n]$. Moreover, while the pairs of facets of operadic diagonals are intervals of the facial weak order (Section 5.6), the shift lattices are not sub-lattices of this order's product (see Figure 20).

Finally, we present the alternative cubical (Section 6.4) and matrix (Section 6.5) descriptions of the SU diagonal from [SU04, SU22], providing proofs of their equivalence with the other descriptions, and giving their LA counterparts. The existence of this cubical description, based on a subdivision of the cube combinatorially isomorphic to the permutahedron, finds its conceptual root in the bar-cobar resolution of the associative permutad. Indeed, this resolution is encoded by the dual subdivision of the permutahedron, which is cubical since $\text{Perm}(n)$ is a simple polytope, and a diagonal can be obtained from the classical Serre diagonal via retraction, in the same fashion as for the associahedra, see [MS06, Lod11] and [LAM23, Sec. 5.1].

Part III. Higher algebraic structures. In this shorter third part of the paper, we derive some higher algebraic consequences of the preceding results, which were the original motivation for the present study. They concern the *operahedra*, a family of polytopes indexed by planar trees, which encode (non-symmetric non-unital) homotopy operads [LA22], and the *multiplihedra*, a family of polytopes indexed by 2-colored nested linear trees, which encode A_∞ -morphisms [LAM23]. Both of these admit realizations “à la Loday”, which generalize the Loday realizations of the associahedra. The faces of an operahedron are in bijection with *nestings*, or parenthesization, of the corresponding planar tree, while the faces of a multiplihedron are in bijection with 2-colored nestings of the corresponding linear tree. The main results concerning the operahedra are summarized as follows.

Theorem (Theorems 7.3, 7.12 and 7.18). *There are exactly*

- (1) *two geometric operadic diagonals of the Loday operahedra, the LA and SU diagonals,*
- (2) *two geometric topological cellular colored operad structures on the Loday operahedra,*
- (3) *two geometric universal tensor products of homotopy operads,*

which agree with the generalized Tamari order on fully nested trees. Moreover, the two topological operad structures are isomorphic, and the two tensor products are not strictly isomorphic, but are related by an ∞ -isotopy.

As the associahedra and the permutahedra are part of the family of operahedra, we get analogous results for A_∞ -algebras and permutadic A_∞ -algebras. The main results concerning the multiplihedra are summarized as follows.

Theorem (Theorems 7.8, 7.16 and 7.22). *There are exactly*

- (1) *two geometric operadic diagonals of the Forcey multiplihedra, the LA and SU diagonals,*
- (2) *two geometric topological cellular operadic bimodule structures (over the Loday associahedra) on the Forcey multiplihedra,*
- (3) *two compatible geometric universal tensor products of A_∞ -algebras and A_∞ -morphisms,*

which agree with the Tamari-type order on atomic 2-colored nested linear trees. Moreover, the two topological operadic bimodule structures are isomorphic, and the two tensor products are not strictly isomorphic, but are related by an ∞ -isotopy.

Here, by the adjective “geometric”, we mean diagonal, operadic structure and tensor product which are obtained geometrically on the polytopes via the Fulton–Sturmfelds method. By “universal”, we mean formulas for the tensor products which apply to *any* pair of homotopy operads or A_∞ -morphisms.

However, the isomorphisms of topological operads (resp. operadic bimodules) takes place in a category of polytopes Poly for which the morphisms are *not* affine maps [LA22, Def. 4.13], and it does *not* commute with the diagonal maps (Examples 7.14 and 7.17). Moreover, the pairs of faces in the image of the two operadic diagonals are in general not in bijection (see Examples 7.20 and 7.24), yielding different (but ∞ -isomorphic) tensor products of homotopy operads (resp. A_∞ -morphisms).

ACKNOWLEDGEMENTS

We are indebted to Matthieu Josuat-Vergès for taking part in the premises of this paper, in particular for conjecturing the case $\ell = 2$ of Theorem 2.19, for working on the proof of Theorem 5.24, and for implementing some sage code used during the project. GLA is grateful to Hugh Thomas for raising the question to count the facets of the LA diagonal and for preliminary discussions during a visit at the LACIM in the summer of 2021 where the project started, and to the Max Planck Institute for Mathematics in Bonn where part of this work was carried out. We are grateful to Sylvie Corteel for pointing out the relevance of the dual perspective for the purpose of counting. VP is grateful to the organizers (Karim Adiprasito, Alexey Glazyrin, Isabella Novic, and Igor Pak) of the workshop “Combinatorics and Geometry of Convex Polyhedra” held at the Simons Center for Geometry and Physics in March 2023 for the opportunity to present a preliminary version of our enumerative results, and to Pavel Galashin for asking about the characteristic polynomial of the multiple braid arrangement during this presentation. We thank Samson Sanedidze and Ron Umble for useful correspondence.

Part I. Combinatorics of multiple braid arrangements

In this first part, we study the combinatorics of hyperplane arrangements obtained as unions of generically translated copies of the braid arrangement. In Section 1, we first recall some classical facts on the enumeration of hyperplane arrangements (Section 1.1), present the classical braid arrangement (Section 1.2), and define our multiple braid arrangements (Section 1.3). Then in Section 2, we describe their flat posets in terms of partition forests (Section 2.1) and rainbow forests (Section 2.3), from which we derive their Möbius polynomials (Section 2.2), and some surprising formulas for their numbers of vertices (Section 2.4) and regions (Section 2.5). Finally, in Section 3, we describe their face posets in terms of ordered partition forests (Section 3.1), and explore some combinatorial criteria to describe the ordered partition forests that appear as faces of a given multiple braid arrangement (Sections 3.2 and 3.3).

1. RECOLLECTION ON HYPERPLANE ARRANGEMENTS AND BRAID ARRANGEMENTS

1.1. Hyperplane arrangements. We first briefly recall classical results on the combinatorics of affine hyperplane arrangements, in particular the enumerative connection between their intersection posets and their face lattices due to T. Zaslavsky [Zas75].

Definition 1.1. A finite affine real *hyperplane arrangement* is a finite set \mathcal{A} of affine hyperplanes in \mathbb{R}^d .

Definition 1.2. A *region* of \mathcal{A} is a connected component of $\mathbb{R}^d \setminus \bigcup_{H \in \mathcal{A}} H$. The *faces* of \mathcal{A} are the closures of the regions of \mathcal{A} and all their intersections with a hyperplane of \mathcal{A} . The *face poset* of \mathcal{A} is the poset $\text{Fa}(\mathcal{A})$ of faces of \mathcal{A} ordered by inclusion. The *f-polynomial* $\mathbf{f}_{\mathcal{A}}(x)$ and *b-polynomial* $\mathbf{b}_{\mathcal{A}}(x)$ of \mathcal{A} are the polynomials

$$\mathbf{f}_{\mathcal{A}}(x) := \sum_{k=0}^d f_k(\mathcal{A}) x^k \quad \text{and} \quad \mathbf{b}_{\mathcal{A}}(x) := \sum_{k=0}^d b_k(\mathcal{A}) x^k,$$

where $f_k(\mathcal{A})$ denotes the number of k -dimensional faces of \mathcal{A} , while $b_k(\mathcal{A})$ denotes the number of bounded k -dimensional faces of \mathcal{A} .

Definition 1.3. A *flat* of \mathcal{A} is a non-empty affine subspace of \mathbb{R}^d that can be obtained as the intersection of some hyperplanes of \mathcal{A} . The *flat poset* of \mathcal{A} is the poset $\text{Fl}(\mathcal{A})$ of flats of \mathcal{A} ordered by reverse inclusion.

Definition 1.4. The *Möbius polynomial* $\mu_{\mathcal{A}}(x, y)$ of \mathcal{A} is the polynomial defined by

$$\mu_{\mathcal{A}}(x, y) := \sum_{F \leq G} \mu_{\text{Fl}(\mathcal{A})}(F, G) x^{\dim(F)} y^{\dim(G)},$$

where $F \leq G$ ranges over all intervals of the flat poset $\text{Fl}(\mathcal{A})$, and $\mu_{\text{Fl}(\mathcal{A})}(F, G)$ denotes the *Möbius function* on the flat poset $\text{Fl}(\mathcal{A})$ defined as usual by

$$\mu_{\text{Fl}(\mathcal{A})}(F, F) = 1 \quad \text{and} \quad \sum_{F \leq G \leq H} \mu_{\text{Fl}(\mathcal{A})}(F, G) = 0$$

for all $F < H$ in $\text{Fl}(\mathcal{A})$.

Remark 1.5. Our definition of the Möbius polynomial slightly differs from that of [Zas75] as we use the dimension of F instead of its codimension, in order to simplify slightly the following statement.

Theorem 1.6 ([Zas75, Thm. A]). *The f-polynomial, the b-polynomial, and the Möbius polynomial of the hyperplane arrangement \mathcal{A} are related by*

$$\mathbf{f}_{\mathcal{A}}(x) = \mu_{\mathcal{A}}(-x, -1) \quad \text{and} \quad \mathbf{b}_{\mathcal{A}}(x) = \mu_{\mathcal{A}}(-x, 1).$$

Example 1.7. For the arrangement \mathcal{A} of 5 hyperplanes of Figure 1, we have

$$\mu_{\mathcal{A}}(x, y) = x^2 y^2 - 5x^2 y + 6x^2 + 5xy - 10x + 4,$$

so that

$$\mathbf{f}_{\mathcal{A}}(x) = \mu_{\mathcal{A}}(-x, -1) = 12x^2 + 15x + 4 \quad \text{and} \quad \mathbf{b}_{\mathcal{A}}(x) = \mu_{\mathcal{A}}(-x, 1) = 2x^2 + 5x + 4.$$

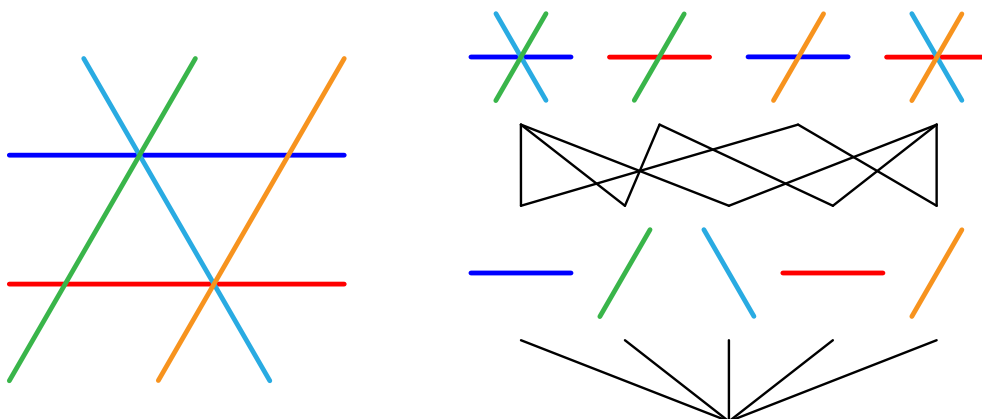


FIGURE 1. A hyperplane arrangement (left) and its intersection poset (right).

Remark 1.8. The coefficient of x^d in the Möbius polynomial $\mu_{\mathcal{A}}(x, y)$ gives the more classical *characteristic polynomial*

$$\chi_{\mathcal{A}}(y) := [x^d] \mu_{\mathcal{A}}(x, y) = \sum_F \mu_{\text{Fl}(\mathcal{A})}(\mathbb{R}^d, F) y^{\dim(F)}.$$

By Theorem 1.6, we thus have

$$f_d(\mathcal{A}) = (-1)^d \chi_{\mathcal{A}}(-1) \quad \text{and} \quad b_d(\mathcal{A}) = (-1)^d \chi_{\mathcal{A}}(1).$$

1.2. The braid arrangement. We now briefly recall the classical combinatorics of the braid arrangement. See Figures 2 to 4 for illustrations when $n = 3$ and $n = 4$.

Definition 1.9. Fix $n \geq 1$ and denote by \mathbb{H} the hyperplane of \mathbb{R}^n defined by $\sum_{s \in [n]} x_s = 0$. The *braid arrangement* \mathcal{B}_n is the arrangement of the hyperplanes $\{\mathbf{x} \in \mathbb{H} \mid x_s = x_t\}$ for all $1 \leq s < t \leq n$.

Remark 1.10. Note that we have decided to work in the space \mathbb{H} rather than in the space \mathbb{R}^n . The advantage is that the braid arrangement \mathcal{B}_n in \mathbb{H} is essential, so that we can speak of its rays. Working in \mathbb{R}^n would change rays to walls, and would multiply all Möbius polynomials by a factor xy .

The combinatorics of the braid arrangement \mathcal{B}_n is well-known. The descriptions of its face and flat posets involve both ordered and unordered set partitions. To avoid confusions, we will always mark with an arrow the ordered structures (ordered set partitions, ordered partition forests, etc.). Hence, the letter π denotes an unordered set partition (the order is irrelevant, neither inside each part, nor between two distinct parts), while $\vec{\pi}$ denotes an ordered set partition (the order inside each part is irrelevant, but the order between distinct parts is relevant).

The braid arrangement \mathcal{B}_n has a k -dimensional face

$$\Phi(\vec{\pi}) := \{\mathbf{x} \in \mathbb{R}^n \mid x_s \leq x_t \text{ for all } s, t \text{ such that the part of } s \text{ is weakly before the part of } t \text{ in } \vec{\pi}\}$$

for each ordered set partition $\vec{\pi}$ of $[n]$ into $k + 1$ parts, or equivalently, for each surjection from $[n]$ to $[k + 1]$. The face poset $\text{Fa}(\mathcal{B}_n)$ is thus isomorphic to the refinement poset $\vec{\Pi}_n$ on ordered set partitions, where an ordered partition $\vec{\pi}$ is smaller than an ordered partition $\vec{\omega}$ if each part of $\vec{\pi}$ is the union of an interval of consecutive parts in $\vec{\omega}$. In particular, it has a single vertex corresponding to the ordered partition $[n]$, $2^n - 2$ rays corresponding to the proper nonempty subsets of $[n]$ (ordered partitions of $[n]$ into 2 parts), and $n!$ regions corresponding to the permutations of $[n]$ (ordered partitions of $[n]$ into n parts). As an example, Figure 2 illustrates the face poset of the braid arrangement \mathcal{B}_3 .

The braid arrangement \mathcal{B}_n has a k -dimensional flat

$$\Psi(\pi) := \{\mathbf{x} \in \mathbb{R}^n \mid x_s = x_t \text{ for all } s, t \text{ which belong to the same part of } \pi\}$$

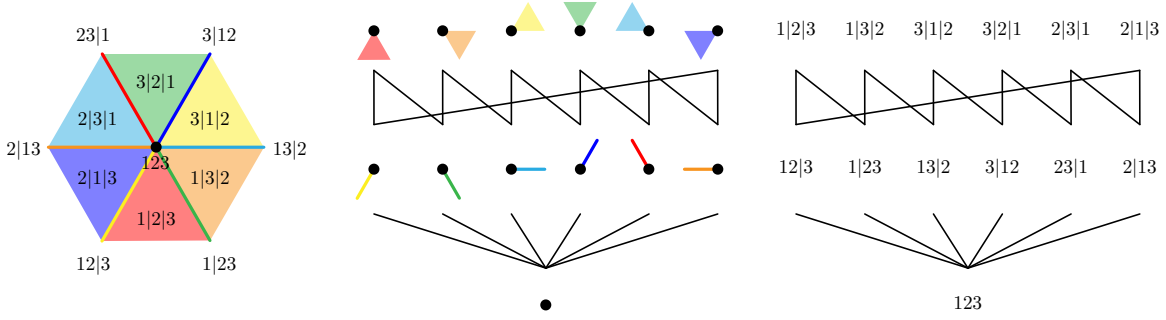


FIGURE 2. The face poset $\text{Fa}(\mathcal{B}_3)$ of the braid arrangement \mathcal{B}_3 (left), where faces are represented as cones (middle) or as ordered set partitions of $[3]$ (right).

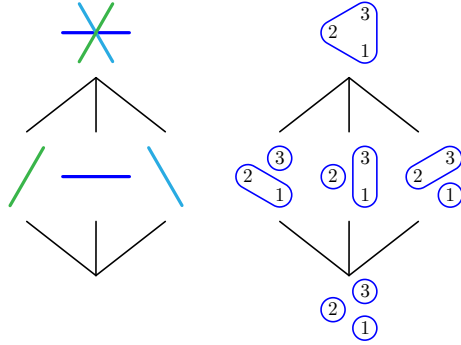


FIGURE 3. The flat poset $\text{Fl}(\mathcal{B}_3)$ of the braid arrangement \mathcal{B}_3 , where flats are represented as intersections of hyperplanes (left) or as set partitions of $[3]$ (right).

for each unordered set partition π of $[n]$ into $k+1$ parts. The flat poset $\text{Fl}(\mathcal{B}_n)$ is thus isomorphic to the refinement poset $\mathbf{\Pi}_n$ on set partitions of $[n]$, where a partition π is smaller than a partition ω if each part of π is contained in a part of ω . For instance, Figures 3 and 4 illustrate the flat posets of the braid arrangements \mathcal{B}_3 and \mathcal{B}_4 . Note that the refinement in $\overline{\mathbf{\Pi}}_n$ and in $\mathbf{\Pi}_n$ are in opposite direction.

The Möbius function of the set partitions poset $\mathbf{\Pi}_n$ is given by

$$\mu_{\mathbf{\Pi}_n}(\pi, \omega) = \prod_{p \in \omega} (-1)^{\#\pi[p]-1} (\#\pi[p] - 1)!,$$

where $\pi[p]$ denotes the restriction of the partition π to the part p of the partition ω , and $\#\pi[p]$ denotes its number of parts. See for instance [Bir95, Rot64]. The Möbius polynomial of the braid arrangement \mathcal{B}_n is given by

$$\mu_{\mathcal{B}_n}(x, y) = \sum_{k \in [n]} x^{k-1} S(n, k) \prod_{i \in [k-1]} (y - i),$$

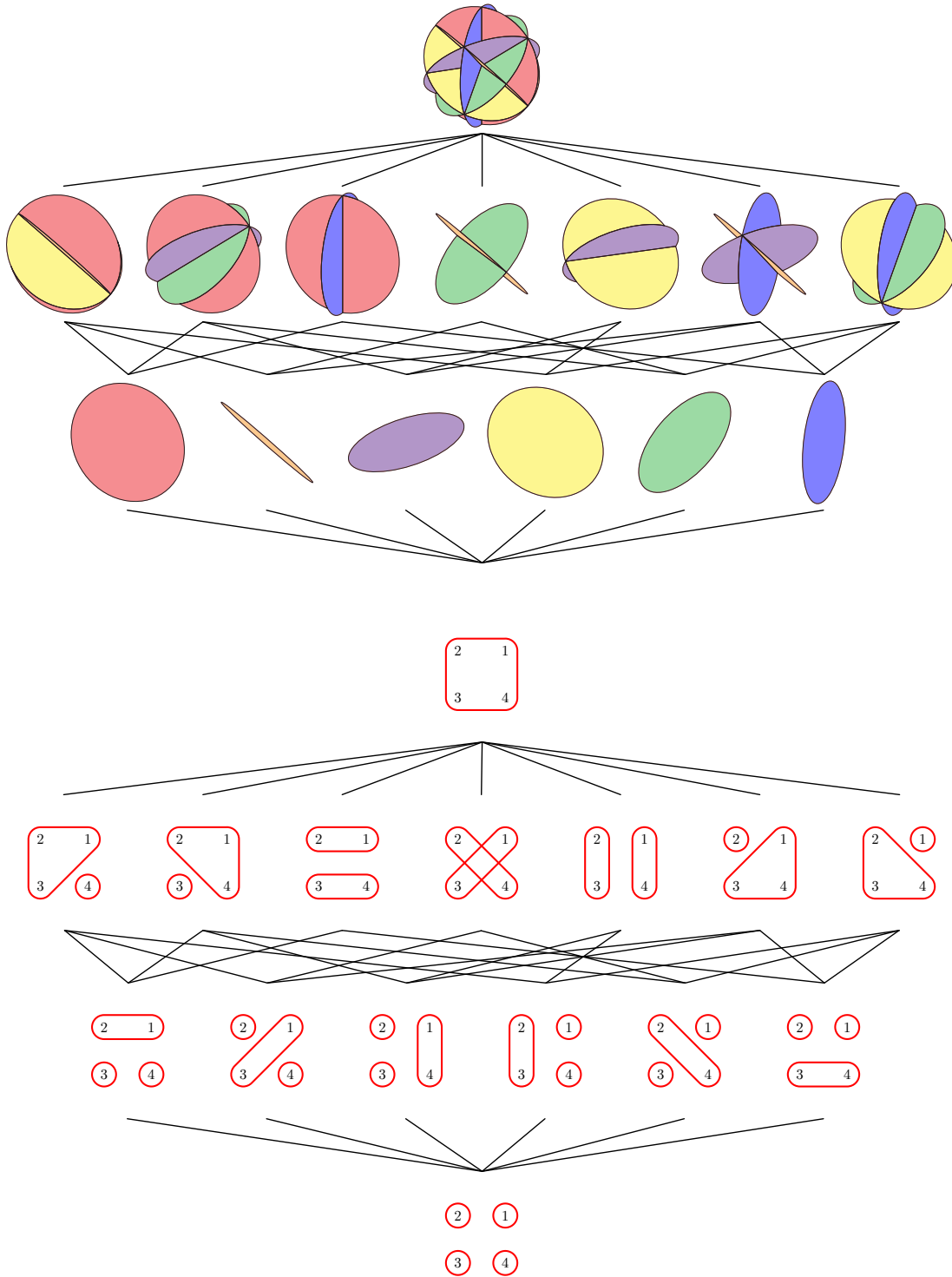


FIGURE 4. The flat poset $\text{Fl}(\mathcal{B}_4)$ of the braid arrangement \mathcal{B}_4 , where flats are represented as intersections of hyperplanes (top) or as set partitions of $[4]$ (bottom).

where $S(n, k)$ denotes the Stirling number of the second kind [OEI10, A008277], *i.e.* the number of set partitions of $[n]$ into k parts. For instance

$$\begin{aligned}\mu_{\mathcal{B}_1}(x, y) &= 1 \\ \mu_{\mathcal{B}_2}(x, y) &= xy - x + 1 = x(y - 1) + 1 \\ \mu_{\mathcal{B}_3}(x, y) &= x^2y^2 - 3x^2y + 2x^2 + 3xy - 3x + 1 = x^2(y - 1)(y - 2) + 3x(y - 1) + 1 \\ \mu_{\mathcal{B}_4}(x, y) &= x^3y^3 - 6x^3y^2 + 11x^3y - 6x^3 + 6x^2y^2 - 18x^2y + 12x^2 + 7xy - 7x + 1 \\ &= x^3(y - 1)(y - 2)(y - 3) + 6x^2(y - 1)(y - 2) + 7x(y - 1) + 1.\end{aligned}$$

In particular, the characteristic polynomial of the braid arrangement \mathcal{B}_n is given by

$$\chi_{\mathcal{B}_n}(y) = (y - 1)(y - 2) \dots (y - n - 1).$$

Working in \mathbb{R}^n rather than in \mathbb{H} would lead to an additional y factor in this formula, which might be more familiar to the reader. See Remark 1.10.

Finally, we will consider the evaluation of the Möbius polynomial $\mu_{\mathcal{B}_n}(x, y)$ at $y = 0$:

$$\pi_n(x) := \mu_{\mathcal{B}_n}(x, 0) = \sum_{k \in [n]} (-1)^{k-1} (k-1)! S(n, k) x^{k-1}.$$

The coefficients of this polynomial are given by the sequence [OEI10, A028246]. We just observe here that it is connected to the \mathbf{f} -polynomial of \mathcal{B}_n .

Lemma 1.11. *We have $\pi_n(x) = (1 - x) \mathbf{f}_{\mathcal{B}_n}(x)$.*

Proof. This lemma is equivalent to the equality

$$\sum_{k=1}^n (-1)^{k-1} (k-1)! S(n, k) x^{k-1} = (1 - x) \sum_{k=1}^{n-1} (-1)^{k-1} k! S(n-1, k) x^{k-1}.$$

Distributing $(1 - x)$ in the right hand side gives:

$$\begin{aligned}& (1 - x) \sum_{k=1}^{n-1} (-1)^{k-1} k! S(n-1, k) x^{k-1} \\ &= \sum_{k=1}^{n-1} k! S(n-1, k) (-x)^{k-1} + \sum_{k=1}^{n-1} k! S(n-1, k) (-x)^k \\ &= \sum_{k=1}^{n-1} k! S(n-1, k) (-x)^{k-1} + \sum_{k=2}^n (k-1)! S(n-1, k-1) (-x)^{k-1} + (n-1)! S(n-1, n-1) (-x)^{n-1} \\ &= S(n-1, 1) (-x)^0 + \sum_{k=2}^{n-1} (k-1)! (S(n-1, k-1) + k S(n-1, k)) (-x)^{k-1}.\end{aligned}$$

The result thus follows from the inductive formula on Stirling numbers of the second kind

$$S(n+1, k) = k S(n, k) + S(n, k-1)$$

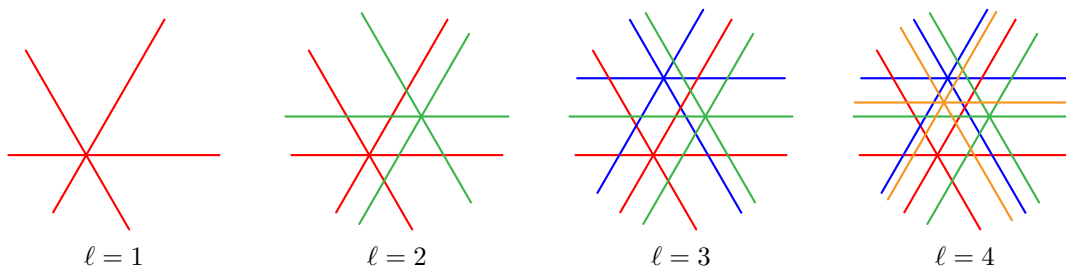
for $0 < k < n$. □

1.3. The (ℓ, n) -braid arrangement. We now focus on the following specific hyperplane arrangements, illustrated in Figure 5. We still denote by \mathbb{H} the hyperplane of \mathbb{R}^n defined by $\sum_{s \in [n]} x_s = 0$.

Definition 1.12. For any integers $\ell, n \geq 1$, and any matrix $\mathbf{a} := (a_{i,j}) \in M_{\ell, n-1}(\mathbb{R})$, the **\mathbf{a} -braid arrangement** $\mathcal{B}_n^\ell(\mathbf{a})$ is the arrangement of hyperplanes $\{\mathbf{x} \in \mathbb{H} \mid x_s - x_t = A_{i,s,t}\}$ for all $1 \leq s < t \leq n$ and $i \in [\ell]$, where $A_{i,s,t} := \sum_{s \leq j < t} a_{i,j}$.

In other words, the \mathbf{a} -braid arrangement $\mathcal{B}_n^\ell(\mathbf{a})$ is the union of ℓ copies of the braid arrangement \mathcal{B}_n translated according to the matrix \mathbf{a} . Of course, the \mathbf{a} -braid arrangement $\mathcal{B}_n^\ell(\mathbf{a})$ highly depends on \mathbf{a} . In this paper, we are interested in the case where \mathbf{a} is generic in the following sense.

Definition 1.13. A matrix $\mathbf{a} := (a_{i,j}) \in M_{\ell, n-1}(\mathbb{R})$ is **generic** if for any $i_1, \dots, i_k \in [\ell]$ and distinct $r_1, \dots, r_k \in [n]$, the equality $\sum_{j \in [k]} A_{i_j, r_{j-1}, r_j} = 0$ implies $i_1 = \dots = i_k$ (with the notation $A_{i,s,t} := \sum_{s \leq j < t} a_{i,j}$ and the convention $r_0 = r_k$).

FIGURE 5. The $(\ell, 3)$ -braid arrangements for $\ell \in [4]$.

We will see that many combinatorial aspects of $\mathcal{B}_n^\ell(\mathbf{a})$, in particular its flat poset and thus its Möbius, f - and b -polynomials, are in fact independent of the matrix \mathbf{a} as long as it is generic. We therefore consider the following definition.

Definition 1.14. The (ℓ, n) -braid arrangement \mathcal{B}_n^ℓ is the arrangement in \mathbb{H} obtained as the union of ℓ generically translated copies of the braid arrangement \mathcal{B}_n (that is, any \mathbf{a} -braid arrangement for some generic matrix $\mathbf{a} \in M_{\ell, n-1}(\mathbb{R})$).

The objective of Part I is to explore the combinatorics of these multiple braid arrangements. We have split our presentation into two sections:

- In Section 2, we describe the flat poset $\text{Fl}(\mathcal{B}_n^\ell)$ of the (ℓ, n) -braid arrangement \mathcal{B}_n^ℓ in terms of (ℓ, n) -partition forests (Section 2.1) and labeled (ℓ, n) -rainbow forests (Section 2.3), which enables us to derive its Möbius, f - and b -polynomials (Section 2.2), from which we extract interesting formulas for the number of vertices (Section 2.4) and regions (Section 2.5). Note that all these results are independent of the translation matrix.
- In Section 3, we describe the face poset $\text{Fa}(\mathcal{B}_n^\ell(\mathbf{a}))$ of the \mathbf{a} -braid arrangement $\mathcal{B}_n^\ell(\mathbf{a})$ in terms of ordered (ℓ, n) -partition forests (Section 3.1). In contrast to the flat poset, this description of the face poset depends on the translation matrix \mathbf{a} . For a given choice of \mathbf{a} , we describe in particular the ordered (ℓ, n) -partition forests with a given underlying (unordered) (ℓ, n) -partition forest (Section 3.2). We then give a criterion to decide whether a given ordered (ℓ, n) -partition forest corresponds to a face of $\mathcal{B}_n^\ell(\mathbf{a})$ (Section 3.3).

Remark 1.15. Note that each hyperplane of the (ℓ, n) -braid arrangement \mathcal{B}_n^ℓ is orthogonal to a root $e_i - e_j$ of the type A root system. Many such arrangements have been studied previously, for instance, the *Shi arrangement* [Shi86, Shi87], the *Catalan arrangement* [PS00, Sect. 7], the *Linial arrangement* [PS00, Sect. 8], the *generic arrangement* of [PS00, Sect. 5], or the *discrimantal arrangements* of [MS89, BB97]. We refer to the work of A. Postnikov and R. Stanley [PS00] and of O. Bernardi [Ber18] for much more references. However, in all these examples, either the copies of the braid arrangement are perturbed, or they are translated non-generically. We have not been able to find the (ℓ, n) -braid arrangement \mathcal{B}_n^ℓ properly treated in the literature.

Remark 1.16. Part of our discussion on the (ℓ, n) -braid arrangement \mathcal{B}_n^ℓ could actually be developed for a hyperplane arrangement \mathcal{A}^ℓ obtained as the union of ℓ generically translated copies of an arbitrary linear hyperplane arrangement \mathcal{A} . Similarly to Proposition 2.3, the flat poset $\text{Fl}(\mathcal{A}^\ell)$ is isomorphic to the lower set of the ℓ^{th} Cartesian power of the flat poset $\text{Fl}(\mathcal{A})$ induced by the ℓ -tuples whose meet in the flat poset $\text{Fl}(\mathcal{A})$ is the bottom element $\mathbf{0}$ (these are sometimes called strong antichains) and which are minimal for this property. Similar to Theorem 2.4, this yields a general formula for the Möbius polynomial of \mathcal{A}^ℓ in terms of the Möbius function of the flat poset $\text{Fl}(\mathcal{A})$. Here, we additionally benefit from the nice properties of the Möbius polynomial of the braid arrangement \mathcal{B}_n to obtain appealing formulas for the vertices, regions and bounded regions of the (ℓ, n) -braid arrangement \mathcal{B}_n^ℓ (see Theorems 2.18 to 2.21). We have therefore decided to restrict our attention to the (ℓ, n) -braid arrangement \mathcal{B}_n^ℓ .

2. FLAT POSET AND ENUMERATION OF \mathcal{B}_n^ℓ

In this section, we describe the flat poset of the (ℓ, n) -braid arrangement \mathcal{B}_n^ℓ in terms of (ℓ, n) -partition forests and derive explicit formulas for its f -vector. Remarkably, the flat poset (and thus the Möbius, f - and b - polynomials) of \mathcal{B}_n^ℓ is independent of the translation vectors as long as they are generic.

2.1. Partition forests. We first introduce the main characters of this section, which will describe the combinatorics of the flat poset of the (ℓ, n) -braid arrangement \mathcal{B}_n^ℓ of Definition 1.14.

Definition 2.1. The *intersection hypergraph* of a ℓ -tuple $\mathbf{F} := (F_1, \dots, F_\ell)$ of set partitions of $[n]$ is the ℓ -regular ℓ -partite hypergraph on all parts of all the partitions F_i for $i \in [\ell]$, with a hyperedge connecting the parts containing j for each $j \in [n]$.

Definition 2.2. An (ℓ, n) -*partition forest* (resp. (ℓ, n) -*partition tree*) is a ℓ -tuple $\mathbf{F} := (F_1, \dots, F_\ell)$ of set partitions of $[n]$ whose intersection hypergraph is a hyperforest (resp. hypertree). See Figure 6. The *dimension* of \mathbf{F} is $\dim(\mathbf{F}) := n - 1 - \ell n + \sum_{i \in [\ell]} \#F_i$. The (ℓ, n) -*partition forest poset* is the poset Φ_n^ℓ on (ℓ, n) -partition forests ordered by componentwise refinement.

In other words, Φ_n^ℓ is the lower set of the ℓ^{th} Cartesian power of the partition poset Π_n induced by (ℓ, n) -partition forests. Note that the maximal elements of Φ_n^ℓ are the (ℓ, n) -partition trees.

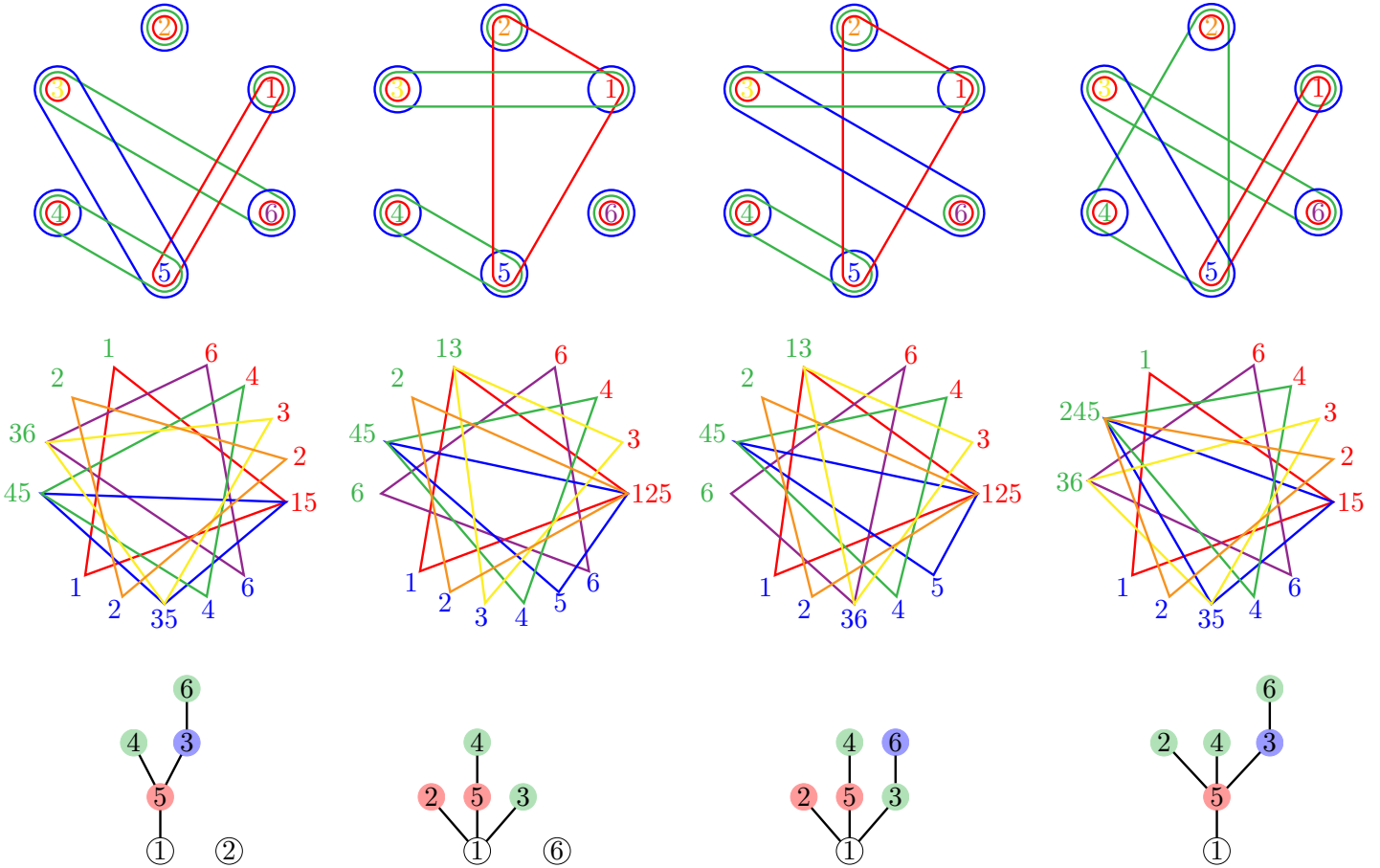


FIGURE 6. Some $(3, 6)$ -partition forests (top) with their intersection hypergraphs (middle) and the corresponding labeled $(3, 6)$ -rainbow forests (bottom). The last two are trees. The order of the colors in the bottom pictures is red, green, blue.

The following statement is illustrated in Figure 7.

Proposition 2.3. *The flat poset $\text{Fl}(\mathcal{B}_n^\ell)$ of the (ℓ, n) -braid arrangement \mathcal{B}_n^ℓ is isomorphic to the (ℓ, n) -partition forest poset.*

Proof. Consider that \mathcal{B}_n^ℓ is the \mathbf{a} -braid arrangement $\mathcal{B}_n^\ell(\mathbf{a})$ for some generic matrix \mathbf{a} . In view of our discussion in Section 1.2, observe that, for each $i \in [\ell]$, each set partition π of $[n]$ corresponds to a $(\#\pi)$ -dimensional flat

$$\Psi_i(\pi) := \{\mathbf{x} \in \mathbb{H} \mid x_s - x_t = A_{i,s,t} \text{ for all } s, t \text{ in the same part of } \pi\}$$

of the i^{th} copy of the braid arrangement \mathcal{B}_n . The flats of the (ℓ, n) -braid arrangement \mathcal{B}_n^ℓ are thus all of the form

$$\Psi(\mathbf{F}) := \bigcap_{i \in [\ell]} \Psi_i(F_i)$$

for certain ℓ -tuples $\mathbf{F} := (F_1, \dots, F_\ell)$ of set partitions of $[n]$. Since the matrix \mathbf{a} is generic, $\Psi(\mathbf{F})$ is non-empty if and only if the intersection hypergraph of \mathbf{F} is acyclic. Moreover, $\Psi(\mathbf{F})$ is included in $\Psi(\mathbf{G})$ if and only if \mathbf{F} refines \mathbf{G} componentwise. Hence, the flat poset of \mathcal{B}_n^ℓ is isomorphic to the (ℓ, n) -partition forest poset. Finally, notice that the codimension of the flat $\Psi(\mathbf{F})$ is the sum of the codimensions of the flats $\Psi_i(F_i)$ for $i \in [\ell]$, so that $\dim(\mathbf{F}) := n - 1 - \ell n + \sum_{i \in [\ell]} \#F_i$ is indeed the dimension of the flat $\Psi(\mathbf{F})$. \square

2.2. Möbius polynomial. We now derive from Definition 1.4 and Proposition 2.3 the Möbius polynomial of the (ℓ, n) -braid arrangement \mathcal{B}_n^ℓ .

Theorem 2.4. *The Möbius polynomial of the (ℓ, n) -braid arrangement \mathcal{B}_n^ℓ is given by*

$$\mu_{\mathcal{B}_n^\ell}(x, y) = x^{n-1-\ell n} y^{n-1-\ell n} \sum_{\mathbf{F} \leq \mathbf{G}} \prod_{i \in [\ell]} x^{\#F_i} y^{\#G_i} \prod_{p \in G_i} (-1)^{\#F_i[p]-1} (\#F_i[p] - 1)!,$$

where $\mathbf{F} \leq \mathbf{G}$ ranges over all intervals of the (ℓ, n) -partition forest poset Φ_n^ℓ , and $F_i[p]$ denotes the restriction of the partition F_i to the part p of G_i .

Proof. Observe that for $\mathbf{F} := (F_1, \dots, F_\ell)$ and $\mathbf{G} := (G_1, \dots, G_\ell)$ in Φ_n^ℓ , we have

$$[\mathbf{F}, \mathbf{G}] = \prod_{i \in [\ell]} [F_i, G_i] \simeq \prod_{i \in [\ell]} \prod_{p \in G_i} \Pi_{\#F_i[p]}.$$

Recall that the Möbius function is multiplicative: $\mu_{P \times Q}((p, q), (p', q')) = \mu_P(p, p') \cdot \mu_Q(q, q')$, for all $p, p' \in P$ and $q, q' \in Q$. Hence, we obtain that

$$\mu_{\Phi_n^\ell}(\mathbf{F}, \mathbf{G}) = \prod_{i \in [\ell]} \prod_{p \in G_i} (-1)^{\#F_i[p]-1} (\#F_i[p] - 1)!.$$

Hence, we derive from Definition 1.4 and Proposition 2.3 that

$$\begin{aligned} \mu_{\mathcal{B}_n^\ell}(x, y) &= \sum_{\mathbf{F} \leq \mathbf{G}} \mu_{\Phi_n^\ell}(\mathbf{F}, \mathbf{G}) x^{\dim(\mathbf{F})} y^{\dim(\mathbf{G})} \\ &= x^{n-1-\ell n} y^{n-1-\ell n} \sum_{\mathbf{F} \leq \mathbf{G}} \prod_{i \in [\ell]} x^{\#F_i} y^{\#G_i} \prod_{p \in G_i} (-1)^{\#F_i[p]-1} (\#F_i[p] - 1)!. \end{aligned} \quad \square$$

By using the polynomial

$$\pi_n(x) := \mu_{\mathcal{B}_n^\ell}(x, 0) = \sum_{k \in [n]} (-1)^{k-1} (k-1)! S(n, k) x^{k-1}$$

introduced at the end of Section 1.2, the Möbius polynomial $\mu_{\mathcal{B}_n^\ell}(x, y)$ can also be expressed as follows.

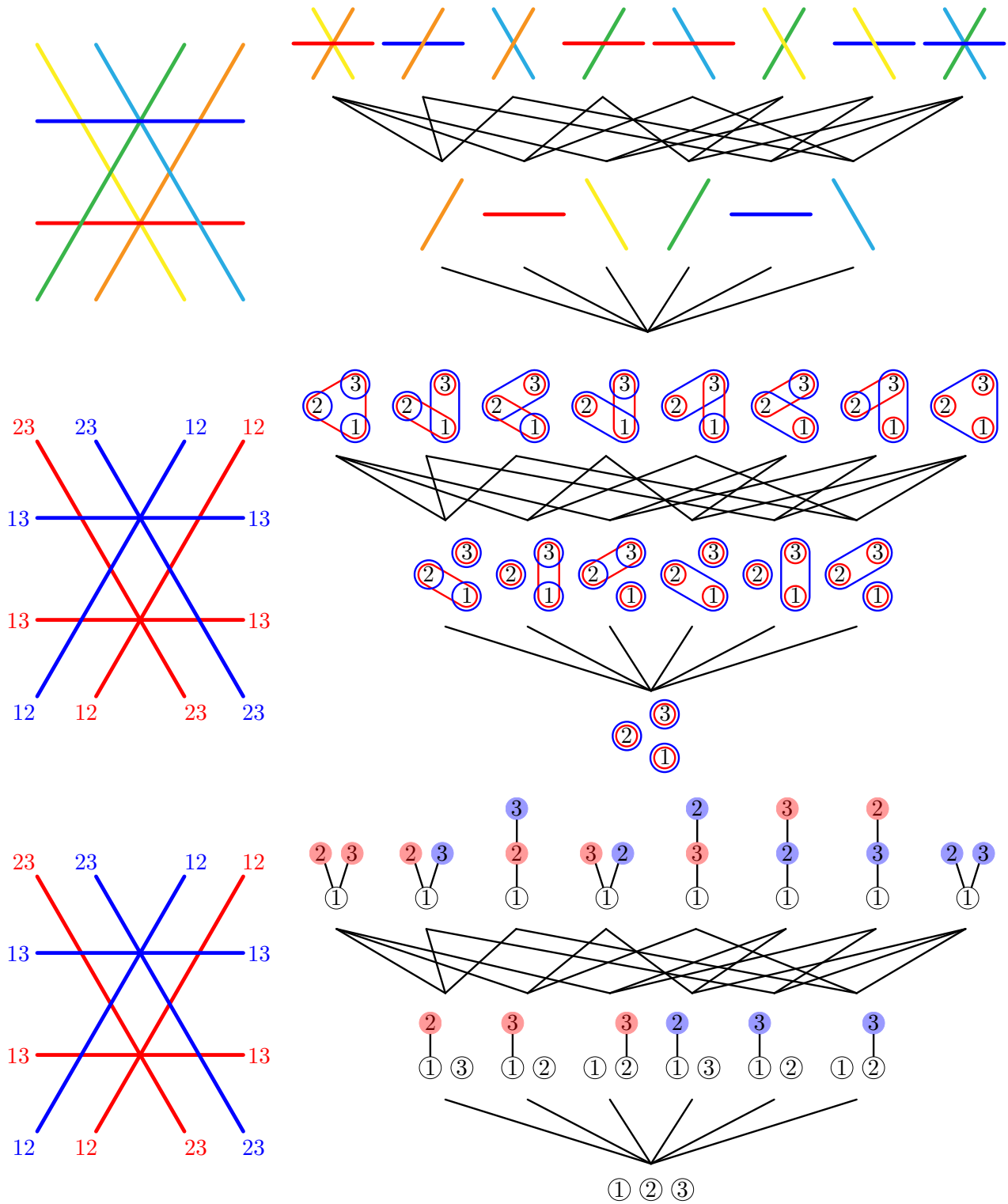


FIGURE 7. The (2,3)-braid arrangement \mathcal{B}_3^2 (left), and its flat poset (right), where flats are represented as intersections of hyperplanes (top), as (2,3)-partitions forests (middle), and as labeled (2,3)-rainbow forests (bottom).

$\ell = 1$						$\ell = 2$						$\ell = 3$						$\ell = 4$						
$n \setminus k$	0	1	2	3	Σ	$n \setminus k$	0	1	2	3	Σ	$n \setminus k$	0	1	2	3	Σ	$n \setminus k$	0	1	2	3	Σ	
1	1				1	1	1				1	1	1				1	1	1					1
2	2	1			3	2	3	2			5	2	4	3			7	2	5	4				9
3	6	6	1		13	3	17	24	8		49	3	34	54	21		109	3	57	96	40			193
4	24	36	14	1	75	4	149	324	226	50	749	4	472	1152	924	243	2791	4	1089	2808	2396	676		6969
1	1				1	1	1				1	1	1				1	1	1					1
2	0	1			1	2	1	2			3	2	2	3			5	2	3	4				7
3	0	0	1		1	3	5	12	8		25	3	16	36	21		73	3	33	72	40			145
4	0	0	0	1	1	4	43	132	138	50	363	4	224	684	702	243	1853	4	639	1944	1980	676		5239

TABLE 1. The face numbers (top) and the bounded face numbers (bottom) of the (ℓ, n) -braid arrangements for $\ell, n \in [4]$.

Proposition 2.5. *The Möbius polynomial of the (ℓ, n) -braid arrangement \mathcal{B}_n^ℓ is given by*

$$\mu_{\mathcal{B}_n^\ell}(x, y) = x^{(n-1)(1-\ell)} \sum_{G \in \Phi_n^\ell} y^{n-1-\ell n + \sum_{i \in [\ell]} \#G_i} \prod_{i \in [\ell]} \pi_{\#G_i}(x).$$

Proof. As already mentioned, the (ℓ, n) -partition forest poset Φ_n^ℓ is a lower set of the ℓ^{th} Cartesian power of the partition poset Π_n . In other words, given a (ℓ, n) -partition forest $\mathbf{G} := (G_1, \dots, G_\ell)$, any ℓ -tuple $\mathbf{F} := (F_1, \dots, F_\ell)$ of partitions satisfying $F_i \leq_{\Pi_n} G_i$ for all $i \in [\ell]$ is a (ℓ, n) -partition forest. Hence, we obtain from Definition 1.4 and Proposition 2.3 that

$$\begin{aligned} \mu_{\mathcal{B}_n^\ell}(x, y) &= \sum_{G \in \Phi_n^\ell} y^{n-\ell n-1+\sum_{i \in [\ell]} \#G_i} \prod_{i \in [\ell]} \sum_{F_i \leq_{\Pi_n} G_i} \mu_{\Pi_n}(F_i, G_i) x^{n-\ell n-1+\sum_{i \in [\ell]} \#F_i}, \\ &= \sum_{G \in \Phi_n^\ell} y^{n-\ell n-1+\sum_{i \in [\ell]} \#G_i} x^{(n-1)(1-\ell)} \prod_{i \in [\ell]} \sum_{\pi_i \in \Pi_{\#G_i}} \mu_{\Pi_{\#G_i}}(\pi_i, \hat{1}) x^{\#\pi_i-1}, \end{aligned}$$

where $\hat{1}$ denotes the maximal element in $\Pi_{\#G_i}$ and π_i is obtained from F_i by merging elements in the same part of G_i . The result follows since $\pi_{\#G_i}(x) = \sum_{\pi_i \in \Pi_{\#G_i}} \mu_{\Pi_{\#G_i}}(\pi_i, \hat{1}) x^{\#\pi_i-1}$. \square

From Theorems 1.6 and 2.4, we thus obtain the face numbers and bounded face numbers of \mathcal{B}_n^ℓ , whose first few values are gathered in Table 1.

Corollary 2.6. *The f - and b -polynomials of the (ℓ, n) -braid arrangement \mathcal{B}_n^ℓ are given by*

$$\begin{aligned} \mathbf{f}_{\mathcal{B}_n^\ell}(x) &= x^{n-1-\ell n} \sum_{\mathbf{F} \leq \mathbf{G}} \prod_{i \in [\ell]} x^{\#F_i} \prod_{p \in G_i} (\#F_i[p] - 1)! \\ \text{and } \mathbf{b}_{\mathcal{B}_n^\ell}(x) &= (-1)^\ell x^{n-1-\ell n} \sum_{\mathbf{F} \leq \mathbf{G}} \prod_{i \in [\ell]} x^{\#F_i} \prod_{p \in G_i} -(\#F_i[p] - 1)!, \end{aligned}$$

where $\mathbf{F} \leq \mathbf{G}$ ranges over all intervals of the (ℓ, n) -partition forest poset Φ_n^ℓ , and $F_i[p]$ denotes the restriction of the partition F_i to the part p of G_i .

Example 2.7. For $n = 1$, we have

$$\mu_{\mathcal{B}_1^\ell}(x, y) = \mathbf{f}_{\mathcal{B}_1^\ell}(x) = \mathbf{b}_{\mathcal{B}_1^\ell}(x) = 1.$$

For $n = 2$, we have

$$\mu_{\mathcal{B}_2^\ell}(x, y) = xy - \ell x + \ell, \quad \mathbf{f}_{\mathcal{B}_2^\ell}(x) = (\ell + 1)x + \ell \quad \text{and} \quad \mathbf{b}_{\mathcal{B}_2^\ell}(x) = (\ell - 1)x + \ell.$$

The case $n = 3$ is already more interesting. Consider the set partitions $P := \{\{1\}, \{2\}, \{3\}\}$, $Q_i := \{\{i\}, [3] \setminus \{i\}\}$ for $i \in [3]$, and $R := \{[3]\}$. Observe that the $(\ell, 3)$ -partition forests are all of the form

$$\mathbf{F} := P^\ell, \quad \mathbf{G}_i^p := P^p Q_i P^{\ell-p-1}, \quad \mathbf{H}_{i,j}^{p,q} := P^p Q_i P^{\ell-p-q-2} Q_j P^q \quad (i \neq j) \quad \text{or} \quad \mathbf{K}^p := P^p R P^{\ell-p-1}.$$

(where we write a tuple of partitions of $[3]$ as a word on $\{P, Q_1, Q_2, Q_3, R\}$). Moreover, the cover relations in the $(\ell, 3)$ -partition forest poset are precisely the relations

$$\begin{array}{c} \swarrow \mathbf{H}_{i,j}^{p,q} \\ \mathbf{F} \leq \mathbf{G}_i^p \leq \mathbf{K}^p \\ \searrow \mathbf{H}_{j,i}^{\ell-q-1, \ell-p-1} \end{array}$$

for $i \neq j$ and p, q such that $p + q \leq \ell - 2$. Hence, we have

$$\begin{aligned} \mu_{\mathcal{B}_3^\ell}(x, y) &= x^2 y^2 - 3\ell x^2 y + \ell(3\ell - 1)x^2 + 3\ell xy - 3\ell(2\ell - 1)x + \ell(3\ell - 2), \\ \mathbf{f}_{\mathcal{B}_3^\ell}(x) &= (3\ell^2 + 2\ell + 1)x^2 + 6\ell^2 x + \ell(3\ell - 2), \\ \text{and } \mathbf{b}_{\mathcal{B}_3^\ell}(x) &= (3\ell^2 - 4\ell + 1)x^2 + 6\ell(\ell - 1)x + \ell(3\ell - 2). \end{aligned}$$

Observe that $3\ell^2 + 2\ell + 1$ is [OEI10, A056109], that $\ell(3\ell - 2)$ is [OEI10, A000567], and that $3\ell^2 - 4\ell + 1$ is [OEI10, A045944].

2.3. Rainbow forests. In order to obtain more explicit formulas for the number of vertices and regions of the (ℓ, n) -braid arrangement \mathcal{B}_n^ℓ in Sections 2.4 and 2.5, we now introduce another combinatorial model for (ℓ, n) -partition forests which is more adapted to their enumeration.

Definition 2.8. An ℓ -rainbow coloring of a rooted plane forest F is an assignment of colors of $[\ell]$ to the non-root nodes of F such that

- (i) there is no monochromatic edge,
- (ii) the colors of siblings are increasing from left to right.

We denote by $\|F\|$ the number of nodes of F and by $\#F$ the number of trees of the forest F (i.e. its number of connected components). An (ℓ, n) -rainbow forest (resp. tree) is a ℓ -rainbow colored forest (resp. tree) with $\|F\| = n$ nodes. We denote by Ψ_n^ℓ (resp. \mathbf{T}_n^ℓ) the set of (ℓ, n) -rainbow forests (resp. trees), and set $\Psi^\ell := \bigsqcup_n \Psi_n^\ell$ (resp. $\mathbf{T}^\ell := \bigsqcup_n \mathbf{T}_n^\ell$).

For instance, we have listed the 14 $(2, 4)$ -rainbow trees in Figure 8 (top). This figure actually illustrates the following statement.

Lemma 2.9. *The (ℓ, m) -rainbow trees are counted by the Fuss-Catalan number*

$$\#\mathbf{T}_m^\ell = F_{\ell, m} := \frac{1}{(\ell - 1)m + 1} \binom{\ell m}{m} \quad [\text{OEI10, A062993}].$$

Proof. We can transform a ℓ -rainbow tree R to an ℓ -ary tree T as illustrated in Figure 8. Namely, the parent of a node N in T is the previous sibling colored as N in R if it exists, and the parent of N in R otherwise. This classical map is a bijection from ℓ -rainbow trees to ℓ -ary trees, which are counted by the Fuss-Catalan numbers [Kla70, HP91]. \square

Remark 2.10. Recall that the corresponding generating function $F_\ell(z) := \sum_{m \geq 0} F_{\ell, m} z^m$ satisfies the functional equation

$$F_\ell(z) = 1 + z F_\ell(z)^\ell.$$

Definition 2.11. For a (ℓ, n) -rainbow forest F , we define

$$\omega(F) := \prod_{i \in [\ell]} \prod_{N \in F} \#C_i(N)!,$$

where N ranges over all nodes of F and $C_i(N)$ denotes the children of N colored by i .

Definition 2.12. A labeling of a (ℓ, n) -rainbow forest F is a bijective map from the nodes of F to $[n]$ such that

- (i) the label of each root is minimal in its tree,
- (ii) the labels of siblings with the same color are increasing from left to right.

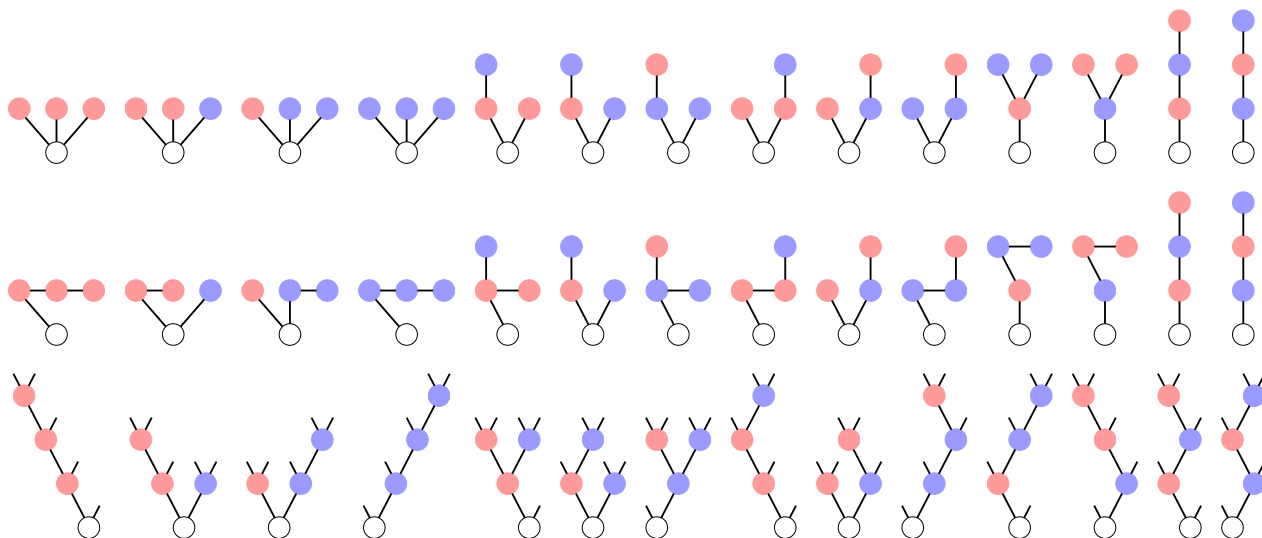


FIGURE 8. The 14 (2, 4)-rainbow trees (top) and 14 binary trees (bottom), and the simple bijection between them (middle). The order of the colors is red, blue.

$m \setminus \ell$	1	2	3	4	5	6	7	8	9
1	1	1	1	1	1	1	1	1	1
2	1	2	3	4	5	6	7	8	9
3	1	5	12	22	35	51	70	92	117
4	1	14	55	140	285	506	819	1240	1785
5	1	42	273	969	2530	5481	10472	18278	29799
6	1	132	1428	7084	23751	62832	141778	285384	527085
7	1	429	7752	53820	231880	749398	1997688	4638348	9706503
8	1	1430	43263	420732	2330445	9203634	28989675	77652024	184138713
9	1	4862	246675	3362260	23950355	115607310	430321633	1329890705	3573805950

TABLE 2. The Fuss-Catalan numbers $F_{\ell,m} = \frac{1}{(\ell-1)m+1} \binom{\ell m}{m}$ for $\ell, m \in [9]$. See [OEI10, A062993].

Lemma 2.13. *The number $\lambda(F)$ of labelings of a (ℓ, n) -rainbow forest F is given by*

$$\lambda(F) = \frac{n!}{\omega(F) \prod_{T \in F} \|T\|}.$$

Proof. Out of all $n!$ bijective maps from the nodes of F to $[n]$, only $1/\prod_{T \in F} \|T\|$ satisfy Condition (i) of Definition 2.12, and only $1/\prod_{i \in [\ell]} \prod_{N \in F} \#C_i(N)! = 1/\omega(F)$ satisfy Condition (ii) of Definition 2.12. \square

The following statement is illustrated in Figure 6.

Proposition 2.14. *There is a bijection from (ℓ, n) -partition forests to labeled (ℓ, n) -rainbow forests, such that if the partition forest \mathbf{F} is sent to the labeled rainbow forest F , then*

$$\dim(\mathbf{F}) = \#F - 1 \quad \text{and} \quad \mu_{\Phi_\ell}(\mathbb{H}, \mathbf{F}) = (-1)^{n-\#F} \omega(F).$$

Proof. From a labeled (ℓ, n) -rainbow forest F , we construct a (ℓ, n) -partition forest $\mathbf{F} := (F_1, \dots, F_\ell)$ whose i^{th} partition F_i has a part $\{N\} \cup C_i(N)$ for each node N of F not colored i . Condition (i) of Definition 2.8 ensures that each F_i is indeed a partition.

Conversely, start from a (ℓ, n) -partition forest $\mathbf{F} := (F_1, \dots, F_\ell)$. Consider the colored clique graph $K_{\mathbf{F}}$ on $[n]$ obtained by replacing each part in F_i by a clique of edges colored by i . For each $1 < j \leq n$, there is a unique shortest path in $K_{\mathbf{F}}$ from the vertex j to the smallest vertex in

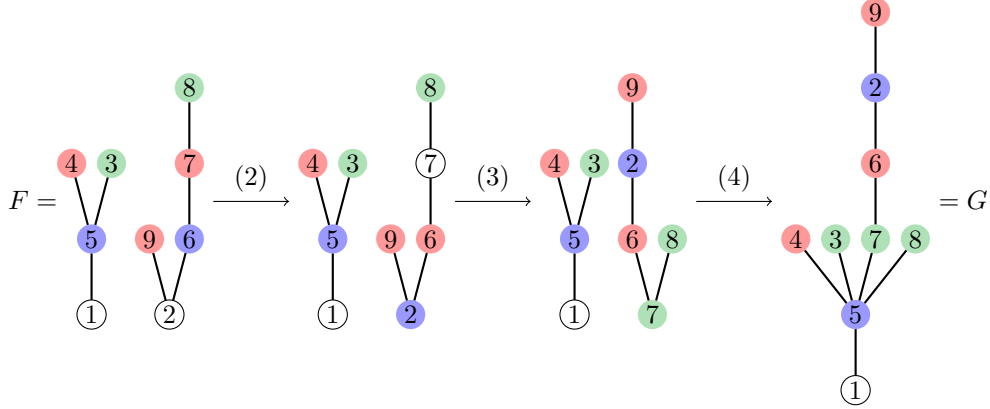


FIGURE 9. A covering relation described in Proposition 2.15, choosing c to be green, a to be 5 and b to be 7.

the connected component of j . Define the parent p of j to be the next vertex along this path, and color the node j by the color of the edge between j and p . This defines a labeled (ℓ, n) -rainbow forest F .

Finally, observe that

$$\dim(\mathbf{F}) = n - 1 - \ell n + \sum_{i \in [\ell]} \#F_i = \#F - 1, \quad \text{and}$$

$$\mu_{\Phi_n^\ell}(\mathbb{H}, \mathbf{F}) = \prod_{i \in [\ell]} \prod_{p \in F_i} (-1)^{\#p-1} (\#p - 1) = \prod_{i \in [\ell]} \prod_{N \in F} (-1)^{\#C_i(N)} \#C_i(N)! = (-1)^{n - \#F} \omega(\mathbf{F}). \square$$

We now transport via this bijection the partial order of the flat lattice on rainbow forests. For a node a of a forest F , we denote by $\text{Root}(a)$ the root of the tree of F containing a . The following statement is illustrated in Figure 9, choosing c to be green, a to be 5 and b to be 7.

Proposition 2.15. *In the flat poset $\text{Fl}(\mathcal{B}_n^\ell)$ labeled by rainbow forests using Propositions 2.3 and 2.14, a rainbow forest F is covered by a rainbow forest G if and only if G can be obtained from F by:*

- (1) choosing a color c , and two vertices a and b not colored with c and with $\text{Root}(a) < \text{Root}(b)$,
- (2) shifting the colors along the path from $\text{Root}(b)$ to b , so that each node along this path is now colored by the former color of its child and b is not colored anymore,
- (3) rerooting at b the tree containing b at b , and coloring b with c ,
- (4) adding an edge (a, b) and replacing the edge (b, e) by an edge (a, e) for each child e of b colored with c .

Proof. Let us first remark that the graph obtained by these operations is indeed a rainbow forest. First, we add an edge between two distinct connected components, so that the result is indeed acyclic. Moreover, the condition on the color of a and on the deletion of edges between b and vertices of color c ensures that we do not add an edge between two vertices of the same color. Note that the parent of b inherits the color of b which is not c .

Let us recall that the cover relations in the flat poset $\text{Fl}(\mathcal{B}_n^\ell)$ are given in terms of (ℓ, n) -partition forests by choosing a partition π of the partition tuple (which corresponds directly to choosing a color), choosing two parts π_a and π_b in the partition π , and merging them, without creating a loop in the intersection hypergraph.

By choosing two vertices in different connected components of the rainbow forest, we are sure that the intersection hypergraph obtained by adding an edge is still acyclic.

The last point that has to be explained is the link between the condition on the color of a and merging two parts in the same partition. If one of the two nodes, say a for instance is of color c , then it belongs to the same part of π as its parent z . The merging is the same if we choose z

$n \setminus \ell$	1	2	3	4	5	6	7	8
1	1	1	1	1	1	1	1	1
2	1	2	3	4	5	6	7	8
3	1	8	21	40	65	96	133	176
4	1	50	243	676	1445	2646	4375	6728
5	1	432	3993	16384	46305	105456	208537	373248
6	1	4802	85683	521284	1953125	5541126	13119127	27350408
7	1	65536	2278125	20614528	102555745	362797056	1029059101	2500000000
8	1	1062882	72412707	976562500	6457339845	28500625446	96889010407	274371577992

TABLE 3. The numbers $f_0(\mathcal{B}_n^\ell) = \ell((\ell - 1)n + 1)^{n-2}$ of vertices of \mathcal{B}_n^ℓ for $\ell, n \in [8]$.

which is not colored c . Moreover, as b is in a different connected component, the corresponding two parts are distinct in π . Finally, a part is just a corolla so the merging corresponds to building a corolla with a , b and their children of color c . \square

We finally recast Proposition 2.5 in terms of rainbow forests.

Proposition 2.16. *The Möbius polynomial of the (ℓ, n) -braid arrangement \mathcal{B}_n^ℓ is given by*

$$\mu_{\mathcal{B}_n^\ell}(x, y) = x^{(n-1)(1-\ell)} \sum_{G \in \Psi_n^\ell} y^{n-1+\#E(G)} \prod_{i \in [\ell]} \pi_{n-\#E(G,i)}(x).$$

Remark 2.17. To further simplify this expression, we would need to count the number of rainbow forests with a prescribed number of colored edges. However, this number does not admit a known multiplicative formula, up to our knowledge. When there is only one color, the corresponding sequence (counting non-colored forests on n nodes and k edges, rooted in the minimal label of each connected component) is [OEI10, A138464].

2.4. Enumeration of vertices of \mathcal{B}_n^ℓ . We now use the labeled (ℓ, n) -rainbow forests of Section 2.3 to derive more explicit formulas for the number of vertices of the (ℓ, n) -braid arrangement \mathcal{B}_n^ℓ . The first few values are gathered in Table 3.

Theorem 2.18. *The number of vertices of the (ℓ, n) -braid arrangement \mathcal{B}_n^ℓ is*

$$f_0(\mathcal{B}_n^\ell) = \ell((\ell - 1)n + 1)^{n-2}.$$

Proof. By Propositions 2.3 and 2.14, we just need to count the labeled (ℓ, n) -rainbow trees. A common reasoning for counting Cayley trees is the use of its Prüfer code defined by recursively pruning the smallest leaf while writing down the label of its parent. This bijection can be adapted to colored Cayley trees by writing down the label of the parent colored by the color of the pruned leaf. This leads to a bijection with certain colored words of length $n - 1$. Namely, there are two possibilities:

- either the pruned leaf is attached to the node 1 and it can have all ℓ colors,
- or it is attached to one of the $n - 1$ other nodes and it can only have $\ell - 1$ colors.

Note that the last letter in the Prüfer code (obtained by removing the last edge) is necessarily the root 1, with ℓ possible different colors. Hence, there are

$$(\ell + (n - 1)(\ell - 1))^{n-2} \ell = \ell((\ell - 1)n + 1)^{n-2}$$

such words. Similar ideas were used in [Lew99]. \square

We can refine the formula of Theorem 2.18 according to the dimension of the flats of the different copies intersected to obtain the vertices of the (ℓ, n) -braid arrangement \mathcal{B}_n^ℓ .

Theorem 2.19. *For any k_1, \dots, k_ℓ such that $0 \leq k_i \leq n - 1$ for $i \in [\ell]$ and $\sum_{i \in [\ell]} k_i = n - 1$, the number of vertices v of the (ℓ, n) -braid arrangement \mathcal{B}_n^ℓ such that the smallest flat of the i^{th} copy of \mathcal{B}_n containing v has dimension $n - k_i - 1$ is given by*

$$n^{\ell-1} \binom{n-1}{k_1, \dots, k_\ell} \prod_{i \in [\ell]} (n - k_i)^{k_i-1}.$$

Proof. By Propositions 2.3 and 2.14, we just need to count the labeled (ℓ, n) -rainbow trees with k_i nodes colored by i . Forgetting the labels, the (ℓ, n) -rainbow trees with k_i nodes colored by i are precisely the spanning trees of the complete multipartite graph $K_{k_1, \dots, k_\ell, 1}$ (where the last 1 stands for the uncolored root). Using a Prüfer code similar to that of the proof of Theorem 2.18, R. Lewis proved in [Lew99] that the latter are counted by $n^{\ell-1} \prod_{i \in [\ell]} (n - k_i)^{k_i-1}$. Finally, the possible labelings are counted by the multinomial coefficient $\binom{n-1}{k_1, \dots, k_\ell}$. \square

2.5. Enumeration of regions and bounded regions of \mathcal{B}_n^ℓ . We finally use the labeled (ℓ, n) -rainbow forests of Section 2.3 to derive more explicit formulas for the number of regions and bounded regions of the (ℓ, n) -braid arrangement \mathcal{B}_n^ℓ . The first few values are gathered in Tables 4 and 5. We first compute the characteristic polynomial of \mathcal{B}_n^ℓ .

Theorem 2.20. *The characteristic polynomial $\chi_{\mathcal{B}_n^\ell}(y)$ of the (ℓ, n) -braid arrangement \mathcal{B}_n^ℓ is given by*

$$\chi_{\mathcal{B}_n^\ell}(y) = \frac{(-1)^n n!}{y} [z^n] \exp \left(- \sum_{m \geq 1} \frac{F_{\ell, m} y z^m}{m} \right),$$

where $F_{\ell, m} := \frac{1}{(\ell-1)m+1} \binom{\ell m}{m}$ is the Fuss-Catalan number.

Proof. By Theorem 2.4 and Proposition 2.14, the characteristic polynomial $\chi_{\mathcal{B}_n^\ell}(y)$ is

$$\chi_{\mathcal{B}_n^\ell}(y) = \sum_{F \in \Phi_n^\ell} \mu_{\Phi_n^\ell}(\mathbb{H}, F) y^{\dim(F)} = \sum_{F \in \Psi_n^\ell} \lambda(F) (-1)^{n-\#F} \omega(F) y^{\#F-1}.$$

From Lemma 2.13, we observe that

$$\frac{\lambda(F) \omega(F) (-y)^{\#F} z^{\|F\|}}{\|F\|!} = \prod_{T \in F} \frac{-y z^{\|T\|}}{\|T\|},$$

where T ranges over the trees of F . Now using that rainbow forests are exactly sets of rainbow trees, we obtain that

$$\sum_{F \in \Psi_n^\ell} \frac{\lambda(F) \omega(F) (-y)^{\#F} z^{\|F\|}}{\|F\|!} = \sum_{F \in \Psi_n^\ell} \prod_{T \in F} \frac{-y z^{\|T\|}}{\|T\|} = \exp \left(\sum_{T \in \mathbf{T}^\ell} \frac{-y z^{\|T\|}}{\|T\|} \right).$$

From Lemma 2.9, we obtain that

$$\exp \left(\sum_{T \in \mathbf{T}^\ell} \frac{-y z^{\|T\|}}{\|T\|} \right) = \exp \left(- \sum_{m \geq 1} \frac{F_{\ell, m} y z^m}{m} \right).$$

We conclude that

$$\begin{aligned} \chi_{\mathcal{B}_n^\ell}(y) &= \sum_{F \in \Psi_n^\ell} \lambda(F) (-1)^{n-\#F} \omega(F) y^{\#F-1} \\ &= \frac{(-1)^n n!}{y} [z^n] \sum_{F \in \Psi_n^\ell} \frac{\lambda(F) \omega(F) (-y)^{\#F} z^{\|F\|}}{\|F\|!} \\ &= \frac{(-1)^n n!}{y} [z^n] \exp \left(- \sum_{m \geq 1} \frac{F_{\ell, m} y z^m}{m} \right). \end{aligned} \quad \square$$

From the characteristic polynomial of \mathcal{B}_n^ℓ and Remark 1.8, we obtain its numbers of regions and bounded regions.

$n \setminus \ell$	1	2	3	4	5	6	7	8
1	1	1	1	1	1	1	1	1
2	2	3	4	5	6	7	8	9
3	6	17	34	57	86	121	162	209
4	24	149	472	1089	2096	3589	5664	8417
5	120	1809	9328	29937	73896	154465	287904	493473
6	720	28399	241888	1085157	3442816	8795635	19376064	38323753
7	5040	550297	7806832	49075065	200320816	625812385	1629858672	3720648337
8	40320	12732873	302346112	2666534049	14010892416	53536186825	164859458688	434390214657

 TABLE 4. The numbers $f_{n-1}(\mathcal{B}_n^\ell)$ of regions of \mathcal{B}_n^ℓ for $\ell, n \in [8]$.

$n \setminus \ell$	1	2	3	4	5	6	7	8
1	1	1	1	1	1	1	1	1
2	0	1	2	3	4	5	6	7
3	0	5	16	33	56	85	120	161
4	0	43	224	639	1384	2555	4248	6559
5	0	529	4528	17937	49696	111745	219024	389473
6	0	8501	120272	663363	2354624	6455225	14926176	30583847
7	0	169021	3968704	30533409	138995776	464913325	1268796096	2996735329
8	0	4010455	156745472	1684352799	9841053184	40179437975	129465630720	352560518527

 TABLE 5. The numbers $b_{n-1}(\mathcal{B}_n^\ell)$ of bounded regions of \mathcal{B}_n^ℓ for $\ell, n \in [8]$.

Theorem 2.21. *The numbers of regions and of bounded regions of the (ℓ, n) -braid arrangement \mathcal{B}_n^ℓ are given by*

$$f_{n-1}(\mathcal{B}_n^\ell) = n! [z^n] \exp \left(\sum_{m \geq 1} \frac{F_{\ell, m} z^m}{m} \right)$$

and

$$b_{n-1}(\mathcal{B}_n^\ell) = (n-1)! [z^{n-1}] \exp \left((\ell-1) \sum_{m \geq 1} F_{\ell, m} z^m \right),$$

where $F_{\ell, m} := \frac{1}{(\ell-1)m+1} \binom{\ell m}{m}$ is the Fuss-Catalan number.

Proof. By Remark 1.8, we obtain from Theorem 2.20 that

$$f_{n-1}(\mathcal{B}_n^\ell) = (-1)^{n-1} \chi_{\mathcal{B}_n^\ell}(-1) = n! [z^n] \exp \left(\sum_{m \geq 1} \frac{F_{\ell, m} z^m}{m} \right),$$

$$b_{n-1}(\mathcal{B}_n^\ell) = (-1)^{n-1} \chi_{\mathcal{B}_n^\ell}(1) = -n! [z^n] \exp \left(- \sum_{m \geq 1} \frac{F_{\ell, m} z^m}{m} \right).$$

To conclude, we thus just need to observe that $U_\ell(z) = \frac{\partial}{\partial z} V_\ell(z)$ where

$$U_\ell(z) := \exp \left((\ell-1) \sum_{m \geq 1} F_{\ell, m} z^m \right) \quad \text{and} \quad V_\ell(z) := - \exp \left(- \sum_{m \geq 1} \frac{F_{\ell, m} z^m}{m} \right).$$

For this, consider the generating functions

$$F_\ell(z) := \sum_{m \geq 0} F_{\ell, m} z^m \quad \text{and} \quad G_\ell(z) := \sum_{m \geq 1} \frac{F_{\ell, m} z^m}{m}.$$

Recall from Remark 2.10 that $F_\ell(z)$ satisfies the functional equation

$$F_\ell(z) = 1 + z F_\ell(z)^\ell.$$

We thus obtain that

$$F'_\ell(z)(1 - \ell z F_\ell(z)^{\ell-1}) = F_\ell(z)^\ell \quad \text{and} \quad F_\ell(z)(1 - \ell z F_\ell(z)^{\ell-1}) = 1 - (\ell-1) z F_\ell(z)^\ell.$$

Combining these two equations, we get

$$(1) \quad F_\ell(z)^{\ell+1} = F'_\ell(z)(1 - (\ell - 1)z F_\ell(z)^\ell).$$

Observe now that

$$(2) \quad z G'_\ell(z) = F_\ell(z) - 1 = z F_\ell(z)^\ell \quad \text{and} \quad G''_\ell(z) = \ell F_\ell(z)^{\ell-1} F'_\ell(z).$$

Hence

$$U_\ell(z) = \exp((\ell - 1)(F_\ell(z) - 1)) = \exp((\ell - 1)z G'_\ell(z))$$

and

$$V'_\ell(z) = \frac{\partial}{\partial z} - \exp(-G_\ell(z)) = G'_\ell(z) \exp(-G_\ell(z)).$$

Consider now the function

$$W_\ell(z) = V'_\ell(z)/U_\ell(z) = G'_\ell(z) \exp(-G_\ell(z) - (\ell - 1)z G'_\ell(z)).$$

Clearly, $W_\ell(0) = 1$. Moreover, using (2), we obtain that its derivative is

$$\begin{aligned} W'_\ell(z) &= \left(G''_\ell(z)(1 - (\ell - 1)z G'_\ell(z)) - \ell G'_\ell(z)^2 \right) \exp(-G_\ell(z) - (\ell - 1)z G'_\ell(z)) \\ &= \ell F_\ell(z)^{\ell-1} \left(F'_\ell(z)(1 - (\ell - 1)z F_\ell(z)^\ell) - F_\ell(z)^{\ell+1} \right) \exp(-G_\ell(z) - (\ell - 1)z G'_\ell(z)), \end{aligned}$$

which vanishes by (1). \square

3. FACE POSET AND COMBINATORIAL DESCRIPTION OF $\mathcal{B}_n^\ell(\mathbf{a})$

In this section, we describe the face poset of the \mathbf{a} -braid arrangement $\mathcal{B}_n^\ell(\mathbf{a})$ in terms of ordered (ℓ, n) -partition forests. This section highly depends on the choice of the translation matrix \mathbf{a} .

3.1. Ordered partition forests. We now introduce the combinatorial objects that will be used to encode the faces of the \mathbf{a} -braid arrangement $\mathcal{B}_n^\ell(\mathbf{a})$ of Definition 1.12.

Definition 3.1. An *ordered (ℓ, n) -partition forest* (resp. *tree*) is an ℓ -tuple $\vec{F} := (\vec{F}_1, \dots, \vec{F}_\ell)$ of ordered set partitions of $[n]$ such that the corresponding ℓ -tuple $\mathbf{F} := (F_1, \dots, F_\ell)$ of unordered set partitions of $[n]$ forms an (ℓ, n) -partition forest (resp. tree). The *ordered (ℓ, n) -partition forest poset* is the poset $\vec{\Phi}_n^\ell$ on ordered (ℓ, n) -partition forests ordered by componentwise refinement. In other words, $\vec{\Phi}_n^\ell$ is the subposet of the ℓ^{th} Cartesian power of the ordered partition poset $\vec{\Pi}_n$ induced by ordered (ℓ, n) -partition forests. Note that the maximal elements of $\vec{\Phi}_n^\ell$ are the ordered (ℓ, n) -partition trees.

The following statement is the analogue of Proposition 2.3, and is illustrated in Figures 10 and 11.

Proposition 3.2. *The face poset $\text{Fa}(\mathcal{B}_n^\ell(\mathbf{a}))$ of the \mathbf{a} -braid arrangement $\mathcal{B}_n^\ell(\mathbf{a})$ is isomorphic to an upper set $\vec{\Phi}_n^\ell(\mathbf{a})$ of the ordered (ℓ, n) -partition forest poset $\vec{\Phi}_n^\ell$.*

Proof. The proof is based on that of Proposition 2.3. A face of $\mathcal{B}_n^\ell(\mathbf{a})$ is an intersection of faces of the ℓ copies of \mathcal{B}_n^ℓ , hence corresponds to an ℓ -tuple of ordered partitions of $[n]$. Moreover, the flats supporting these faces intersect, so that the corresponding unordered partitions must form an (ℓ, n) -partition forest. Hence, each face of $\mathcal{B}_n^\ell(\mathbf{a})$ corresponds to a certain ordered (ℓ, n) -partition forest. Moreover, the inclusion of faces of $\mathcal{B}_n^\ell(\mathbf{a})$ translates to the componentwise refinement on ordered partitions. Finally, by genericity, it is immediate that we obtain an upper set of this componentwise refinement order. \square

We now fix a generic translation matrix $\mathbf{a} := (a_{i,j})$ and still denote by $A_{i,s,t} := \sum_{s \leq j < t} a_{i,j}$ for all $1 \leq s < t \leq n$ and $i \in [\ell]$ (and often write $A_{i,t,s}$ for $-A_{i,s,t}$). The objective of this section is to describe

- the ordered (ℓ, n) -partitions forests of the upper set $\vec{\Phi}_n^\ell(\mathbf{a})$ with a given underlying (unordered) (ℓ, n) -partition forest (Section 3.2),
- a criterion to decide whether a given ordered (ℓ, n) -partition forest belongs to the upper set $\vec{\Phi}_n^\ell(\mathbf{a})$, i.e. corresponds to a face of $\mathcal{B}_n^\ell(\mathbf{a})$ (Section 3.3).

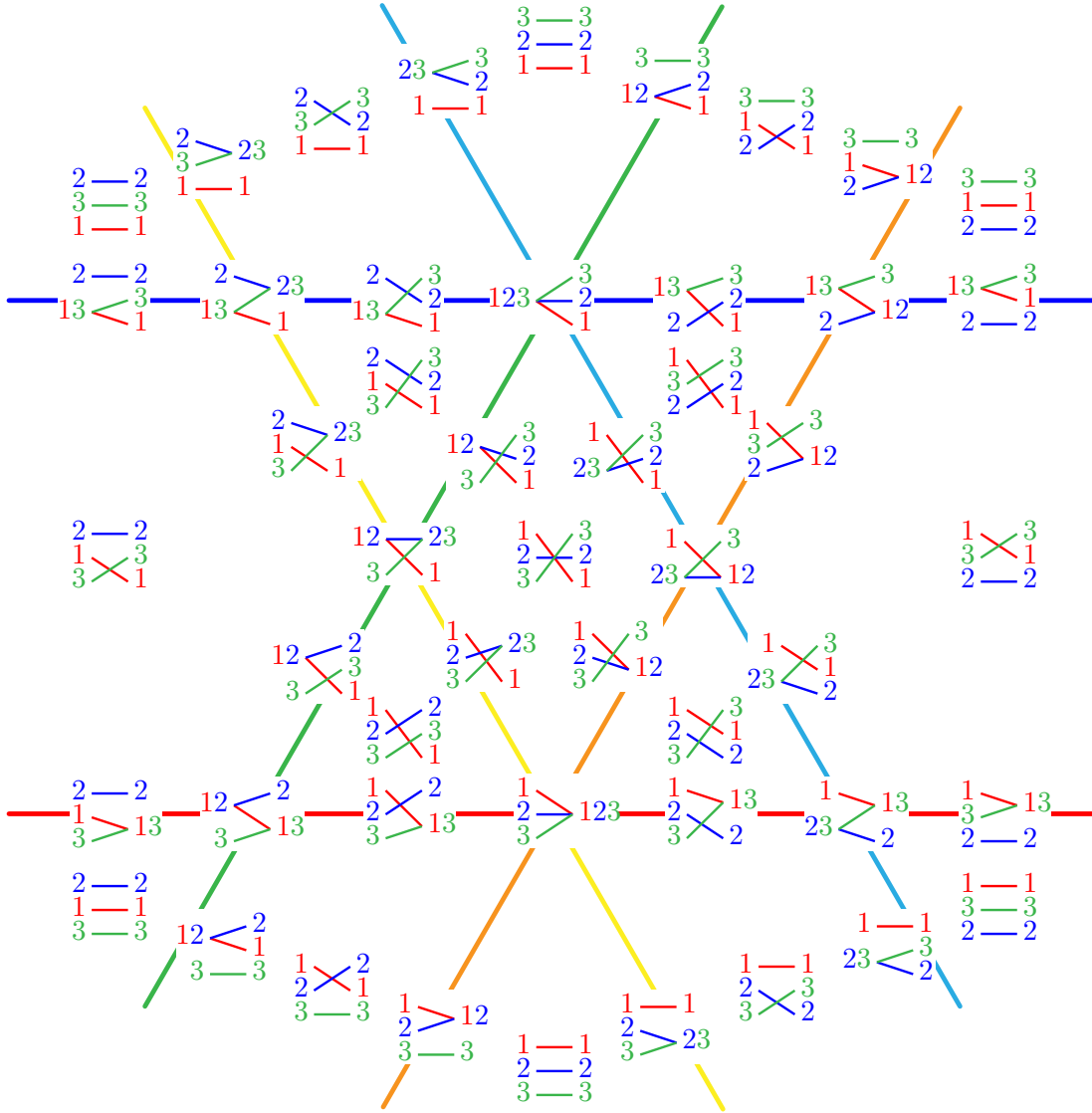


FIGURE 10. Labelings of the faces of the arrangement $\mathcal{B}_3^2(\mathbf{a})$ for $\mathbf{a} = \begin{bmatrix} 0 & 0 \\ -1 & -1 \end{bmatrix}$.

3.2. From partition forests to ordered partition forests. In this section, we describe the ordered (ℓ, n) -partitions forests $\overline{\mathbf{F}}$ of the upper set $\overline{\Phi}_n^\ell(\mathbf{a})$ with a given underlying (ℓ, n) -partition forest \mathbf{F} . We denote by $cc(\mathbf{F})$ the connected components of \mathbf{F} , meaning the partition of $[n]$ given by the hyperedge labels of the connected components of the intersection hypergraph of \mathbf{F} . We first observe that the choice of \mathbf{a} fixes the order of the parts in a common connected component of \mathbf{F} .

Proposition 3.3. *Consider a (ℓ, n) -partition forest $\mathbf{F} := (F_1, \dots, F_\ell)$, and two integers $s, t \in [n]$ labeling two hyperedges in the same connected component of the intersection hypergraph of \mathbf{F} . Assume that the unique path from s to t in the hypergraph of \mathbf{F} passes through the hyperedges labeled by $s = r_0, \dots, r_q = t$ and through parts of the partitions F_{i_1}, \dots, F_{i_q} . Then for any ordered (ℓ, n) -partition forest $\overline{\mathbf{F}} := (\overline{F}_1, \dots, \overline{F}_\ell)$ of the upper set $\overline{\Phi}_n^\ell(\mathbf{a})$ with underlying (ℓ, n) -partition forest \mathbf{F} and any $i \in [\ell]$, the order of s and t in \overline{F}_i is given by the sign of $A_{i,s,t} - \sum_{p \in [q]} A_{i_p, r_{p-1}, r_p}$.*

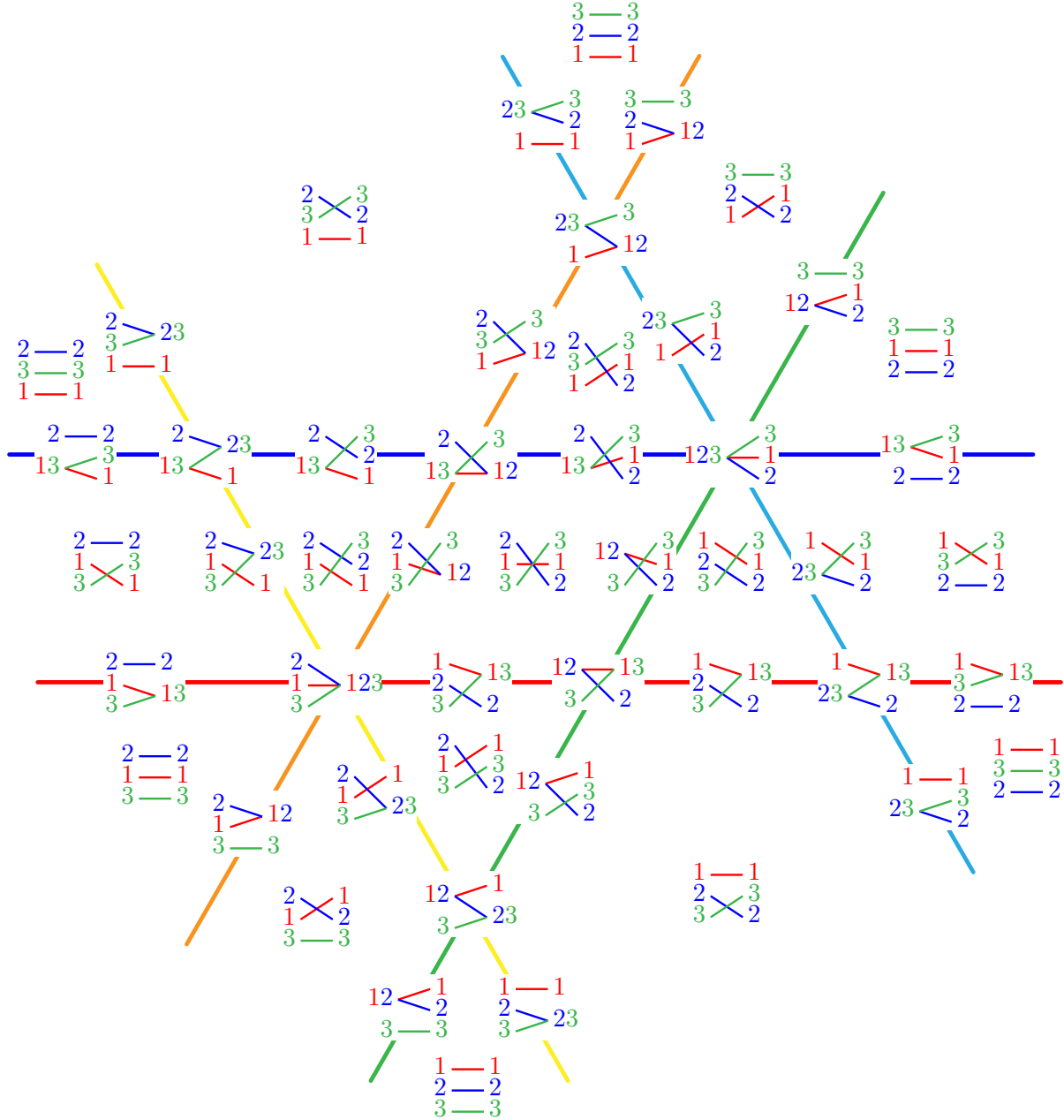


FIGURE 11. Labelings of the faces of the arrangement $\mathcal{B}_3^2(\mathbf{a})$ for $\mathbf{a} = \begin{bmatrix} 0 & 0 \\ 1 & -2 \end{bmatrix}$.

Proof. Consider any point \mathbf{x} in the face of $\mathcal{B}_n^\ell(\mathbf{a})$ corresponding to \vec{F} . Along the path from s to t , we have $x_{r_{p-1}} - x_{r_p} = A_{i_p, r_{p-1}, r_p}$ for each $p \in [q]$. Hence, we obtain that

$$x_s - x_t = \sum_{p \in [q]} (x_{r_{p-1}} - x_{r_p}) = \sum_{p \in [q]} A_{i_p, r_{p-1}, r_p}.$$

The order of s, t in \vec{F}_i is given by the sign of $A_{i, s, t} - (x_s - x_t)$, hence of $A_{i, s, t} - \sum_{p \in [q]} A_{i_p, r_{p-1}, r_p}$. \square

We now describe the different ways to order the parts in distinct connected components of \mathbf{F} . For this, we need the following posets.

Definition 3.4. Consider a (ℓ, n) -partition forest \mathbf{F} and denote by $cc(\mathbf{F})$ the connected components of \mathbf{F} . For each pair $s, t \in [n]$ in distinct connected components of $cc(\mathbf{F})$, we define the chain $<_{s,t}$ on the ℓ triples (i, s, t) for $i \in [\ell]$ given by the order of the values $A_{i,s,t}$. The *inversion poset* $\text{Inv}(\mathbf{F}, \mathbf{a})$ is then the poset obtained by quotienting the disjoint union of the chains $<_{s,t}$ (for all $s, t \in [n]$ in distinct connected components of $cc(\mathbf{F})$) by the equivalence relation $(i, s, t) \equiv (i, s', t')$ if s and s' belong to the same part of F_i and t and t' belong to the same part of F_i . We say that a subset X of $\text{Inv}(\mathbf{F}, \mathbf{a})$ is antisymmetric if $(i, s, t) \in X \iff (i, t, s) \notin X$.

Proposition 3.5. *The ordered (ℓ, n) -partition forests of the upper set $\overrightarrow{\Phi}_n^\ell(\mathbf{a})$ with a given underlying (ℓ, n) -partition forest \mathbf{F} are in bijection with the antisymmetric lower sets of the inversion poset $\text{Inv}(\mathbf{F}, \mathbf{a})$.*

Proof. Consider an ordered (ℓ, n) -partition forest $\overrightarrow{\mathbf{F}}$ of the upper set $\overrightarrow{\Phi}_n^\ell(\mathbf{a})$. Let \mathbf{x} be any point of the face of $\mathcal{B}_n^\ell(\mathbf{a})$ corresponding to $\overrightarrow{\mathbf{F}}$. For each pair $s, t \in [n]$ in distinct connected components of $cc(\mathbf{F})$, let $I_{s,t}(\mathbf{F})$ be the set of indices $i \in [\ell]$ such that $x_s - x_t < A_{i,s,t}$. Note that $I_{s,t}$ is by definition a lower set of the chain $<_{s,t}$ of $\text{Inv}(\mathbf{F}, \mathbf{a})$. Hence, $I(\overrightarrow{\mathbf{F}}) := \bigcup_{s,t} I_{s,t} \equiv$ is a lower set of $\text{Inv}(\mathbf{F}, \mathbf{a})$. Moreover, it is clearly antisymmetric since

$$(i, s, t) \in I(\overrightarrow{\mathbf{F}}) \iff x_s - x_t < A_{i,s,t} \iff x_t - x_s > A_{i,t,s} \iff (i, t, s) \notin I(\overrightarrow{\mathbf{F}}).$$

Conversely, given an antisymmetric lower set I of $\text{Inv}(\mathbf{F}, \mathbf{a})$, we can reconstruct an ordered (ℓ, n) -partition forest $\overrightarrow{\mathbf{F}}$ by ordering each pair $s, t \in [n]$ in F_i

- according to Proposition 3.3 (hence independently of I) if s and t belong to the same connected component of \mathbf{F} ,
- according to I if s and t belong to distinct connected components of \mathbf{F} . Namely, we place the block of \overrightarrow{F}_i containing s before the block of \overrightarrow{F}_i containing t if and only if $(i, s, t) \in I$.

It is then straightforward to check that the resulting ordered (ℓ, n) -partition forest belongs to the upper set $\overrightarrow{\Phi}_n^\ell(\mathbf{a})$, by exhibiting a point \mathbf{x} in of the corresponding face of $\mathcal{B}_n^\ell(\mathbf{a})$. \square

3.3. A criterion for ordered partition forests. We now consider a given ordered (ℓ, n) -partition forest $\overrightarrow{\mathbf{F}}$ and provide a criterion to decide if it belongs to the upper set $\overrightarrow{\Phi}_n^\ell(\mathbf{a})$ corresponding to the faces of $\mathcal{B}_n^\ell(\mathbf{a})$. For this, we need the following directed graph associated to $\overrightarrow{\mathbf{F}}$.

Definition 3.6. For an ordered partition $\overrightarrow{\pi} := \overrightarrow{\pi}_1 | \dots | \overrightarrow{\pi}_k$ of $[n]$, we denote by $D_{\overrightarrow{\pi}}$ the directed graph on $[n]$ with an arc $\max(\overrightarrow{\pi}_j) \rightarrow \min(\overrightarrow{\pi}_{j+1})$ for each $j \in [k-1]$ and a cycle $x_1 \rightarrow \dots \rightarrow x_p \rightarrow x_1$ for each part $\overrightarrow{\pi}_j = \{x_1 < \dots < x_p\}$. Note that $D_{\overrightarrow{\pi}}$ has n vertices and $n + k$ arcs. For an ordered (ℓ, n) -partition forest $\overrightarrow{\mathbf{F}} := (\overrightarrow{F}_1, \dots, \overrightarrow{F}_\ell)$, we denote by $D_{\overrightarrow{\mathbf{F}}}$ the superposition of the directed graphs $D_{\overrightarrow{F}_i}$ for $i \in [\ell]$, where the arcs of $D_{\overrightarrow{F}_i}$ are labeled by i .

Proposition 3.7. *An ordered (ℓ, n) -partition forest $\overrightarrow{\mathbf{F}}$ belongs to the upper set $\overrightarrow{\Phi}_n^\ell(\mathbf{a})$ if and only if $\sum_{\alpha \in \gamma} A_{i(\alpha), s(\alpha), t(\alpha)} \geq 0$ for any (simple) oriented cycle γ in $D_{\overrightarrow{\mathbf{F}}}$, where each arc $\alpha \in \gamma$ has label $i(\alpha)$, source $s(\alpha)$, and target $t(\alpha)$.*

Proof. Consider an ordered (ℓ, n) -partition forest $\overrightarrow{\mathbf{F}} := (\overrightarrow{F}_1, \dots, \overrightarrow{F}_\ell)$. For each $i \in [\ell]$, denote by

- m_i the number of arcs of $D_{\overrightarrow{F}_i}$
- M_i the incidence matrix of $D_{\overrightarrow{F}_i}$, with m_i rows and n columns, with a row for each arc α of $D_{\overrightarrow{F}_i}$ containing a -1 in column $s(\alpha)$, a 1 in column $t(\alpha)$, and 0 elsewhere,
- \mathbf{z}_i the column vector in \mathbb{R}^{m_i} with a row for each arc α of $D_{\overrightarrow{F}_i}$ containing the value $A_{i(\alpha), s(\alpha), t(\alpha)}$.

Then a point $\mathbf{x} \in \mathbb{R}^n$ belongs to the face of the i^{th} braid arrangement corresponding to \overrightarrow{F}_i if and only if it satisfies $M_i \mathbf{x} \leq \mathbf{z}_i$. Hence, $\overrightarrow{\mathbf{F}}$ appears as a face of the \mathbf{a} -braid arrangement if and only if there exists $\mathbf{x} \in \mathbb{R}^n$ such that $M \mathbf{x} \leq \mathbf{z}$, where M is the $(m \times n)$ -matrix (where $m := \sum_{i \in [\ell]} m_i$), obtained by piling the matrices M_i for $i \in [\ell]$ and similarly, \mathbf{z} is the column vector obtained by piling the vectors \mathbf{z}_i . A direct application of the Farkas lemma (see e.g. [Zie98, Prop. 1.7]), there exists $\mathbf{x} \in \mathbb{R}^n$ such that $M \mathbf{x} \leq \mathbf{z}$ if and only if $\mathbf{c} \mathbf{z} \geq 0$ for any $\mathbf{c} \in (\mathbb{R}^m)^*$ with $\mathbf{c} \geq \mathbf{0}$ and $\mathbf{c} M = \mathbf{0}$. Now it is classical that the left kernel of the incidence matrix of a directed graph is generated

by its circuits (non-necessarily oriented cycles), and that the positive cone in this left kernel is generated by its oriented cycles. \square

Remark 3.8. Note that we made some arbitrary choices here by choosing the arc from $\max(\vec{\pi}_j)$ to $\min(\vec{\pi}_{j+1})$ between two consecutive parts $\vec{\pi}_j$ and $\vec{\pi}_{j+1}$ and a cycle inside each part $\vec{\pi}_j$ (while we said that the order in each part is irrelevant). We could instead have considered all arcs connecting two elements of two consecutive parts, or two elements inside the same part. Our choices just limit the amount of oriented cycles in $D_{\vec{\pi}}$.

Part II. Diagonals of permutahedra

In this second part, we study the combinatorics of the diagonals of the permutahedra. In Section 4, we first recall the definition and some known facts about cellular diagonals of polytopes (Section 4.1), which we immediately specialize to the classical permutahedron (Section 4.2), and connect to Part I to derive enumerative statements on the diagonals of permutahedra (Section 4.3). In Section 5, we consider two particular diagonals, the LA and SU diagonals (Section 5.1), we show that these are the only two operadic diagonals which induce the weak order (Section 5.2), and that they are isomorphic (Section 5.3). Using results from Sections 3 and 4, we then characterize their facets in terms of paths in $(2, n)$ -partition trees (Section 5.4), and their vertices as pattern-avoiding pairs of permutations (Section 5.5). Finally, in Section 6, we show that the geometric SU diagonal Δ^{SU} is a topological enhancement of the original Saneblidze-Umble diagonal [SU04] (Section 6.1). In order to prove this result, we define different types of shifts that can be performed on the facets of the SU diagonal, and give several new equivalent definitions of it. These descriptions are directly translated to the LA diagonal via isomorphism (Section 6.2). Moreover, we observe that the shifts define a natural lattice structure on the set of facets of operadic diagonals, that we call the *shift lattice* (Section 6.3). Finally, we present the alternative matrix (Section 6.5) and cubical (Section 6.4) descriptions of the SU diagonal from [SU04, SU22], provide proofs of their equivalence with the other descriptions, and give their LA counterparts.

4. CELLULAR DIAGONALS

4.1. Cellular diagonals for polytopes. As discussed in the introduction, cellular approximations of the thin diagonal for families of polytopes are of fundamental importance in algebraic topology and geometry. They allow one to define the cup product and thus define the ring structure on the cohomology groups of a topological space, and combinatorially on the Chow groups of a toric variety. We now proceed to define thin, cellular, and geometric diagonals.

Definition 4.1. The *thin diagonal* of a set X is the map $\delta : X \rightarrow X \times X$ defined by $\delta(x) := (x, x)$ for all $x \in X$. See Figure 13 (left).

Definition 4.2. A *cellular diagonal* of a d -dimensional polytope P is a continuous map $\Delta : P \rightarrow P \times P$ such that

- (1) its image is a union of d -dimensional faces of $P \times P$ (i.e. it is *cellular*),
- (2) it agrees with the thin diagonal of P on the vertices of P , and
- (3) it is homotopic to the thin diagonal of P , relative to the image of the vertices of P .

See Figure 13 (middle left). A cellular diagonal is said to be *face coherent* if its restriction to a face of P is itself a cellular diagonal for that face.

A powerful geometric technique to define face coherent cellular diagonals on polytopes first appeared in [FS97], was presented in [MTTV21], and was fully developed in [LA22]. We provide in Theorem 4.4 the precise (but slightly technical) definition of these diagonals, even though we will only use the characterization of the faces in their image provided in Theorem 4.6.

The key idea is that any vector \mathbf{v} in generic position with respect to P defines a cellular diagonal of P . For \mathbf{z} a point of P , we denote by $\rho_{\mathbf{z}}P := 2\mathbf{z} - P$ the reflection of P with respect to the point \mathbf{z} .

Definition 4.3. The *fundamental hyperplane arrangement* \mathcal{H}_P of a polytope $P \subset \mathbb{R}^d$ is the set of all linear hyperplanes of \mathbb{R}^d orthogonal to the edges of $P \cap \rho_{\mathbf{z}}P$ for all $\mathbf{z} \in P$. See Figure 12.

A vector is *generic with respect to P* if it does not belong to the union of the hyperplanes of the fundamental hyperplane arrangement \mathcal{H}_P . In particular, such a vector is not perpendicular to any edge of P , and we denote by $\min_{\mathbf{v}}(P)$ (resp. $\max_{\mathbf{v}}(P)$) the unique vertex of P which minimizes (resp. maximizes) the scalar product with \mathbf{v} . Note that the datum of a polytope P together with a vector \mathbf{v} generic with respect to P was called *positively oriented polytope* in [MTTV21, LA22, LAM23].

Theorem 4.4. *For any vector $\mathbf{v} \in \mathbb{R}^d$ generic with respect to P , the tight coherent section $\Delta_{(P,\mathbf{v})}$ of the projection $P \times P \rightarrow P$, $(\mathbf{x}, \mathbf{y}) \mapsto (\mathbf{x} + \mathbf{y})/2$ selected by the vector $(-\mathbf{v}, \mathbf{v})$ defines a cellular diagonal of P . More precisely, $\Delta_{(P,\mathbf{v})}$ is given by the formula*

$$\begin{aligned} \Delta_{(P,\mathbf{v})} : P &\rightarrow P \times P \\ \mathbf{z} &\mapsto (\min_{\mathbf{v}}(P \cap \rho_{\mathbf{z}}P), \max_{\mathbf{v}}(P \cap \rho_{\mathbf{z}}P)). \end{aligned}$$

Definition 4.5. A *geometric diagonal* of a polytope P is a diagonal of the form $\Delta_{(P,\mathbf{v})}$ for some vector $\mathbf{v} \in \mathbb{R}^d$ generic with respect to P .

Note that the geometric diagonal $\Delta_{(P,\mathbf{v})}$ only depends on the region of \mathcal{H}_P containing \mathbf{v} , see [LA22, Prop. 1.23].

Now the following *universal formula* [LA22, Thm. 1.26] expresses combinatorially the faces in the image of the geometric diagonal $\Delta_{(P,\mathbf{v})}$. Recall that the *normal cone* of a face F of a polytope P in \mathbb{R}^d is the cone of directions $\mathbf{c} \in \mathbb{R}^d$ such that the maximum of the scalar product $\langle \mathbf{c} | \mathbf{x} \rangle$ over P is attained for some \mathbf{x} in F .

Theorem 4.6 ([LA22, Thm. 1.26]). *Fix a vector $\mathbf{v} \in \mathbb{R}^d$ generic with respect to P . For each hyperplane H of the fundamental hyperplane arrangement \mathcal{H}_P , denote by $H^{\mathbf{v}}$ the open half space defined by H and containing \mathbf{v} . The faces of $P \times P$ in the image of the geometric diagonal $\Delta_{(P,\mathbf{v})}$ are the faces $F \times G$ where F and G are faces of P such that either the normal cone of F intersects $H^{-\mathbf{v}}$ or the normal cone of G intersects $H^{\mathbf{v}}$, for each $H \in \mathcal{H}_P$.*

The image of $\Delta_{(P,\mathbf{v})}$ is a union of pairs of faces $F \times G$ of the Cartesian product $P \times P$. By drawing the polytopes $(F + G)/2$ for all pairs of faces $(F, G) \in \text{Im } \Delta_{(P,\mathbf{v})}$, we can visualize $\Delta_{(P,\mathbf{v})}$ as a polytopal subdivision of P . See Figure 13 (middle right) and Figure 14.

It turns out that the dual of this complex is just the common refinement of two translated copies of the normal fan of P . See Figure 13 (right). Recall that the *normal fan* of P is the fan formed by the normal cones of all faces of P . We thus obtain the following statement.

Proposition 4.7 ([LA22, Coro. 1.4]). *The inclusion poset on the faces in the image of the diagonal $\Delta_{(P,\mathbf{v})}$ is isomorphic to the reverse inclusion poset on the faces of the common refinement of two copies of the normal fan of P , translated from each other by the vector \mathbf{v} .*

Finally, the following statement relates the image of the diagonal $\Delta_{(P,\mathbf{v})}$ to the intervals of the poset obtained by orienting the skeleton of P in direction \mathbf{v} .

Proposition 4.8 ([LA22, Prop. 1.17]). *For any polytope P and any generic vector \mathbf{v} , we have*

$$(3) \quad \text{Im } \Delta_{(P,\mathbf{v})} \subseteq \bigcup_{\substack{F, G \text{ faces of } P \\ \max_{\mathbf{v}}(F) \leq \min_{\mathbf{v}}(G)}} F \times G.$$

Remark 4.9. For some polytopes such as the simplices [EM54], the cubes [Ser51], the freehedra [San09], and the associahedra [MTTV21], the reverse inclusion also holds (in the case of the simplices and the cubes, the diagonals are known as the *Alexander-Whitney map* [EM54] and *Serre map* [Ser51]). According to [MTTV21], the resulting equality enhancing (3) was called *magical formula* by J.-L. Loday. This equality simplifies the computation of the f -vectors of the diagonals. For instance, the number of k -dimensional faces in the diagonal of the $(n-1)$ -dimensional simplex, cube, and associahedron are respectively given by

$$f_k(\Delta_{\text{Simplex}(n)}) = (k+1) \binom{n+1}{k+2} \quad [\text{OEI10, A127717}],$$

$$f_k(\Delta_{\text{Cube}(n)}) = \binom{n-1}{k} 2^k 3^{n-1-k} \quad [\text{OEI10, A038220}],$$

$$f_k(\Delta_{\text{Asso}(n)}) = \frac{2}{(3n+1)(3n+2)} \binom{n-1}{k} \binom{4n+1-k}{n+1} \quad [\text{BCP23}].$$

Polytopes of greater complexity such as the multiplihedra [LAM23] or the operahedra [LA22], which include the permutahedra, do not possess this exceptional property, and the f -vectors of their diagonals are harder to compute.

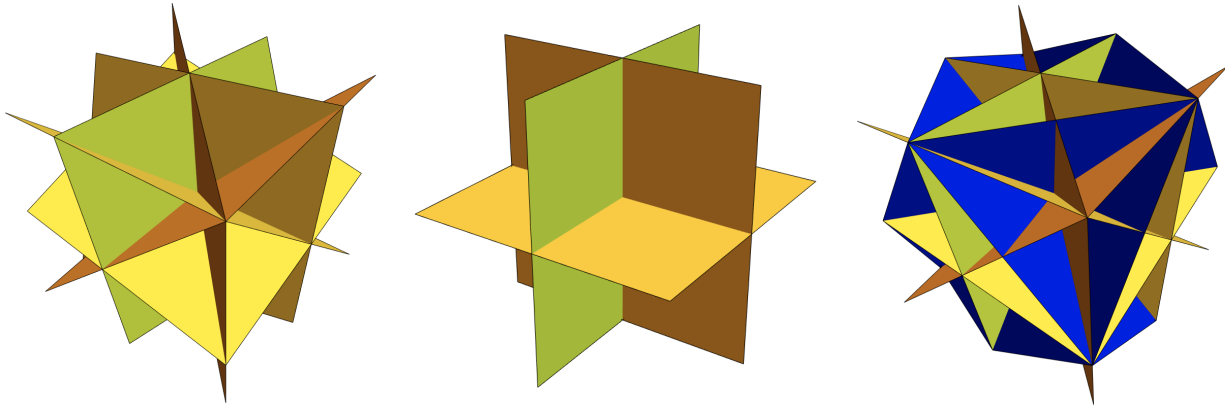


FIGURE 12. The fundamental hyperplane arrangements of the 3-dimensional simplex (left), cube (middle), and permutahedron (right). The hyperplanes perpendicular to edges of some intersection $P \cap \rho_z P$, which are *not* edges of the polytope P , are colored in blue. Left and rightmost illustrations from [LA22, Fig. 12].

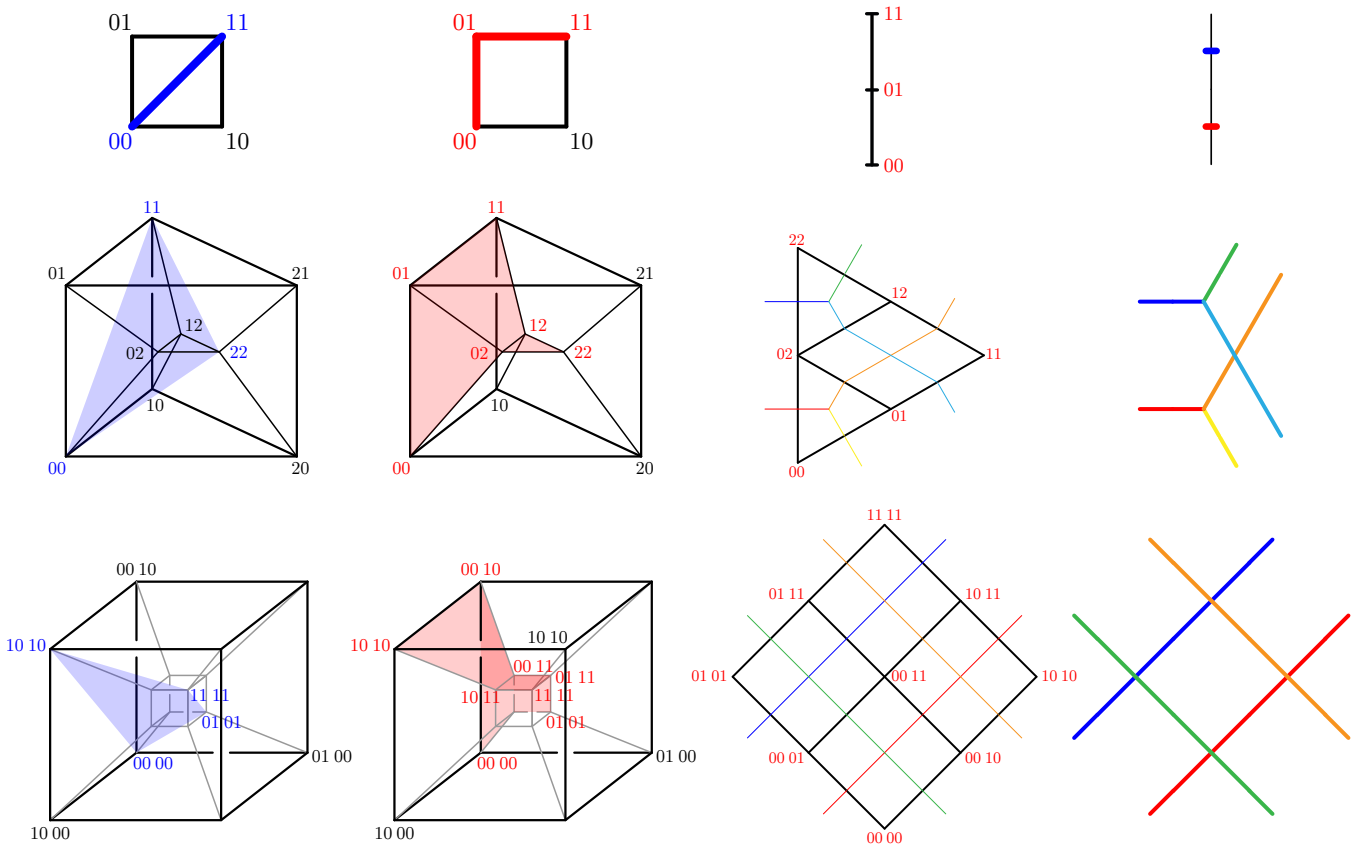


FIGURE 13. Cellular diagonals of the segment (top), the triangle (middle) and the square (bottom). For each of them, we have represented the thin diagonal of P (left, in blue), a cellular diagonal of P (middle left, in red) both in $P \times P$, the associated polytopal subdivision of P (middle right) and the common refinement of the two copies of the normal fan of P (right) both in P .

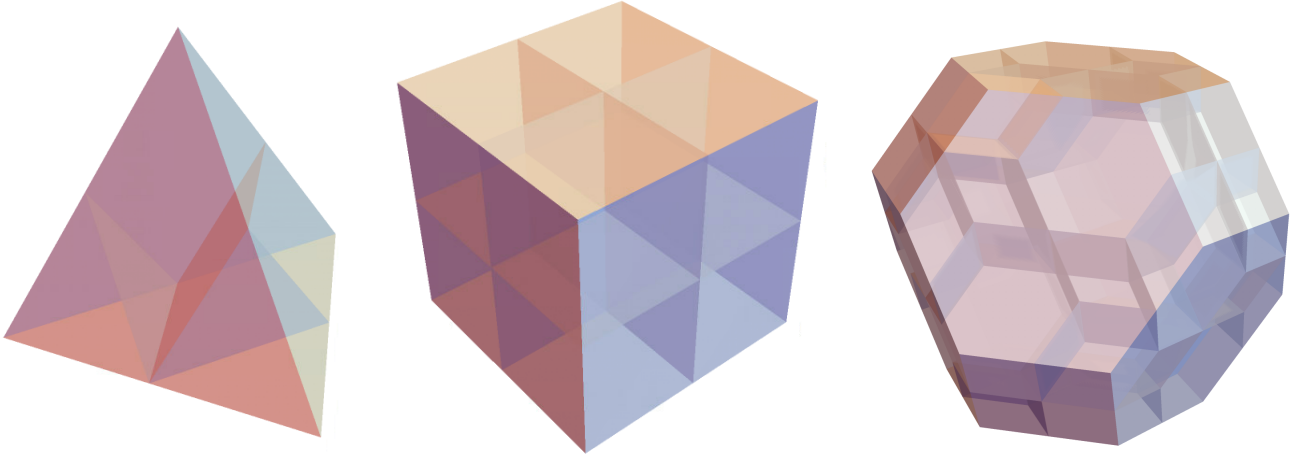


FIGURE 14. The subdivisions induced by cellular diagonals of the 3-dimensional simplex (left), cube (middle), and permutahedron (right). Right illustration from [LA22, Fig. 13].

Remark 4.10. This is in fact precisely the content of the *Fulton–Sturmfels formula* for the intersection product on toric varieties [FS97, Thm. 4.2], where the definition of cellular diagonals as tight coherent sections first appeared.

To conclude, we define the opposite of a geometric diagonal.

Definition 4.11. The *opposite* of the geometric diagonal $\Delta := \Delta_{(P, \mathbf{v})}$ for a vector $\mathbf{v} \in \mathbb{R}^d$ generic with respect to P is the geometric diagonal $\Delta^{\text{op}} := \Delta_{(P, -\mathbf{v})}$ for the vector $-\mathbf{v}$. Observe that

$$F \times G \in \text{Im } \Delta \quad \iff \quad G \times F \in \text{Im } \Delta^{\text{op}}.$$

4.2. Cellular diagonals for the permutahedra. We now specialize the statements of Section 4.1 to the standard permutahedron. We first recall its definition.

Definition 4.12. The *permutahedron* $\text{Perm}(n)$ is the polytope in \mathbb{R}^n defined equivalently as

- the convex hull of the points $\sum_{i \in [n]} i e_{\sigma(i)}$ for all permutations σ of $[n]$, see [Sch11],
- the intersection of the hyperplane $\{\mathbf{x} \in \mathbb{R}^n \mid \sum_{i \in I} x_i = \binom{n+1}{2}\}$ with the affine halfspaces $\{\mathbf{x} \in \mathbb{R}^n \mid \sum_{i \in I} x_i \geq \binom{\#I+1}{2}\}$ for all $\emptyset \neq I \subsetneq [n]$, see [Rad52].

The normal fan of the permutahedron $\text{Perm}(n)$ is the fan defined by the braid arrangement \mathcal{B}_n . In particular, the faces of $\text{Perm}(n)$ correspond to the ordered partitions of $[n]$. Moreover, when oriented in a generic direction, the skeleton of the permutahedron $\text{Perm}(n)$ is isomorphic to the Hasse diagram of the classical weak order on permutations of $[n]$. See Figure 15.

The fundamental hyperplane arrangement of the permutahedron $\text{Perm}(n)$ was described in [LA22, Sect. 3.1]. As we will use the following set throughout the paper, we embed it in a definition.

Definition 4.13. For $n \in \mathbb{N}$, we define

$$U(n) := \{\{I, J\} \mid I, J \subset [n] \text{ with } \#I = \#J \text{ and } I \cap J = \emptyset\}.$$

An *ordering* of $U(n)$ is a set containing exactly one of the two ordered pairs (I, J) or (J, I) for each $\{I, J\} \in U(n)$.

Proposition 4.14 ([LA22, Sect. 3.1]). *The fundamental hyperplane arrangement of the permutahedron $\text{Perm}(n)$ is given by the hyperplanes $\{\mathbf{x} \in \mathbb{R}^n \mid \sum_{i \in I} x_i = \sum_{j \in J} x_j\}$ for all $\{I, J\} \in U(n)$.*

For a vector \mathbf{v} generic with respect to $\text{Perm}(n)$, we denote by $O(\mathbf{v})$ the ordering of $U(n)$ such that $\sum_{i \in I} v_i > \sum_{j \in J} v_j$ for all $(I, J) \in O(\mathbf{v})$. Applying Theorem 4.6, we next describe the faces in the image of the geometric diagonal $\Delta_{(\text{Perm}(n), \mathbf{v})}$. For this, the following definition will be convenient.

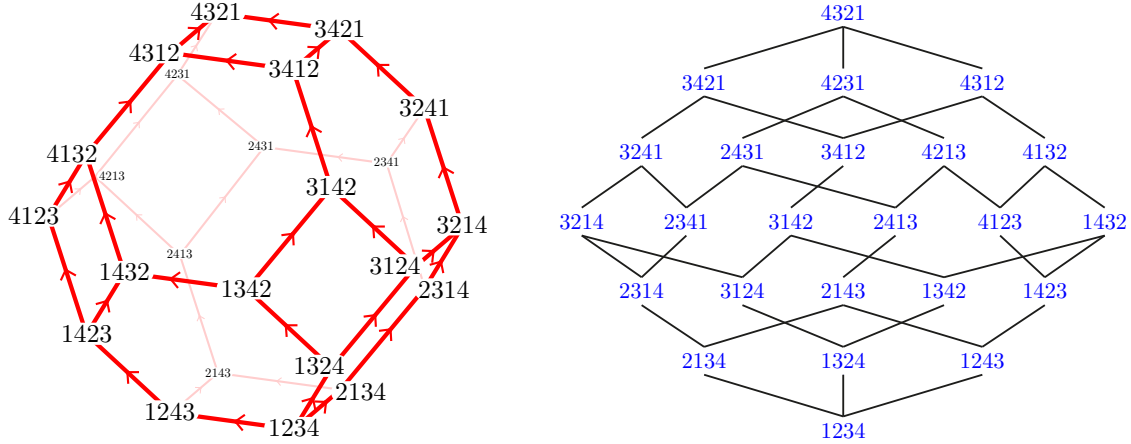


FIGURE 15. The permutahedron $\text{Perm}(4)$ (left) and the weak order on permutations of $[4]$ (right).

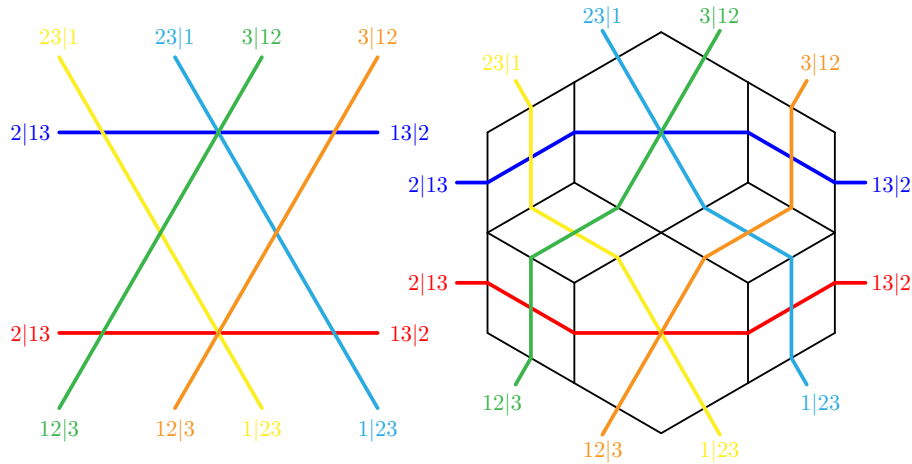


FIGURE 16. The duality between the $(2,3)$ -braid arrangement \mathcal{B}_3^2 (left) and the diagonal of the permutahedron $\text{Perm}(3)$ (right).

Definition 4.15. For $I, J \subseteq [n]$ and an ordered partition σ of $[n]$ into k blocks, we say that I *dominates* J in σ if for all $\ell \in [k]$, the first ℓ blocks of σ contain at least as many elements of I than of J .

Theorem 4.16 ([LA22, Thm. 3.16]). *A pair (σ, τ) of ordered partitions of $[n]$ corresponds to a face in the image of the geometric diagonal $\Delta_{(\text{Perm}(n), \mathbf{v})}$ if and only if, for all $(I, J) \in \mathcal{O}(\mathbf{v})$, J does not dominate I in σ or I does not dominate J in τ .*

As the normal fan of the permutahedron $\text{Perm}(n)$ is the fan defined by the braid arrangement \mathcal{B}_n , we obtain by Proposition 4.7 the following connection between the diagonal of $\text{Perm}(n)$ and the $(2, n)$ -braid arrangement \mathcal{B}_2^n studied in Part I. This connection is illustrated in Figure 16.

Proposition 4.17. *The inclusion poset on the faces in the image of the diagonal $\Delta_{(\text{Perm}(n), \mathbf{v})}$ is isomorphic to the reverse inclusion poset on the faces of the $(2, n)$ -braid arrangement \mathcal{B}_2^n .*

Remark 4.18. To be more precise, the diagonal $\Delta_{(\text{Perm}(n), \mathbf{v})}$ is dual to the \mathbf{a} -braid arrangement $\mathcal{B}_2^n(\mathbf{a})$ where the translation matrix \mathbf{a} has two rows, with first row $\mathbf{a}_{1,j} = 0$ and second

row $\mathbf{a}_{2,j} = v_j - v_{j+1}$ for all $j \in [n-1]$. Since \mathbf{v} is generic with respect to $\text{Perm}(n)$, we have $\sum_{i \in I} v_i \neq \sum_{j \in J} v_j$ for all $(I, J) \in \mathcal{U}(n)$, so that \mathbf{a} is indeed generic.

Remark 4.19. Similarly, the combinatorics of the $(\ell-1)^{\text{st}}$ iteration of a diagonal of the permutahedron $\text{Perm}(n)$ is given by the combinatorics of the (ℓ, n) -braid arrangement.

Finally, the permutahedron $\text{Perm}(n)$ is not magical in the sense of Proposition 4.8. See also Example 5.25.

Proposition 4.20 ([LA22, Sect. 3]). *For any $n > 3$ and any generic vector \mathbf{v} , the diagonal $\Delta_{(\text{Perm}(n), \mathbf{v})}$ of the permutahedron $\text{Perm}(n)$ does not satisfy the magical formula. Namely, we have the strict inclusion*

$$\text{Im } \Delta_{(\text{Perm}(n), \mathbf{v})} \subsetneq \bigcup_{\substack{F, G \text{ faces of } \text{Perm}(n) \\ \max_{\mathbf{v}}(F) \leq \min_{\mathbf{v}}(G)}} F \times G.$$

Remark 4.21. Note that opposite diagonals have opposite orderings. Namely, $\mathcal{O}(-\mathbf{v}) = \mathcal{O}(\mathbf{v})^{\text{op}}$ where $\mathcal{O}^{\text{op}} := \{(J, I) \mid (I, J) \in \mathcal{O}\}$.

4.3. Enumerative results on cellular diagonals of the permutahedra. Relying on Proposition 4.17, we now specialize the results of Part I to the case $\ell = 2$ to derive enumerative results on the diagonals of the permutahedra.

Observe that one can easily compute the full Möbius polynomials of the $(2, n)$ -braid arrangements \mathcal{B}_n^2 from Theorem 2.4:

$$\begin{aligned} \mu_{\mathcal{B}_1^2}(x, y) &= 1, \\ \mu_{\mathcal{B}_2^2}(x, y) &= xy - 2x + 2, \\ \mu_{\mathcal{B}_3^2}(x, y) &= x^2y^2 - 6x^2y + 10x^2 + 6xy - 18x + 8, \\ \mu_{\mathcal{B}_4^2}(x, y) &= x^3y^3 - 12x^3y^2 + 52x^3y - 84x^3 + 12x^2y^2 - 96x^2y + 216x^2 + 44xy - 182x + 50, \\ \mu_{\mathcal{B}_5^2}(x, y) &= x^4y^4 - 20x^4y^3 + 160x^4y^2 - 620x^4y + 1008x^4 \\ &\quad + 20x^3y^3 - 300x^3y^2 + 1640x^3y - 3360x^3 \\ &\quad + 140x^2y^2 - 1430x^2y + 4130x^2 + 410xy - 2210x + 432. \end{aligned}$$

We now focus on the number of vertices, regions, and bounded regions of the $(2, n)$ -braid arrangement \mathcal{B}_n^2 , to obtain the number of facets, vertices, and internal vertices of the diagonal of the permutahedron $\text{Perm}(n)$. The first few values are gathered in Tables 6 and 7.

Corollary 4.22. *The diagonal of the permutahedron $\text{Perm}(n)$ has*

- $2(n+1)^{n-2}$ facets,
- $n \binom{n-1}{k_1} (n-k_1)^{k_1-1} (n-k_2)^{k_2-1}$ facets corresponding to pairs (F_1, F_2) of faces of the permutahedron $\text{Perm}(n)$ with $\dim(F_1) = k_1$ and $\dim(F_2) = k_2$ (thus $k_1 + k_2 = n-1$),
- $n! [z^n] \exp\left(\sum_{m \geq 1} \frac{C_m z^m}{m}\right)$ vertices,
- $(n-1)! [z^{n-1}] \exp\left(\sum_{m \geq 1} C_m z^m\right)$ internal vertices,

where $C_m := \frac{1}{m+1} \binom{2m}{m}$ denotes the m^{th} Catalan number.

Proof. Use the duality between the $(2, n)$ -braid arrangement \mathcal{B}_n^2 and the diagonal of the permutahedron $\text{Perm}(n)$ (see Proposition 4.17 and Figure 16), and specialize Theorems 2.18, 2.19 and 2.21 to the case $\ell = 2$. \square

Remark 4.23. For completeness, we provide an alternative simpler proof of the first point of Corollary 4.22. By Proposition 2.3, we just need to count the $(2, n)$ -partition trees. Consider a $(2, n)$ -partition tree $\mathbf{F} := (F_1, F_2)$ (hence $\#F_1 + \#F_2 = n+1$). Consider the intersection tree T

n	1	2	3	4	5	6	7	8	9	...	OEIS
facets	1	2	8	50	432	4802	65536	1062882	20000000	...	[OEI10, A007334]
vertices	1	3	17	149	1809	28399	550297	12732873	343231361	...	[OEI10, A213507]
int. verts.	1	1	5	43	529	8501	169021	4010455	110676833	...	[OEI10, A251568]

TABLE 6. The numbers of facets, vertices, and internal vertices of the diagonal of the permutahedron $\text{Perm}(n)$ for $n \in [9]$.

$n = 1$		$n = 2$			$n = 3$				$n = 4$				
dim	0	dim	0	1	dim	0	1	2	dim	0	1	2	3
0	1	0	3	1	0	17	12	1	0	149	162	38	1
		1	1		1	12	6		1	162	150	24	
					2	1			2	38	24		
									3	1			

$n = 5$						$n = 6$						
dim	0	1	2	3	4	dim	0	1	2	3	4	5
0	1809	2660	1080	110	1	0	28399	52635	30820	6165	302	1
1	2660	3540	1200	80		1	52635	90870	67580	7785	240	
2	1080	1200	270			2	30820	47580	20480	2160		
3	110	80				3	6165	7785	2160			
4	1					4	302	240				
						5	1					

TABLE 7. Number of pairs of faces in the cellular image of the diagonal of the permutahedron $\text{Perm}(n)$ for $n \in [6]$.

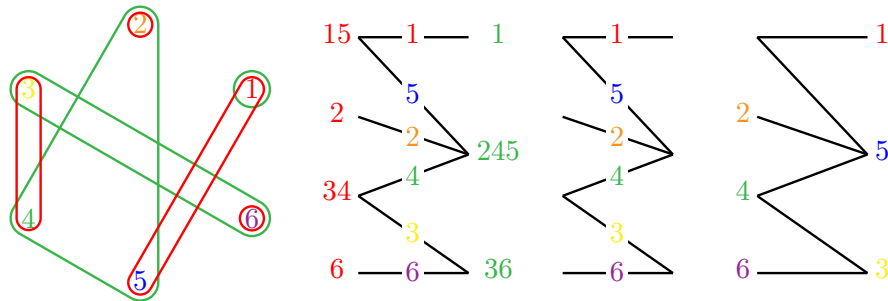


FIGURE 17. The bijection from rooted (ℓ, n) -partition trees (left) to spanning trees of K_{n+1} containing the edge $(0, 1)$ (right).

of \mathbf{F} with vertices labeled by the parts of F_1 and of F_2 and edges labeled by $[n]$, root T at the part of F_1 containing vertex 1, forget the vertex labels of T , and send each edge label of T to the next vertex away from the root, and label the root by 0. See Figure 17. The result is a spanning tree of the complete graph K_{n+1} on $\{0, \dots, n\}$ which must contain the edge $(0, 1)$ (because we have chosen the root to be the part of F_1 containing 1). Finally, by double counting the pairs (T, e) where T is a spanning tree of K_{n+1} and e is an edge of T , we see that n times the number of spanning trees of K_{n+1} equals $\binom{n+1}{2}$ times the number of spanning trees of K_{n+1} containing $(0, 1)$. Hence, by Cayley's formula for spanning trees of K_{n+1} , we obtain that the number of $(2, n)$ -partition trees is

$$\frac{2n}{n(n+1)}(n+1)^{n-1} = 2(n+1)^{n-2}.$$

5. OPERADIC DIAGONALS

This section is devoted to the combinatorics of two specific diagonals of the permutahedra, the LA and SU diagonals, which are shown to be the only operadic geometric diagonals of the permutahedra.

5.1. The LA and SU diagonals. Recall from Section 4.2 that a geometric diagonal of the permutahedron $\text{Perm}(n)$ gives a choice of ordering of the sets $U(n)$ (see Definition 4.13). As we consider in this section diagonals for all permutahedra, we now consider families of orderings.

Definition 5.1. An *ordering* of $U := \{U(n)\}_{n \geq 1}$ is a family $O := \{O(n)\}_{n \geq 1}$ where $O(n)$ is an ordering of $U(n)$ for each $n \geq 1$.

We will be focusing on the following two orderings and their corresponding diagonals.

Definition 5.2. The *LA* and *SU orderings* are defined by

- $\text{LA}(n) := \{(I, J) \mid \{I, J\} \in U(n) \text{ and } \min(I \cup J) = \min I\}$ and
- $\text{SU}(n) := \{(I, J) \mid \{I, J\} \in U(n) \text{ and } \max(I \cup J) = \max J\}$.

Definition 5.3. The *LA diagonal* Δ^{LA} (resp. *SU diagonal* Δ^{SU}) of the permutahedron $\text{Perm}(n)$ is the geometric diagonal $\Delta_{(\text{Perm}(n), \mathbf{v})}$ given by any vector $\mathbf{v} \in \mathbb{R}^n$ satisfying

$$\sum_{i \in I} v_i > \sum_{j \in J} v_j,$$

for all $(I, J) \in \text{LA}(n)$ (resp. $(I, J) \in \text{SU}(n)$).

First note that this definition makes sense, since vectors $\mathbf{v} = (v_1, \dots, v_n)$ such that $O(\mathbf{v})$ is the LA or SU order do exist: take for instance $v_i := 2^{-i+1}$ for Δ^{LA} and $v_i := 2^n - 2^{i-1}$ for Δ^{SU} . Second, note that the LA and SU diagonals coincide up to dimension 2, but differ in dimension ≥ 3 . The former is illustrated in Figure 18, with the faces labeled by ordered $(2, 3)$ -partition forests.

We will prove in Theorem 6.24 that Δ^{SU} is a topological enhancement of the Sanedblidze–Umble diagonal from [SU04]. The faces of the LA and SU diagonals are described by the following specialization of Theorem 4.16.

Theorem 5.4. *A pair (σ, τ) of ordered partitions of $[n]$ is not a face of the LA diagonal Δ^{LA} if and only if there exists $(I, J) \in \text{LA}(n)$ such that J dominates I in σ and I dominates J in τ . The same holds for the SU diagonal by replacing Δ^{LA} by Δ^{SU} and $\text{LA}(n)$ by $\text{SU}(n)$.*

5.2. The operadic property. The goal of this section is to prove that the LA and SU diagonals are the only two operadic diagonals which induce the weak order on the vertices of the permutahedra (Theorem 5.13). We start by properly defining operadic diagonals.

Let $A \sqcup B = [n]$ be a partition of $[n]$ where $A := \{a_1, \dots, a_p\}$ and $B := \{b_1, \dots, b_q\}$. Recall that the ordered partition $B|A$ corresponds to a facet of the permutahedron $\text{Perm}(n)$ defined by the inequality $\sum_{b \in B} x_b \geq \binom{\#B+1}{2}$. This facet is isomorphic to the Cartesian product

$$(\text{Perm}(p) + q\mathbf{1}_{[p]}) \times \text{Perm}(q)$$

of lower dimensional permutahedra, where the first factor is translated by $q\mathbf{1}_{[p]} := q \sum_{i \in [p]} \mathbf{e}_i$, via the permutation of coordinates

$$\Theta : \quad \mathbb{R}^p \times \mathbb{R}^q \quad \xrightarrow{\cong} \quad \mathbb{R}^n \\ (x_1, \dots, x_p) \times (x_{p+1}, \dots, x_n) \quad \longmapsto \quad (x_{\sigma^{-1}(1)}, \dots, x_{\sigma^{-1}(n)}),$$

where σ is the (p, q) -shuffle defined by $\sigma(i) := a_i$ for $i \in [p]$, and $\sigma(p+j) := b_j$ for $j \in [q]$. Note that this map is a particular instance of the eponym map introduced in Point (5) of [LA22, Prop. 2.3].

Definition 5.5. A family of geometric diagonals $\Delta := \{\Delta_n : \text{Perm}(n) \rightarrow \text{Perm}(n) \times \text{Perm}(n)\}_{n \geq 1}$ of the permutahedra is *operadic* if for every face $A_1 | \dots | A_k$ of the permutahedron $\text{Perm}(\#A_1 + \dots + \#A_k)$, the map Θ induces a topological cellular isomorphism

$$\Delta_{\#A_1} \times \dots \times \Delta_{\#A_k} \cong \Delta_{\#A_1 + \dots + \#A_k}.$$

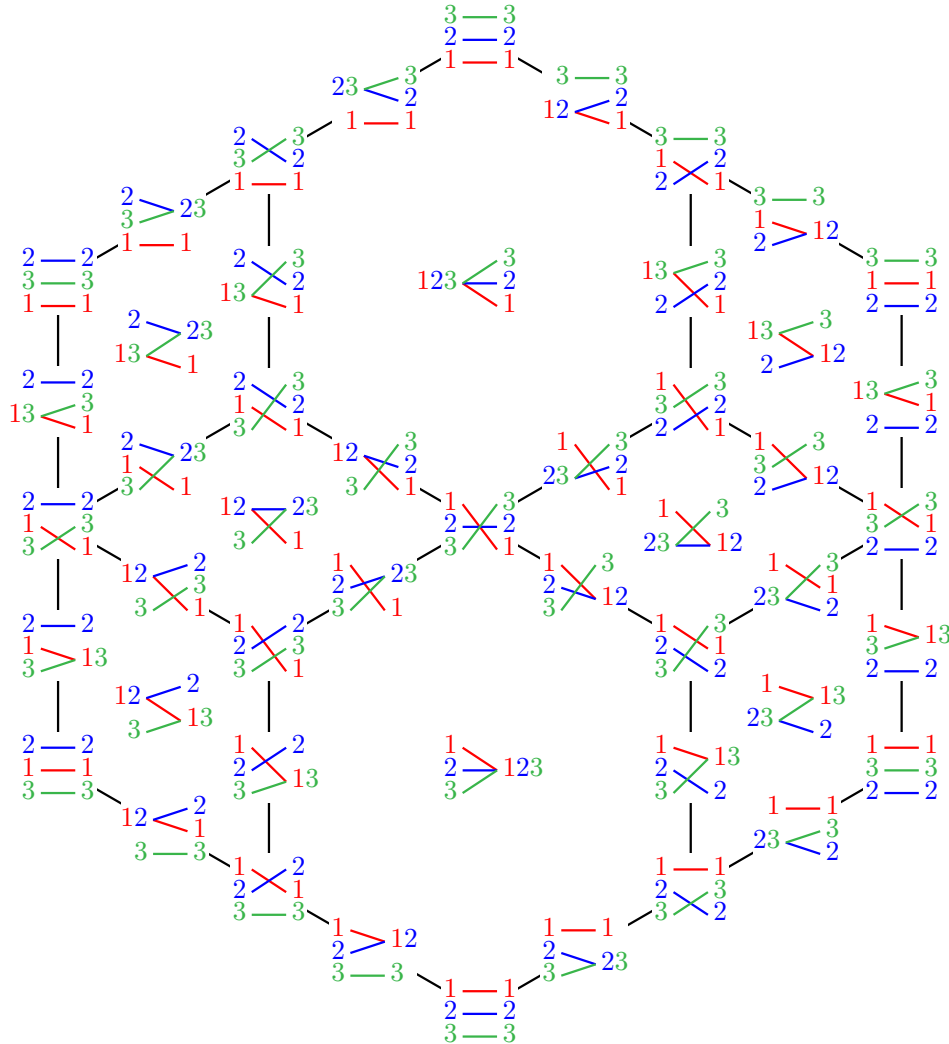


FIGURE 18. The LA (and SU) diagonal of $\text{Perm}(3)$ with faces labeled by ordered $(2, 3)$ -partition forests. (See also Figure 10 for the dual hyperplane arrangement.)

In other words, we require that the diagonal Δ commutes with the map Θ , see [LA22, Sect. 4.2]. At the algebraic level, this property is called “comultiplicativity” in [SU04]. Note that in particular, such an isomorphism respects the poset structures.

We will now translate this operadic property for geometric diagonals to the corresponding orderings \mathcal{O} of \mathcal{U} . We need the following standardization map (this map is classical for permutations or words, but we use it here for pairs of sets).

Definition 5.6. The *standardization* of a pair (I, J) of disjoint subsets of $[n]$ is the only partition $\text{std}(I, J)$ of $[\#I + \#J]$ where the relative order of the elements is the same as in (I, J) . More precisely, it is defined recursively by

- $\text{std}(\emptyset, \emptyset) := (\emptyset, \emptyset)$, and
- if $k := \#I + \#J$ and $\ell := \max(I \cup J)$ belongs to I (resp. J), then $\text{std}(I, J) = (U \cup \{k\}, V)$ (resp. $\text{std}(I, J) = (U, V \cup \{k\})$) where $(U, V) = \text{std}(I \setminus \{\ell\}, J)$ (resp. $(U, V) = \text{std}(I, J \setminus \{\ell\})$).

For example, $\text{std}(\{5, 9, 10\}, \{6, 8, 12\}) = (\{1, 4, 5\}, \{2, 3, 6\})$.

Definition 5.7. An ordering O of U is *operadic* if every $\{I, J\} \in U$ satisfies the following two conditions

- (1) $\text{std}(I, J) \in O$ implies $(I, J) \in O$,
- (2) if there exist $I' \subset I, J' \subset J$ such that $(I', J') \in O$ and $(I \setminus I', J \setminus J') \in O$, then $(I, J) \in O$.

We call *indecomposables* of O the pairs $(I, J) \in O$ for which the only subpair (I', J') satisfying Condition (2) above is the pair (I, J) itself.

Proposition 5.8. *A geometric diagonal $\Delta := (\Delta_{(\text{Perm}(n), \mathbf{v}_n)})_{n \in \mathbb{N}}$ of the permutahedra is operadic if and only if its associated ordering $O := (O(\mathbf{v}_n))_{n \in \mathbb{N}}$ is operadic.*

Proof. Every operadic diagonal satisfies [LA22, Prop. 4.14], which amounts precisely to an operadic ordering of U in the sense of Definition 5.7. \square

We now turn to the study of the LA and SU orderings.

Lemma 5.9. *The LA and SU orderings are operadic, and their indecomposables are the pairs whose standardization are $(\{1\}, \{2\})$ and*

$$\begin{aligned} \text{(LA)} \quad & (\{1, k+2, k+3, \dots, 2k-1, 2k\}, \{2, 3, \dots, k+1\}) \\ \text{(SU)} \quad & (\{k, k+1, \dots, 2k-1\}, \{1, 2, 3, \dots, k-1, 2k\}) \end{aligned}$$

for all $k \geq 1$. The opposite orderings LA^{op} and SU^{op} are also operadic, and generated by the opposite pairs.

Proof. We present the proof for the LA ordering, the proofs for the SU and opposite orders are similar. First, we verify that LA is operadic. Condition (1) follows from the fact that standardizing a pair preserves its minimal element. Condition (2) also holds, since whenever (I', J') and its complement are in LA, we have $\min(I) = \min\{\min(I'), \min(I \setminus I')\}$, and thus (I, J) itself is in LA.

Second, we compute the indecomposables. Let (I, J) be a pair with standardization (LA). If we try to decompose (I, J) as a non-trivial union, there is always one pair (I', J') in this union for which $\min(I \cup J) \notin I'$, so we have $\min(I' \cup J') = \min J'$, which implies that $(I', J') \notin \text{LA}$. Thus, the pair (I, J) is indecomposable.

It remains to show that any pair (I, J) in LA whose standardization is not of the form (LA) can be decomposed as a union of such pairs. Let us denote by (I_k, J_k) the standard form (LA) and let $(I, J) \in \text{LA}$ be such that $\text{std}(I, J) \neq (I_k, J_k)$. Then there exists $i_2 \in I \setminus \min I$ such that $i_2 < \max J$. This means that (I, J) can be decomposed as a union: if we write it as $(\{i_1, \dots, i_k\}, \{j_1, \dots, j_k\})$, where each set ordered smallest to largest, then we must have $\min(I \cup J) = i_1 < i_2 < j_k$, in which case $(\{i_2\}, \{j_k\})$ and $(\{i_1, i_3, \dots, i_k\}, \{j_1, \dots, j_{k-1}\})$ are both smaller LA pairs. Then it must be the case that $\text{std}((\{i_2\}, \{j_k\})) = (\{1\}, \{2\})$, and $\text{std}((\{i_1, i_3, \dots, i_k\}, \{j_1, \dots, j_{k-1}\}))$ is either (I_{k-1}, J_{k-1}) , or we can repeat this decomposition. \square

Remark 5.10. We note that the decomposition in Lemma 5.9 is one of potentially many different decompositions of the pair (I, J) . However, by definition of the LA order, for any decomposition $(I, J) = (\bigsqcup_{a \in A} I_a, \bigsqcup_{a \in A} J_a)$, we have $\text{std}(I_a, J_a) \in \text{LA}$ for all $a \in A$. As such, all decompositions of a pair (I, J) , order it the same way.

Proposition 5.11. *The only operadic orderings of $U = \{U(n)\}_{n \geq 1}$ are the LA, SU, LA^{op} and SU^{op} orderings.*

Proof. We build operadic orderings inductively, showing that the choices for $U(n)$, $n \leq 4$ determine higher ones. We prove the statement for the LA order, the SU and opposite orders are similar. First, we decide to order the unique pair of $U(2)$ as $(\{1\}, \{2\})$. The operadic property then determines the orders of all the pairs of $U(3)$ and $U(4)$, except the pair $\{\{1, 4\}, \{2, 3\}\}$, for which we choose the order $(\{1, 4\}, \{2, 3\})$. Now, we claim that all the higher choices are forced by the operadic property, and lead to the LA diagonal. Starting instead with the orders $(\{1\}, \{2\})$ and $(\{2, 3\}, \{1, 4\})$ would give the SU diagonal, and reversing the pairs would give the opposite orders.

Let $\ell \geq 2$ and suppose that for all $k \leq \ell$, we have given the pair

$$\{I_k, J_k\} := \{\{1, k+2, k+3, \dots, 2k-1, 2k\}, \{2, 3, \dots, k+1\}\}$$

the LA ordering (I_k, J_k) . Then from Lemma 5.9, we know that the only $\{I, J\}$ pair of order $\ell+1$ that will not decompose, and hence be specified by the already chosen conditions, is $\{I_{\ell+1}, J_{\ell+1}\}$. As such, the only way we can vary from LA is to order this element in the opposite direction $(J_{\ell+1}, I_{\ell+1})$. We now consider a particular decomposable pair $\{I'_m, J'_m\}$ where $I'_m := I_m \sqcup \{3\} \setminus \{m+2\}$ and $J'_m := J_m \sqcup \{m+2\} \setminus \{3\}$, of order $m := \ell+2$, that will lead to a contradiction (see Example 5.12). On the one side, we can decompose $\{I'_m, J'_m\} = \{I_a \cup I_b, J_a \cup J_b\}$ with $I_a := \{1, m+3, \dots, 2m\}$, $J_a := \{4, 5, \dots, m+2\}$, $I_b := \{3\}$ and $J_b := \{2\}$. By hypothesis, we have the orders (J_a, I_a) and (J_b, I_b) which imply the order (J'_m, I'_m) since our ordering is operadic. On the other side, we can decompose $\{I'_m, J'_m\} = \{I_c \cup I_d, J_c \cup J_d\}$, where $I_c := \{1, m+3, \dots, 2m-1\}$, $J_c := \{2, 5, \dots, m+1\}$, $I_d := \{3, 2m\}$ and $J_d := \{4, m+2\}$. By hypothesis, we have the orders (I_c, J_c) and (I_d, J_d) , which imply that (I'_m, J'_m) since our ordering is operadic. We arrived at a contradiction. Thus, the only possible operadic choice of ordering for $\{I_{\ell+1}, J_{\ell+1}\}$ is the LA ordering, which finishes the proof. \square

Example 5.12. To illustrate our proof of Proposition 5.11, consider an operadic ordering O for which the LA ordering holds for pairs of order 1 and 2, but is reversed for pairs of order 3, *i.e.*

$$(\{1\}, \{2\}) \in O, \quad (\{1, 4\}, \{2, 3\}) \in O, \quad \text{and} \quad (\{2, 3, 4\}, \{1, 5, 6\}) \in O.$$

Then, the pair $\{I'_4, J'_4\} = \{\{1, 3, 7, 8\}, \{2, 4, 5, 6\}\}$ admits two different orientations. In particular,

$$\begin{aligned} (\{4, 5, 6\}, \{1, 7, 8\}) \in O \text{ and } (\{2\}, \{3\}) \in O &\implies (\{2, 4, 5, 6\}, \{1, 3, 7, 8\}) \in O \text{ and} \\ (\{1, 7\}, \{2, 5\}) \in O \text{ and } (\{3, 8\}, \{4, 6\}) \in O &\implies (\{1, 3, 7, 8\}, \{2, 4, 5, 6\}) \in O. \end{aligned}$$

Combining Proposition 5.8 with Proposition 5.11, we get the main result of this section. Recall that a vector induces the weak order on the vertices of the standard permutahedron if and only if it has strictly decreasing coordinates (see Definition 4.12).

Theorem 5.13. *There are exactly four operadic geometric diagonals of the permutahedra, given by the LA and SU diagonals, and their opposites LA^{op} and SU^{op} . The LA and SU diagonals are the only operadic geometric diagonals which induce the weak order on the vertices of the permutahedron.*

Remark 5.14. This answers by the negative a conjecture regarding unicity of diagonals on the permutahedra, raised at the beginning of [SU04, Sect. 3], and could be seen as an alternative statement. See Section 6 where we prove that the geometric SU diagonal is a topological enhancement of the SU diagonal from [SU04].

5.3. Isomorphisms between operadic diagonals. Let P be a centrally symmetric polytope, and let $s : P \rightarrow P$ be its involution, given by taking a point $\mathbf{p} \in P$ to its reflection $s(\mathbf{p})$ with respect to the center of symmetry of P . Note that this map is cellular, and induces an involution on the face lattice of P . For the permutahedron $\text{Perm}(n)$, this face poset involution is given in terms of ordered partitions of $[n]$ by the map $A_1 | \dots | A_k \mapsto A_k | \dots | A_1$.

The permutahedron $\text{Perm}(n)$ possesses another interesting symmetry, namely, the cellular involution $r : \text{Perm}(n) \rightarrow \text{Perm}(n)$ which sends a point $p \in \text{Perm}(n)$ to its reflection with respect to the hyperplane of equation

$$\sum_{i=1}^{\lfloor n/2 \rfloor} x_i = \sum_{i=1}^{\lfloor n/2 \rfloor} x_{n-i+1}.$$

This involution also respects the face poset structure. In terms of ordered partitions, it replaces each block A_j in $A_1 | \dots | A_k$ by the block $r(A_j) := \{r(i) \mid i \in A_j\}$ where $r(i) := n - i + 1$.

The involution $t : P \times P \rightarrow P \times P$, sending (x, y) to (y, x) , takes a cellular diagonal to another cellular diagonal. As we have already remarked in Definition 4.11, this involution sends a geometric diagonal Δ to its opposite Δ^{op} .

Theorem 5.15. *For the permutahedron $\text{Perm}(n)$, the involutions t and $rs \times rs$ are cellular isomorphisms between the four operadic diagonals, through the following commutative diagram*

$$\begin{array}{ccc} \Delta^{\text{LA}} & \xrightarrow{t} & (\Delta^{\text{LA}})^{\text{op}} \\ rs \times rs \downarrow & & \downarrow rs \times rs \\ \Delta^{\text{SU}} & \xrightarrow{t} & (\Delta^{\text{SU}})^{\text{op}} \end{array}$$

Moreover, they induce poset isomorphisms at the level of the face lattices.

Proof. The result for the transpositions t and the commutativity of the diagram are straightforward, so we prove that $rs \times rs$ is a cellular isomorphism respecting the poset structure. First, since $r(\min(I \cup J)) = \max(r(I) \cup r(J))$, we observe that the map $(I, J) \mapsto (r(J), r(I))$ defines a bijection between $\text{LA}(n)$ and $\text{SU}(n)$. Then, if σ is an ordered partition such that I dominates J in σ (Definition 4.15), it must be the case that J dominates I in $s\sigma$, and consequently rJ dominates rI in $rs\sigma$. As such, the domination characterization of the diagonals (Theorem 5.4), tells us $(\sigma, \tau) \in \Delta^{\text{LA}}$ if and only if $(rs(\sigma), rs(\tau)) \in \Delta^{\text{SU}}$. Finally, since both t, r and s preserve the poset structures, so does their composition, which finishes the proof. \square

Remark 5.16. There is a second, distinct isomorphism given by $t(r \times r)$. This follows from the fact that $s \times s : \Delta^{\text{LA}} \rightarrow (\Delta^{\text{LA}})^{\text{op}}$ is an isomorphism (and also for $s \times s : \Delta^{\text{SU}} \rightarrow (\Delta^{\text{SU}})^{\text{op}}$), as such the composite

$$t(r \times r) : \Delta^{\text{LA}} \xrightarrow{s \times s} (\Delta^{\text{LA}})^{\text{op}} \xrightarrow{rs \times rs} (\Delta^{\text{SU}})^{\text{op}} \xrightarrow{t} \Delta^{\text{SU}}$$

is also an isomorphism. This second isomorphism has the conceptual benefit of sending left shift operators to left shift operators (and right to right), see Proposition 6.27.

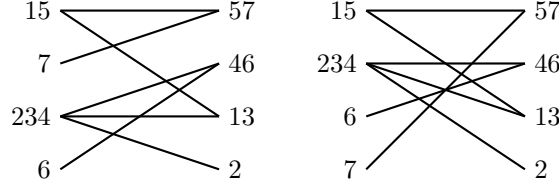
5.4. Facets of operadic diagonals. We now aim at describing the facets of the LA and SU diagonals. We have seen in Section 1.3 that facets of any diagonal of the permutahedron $\text{Perm}(n)$ are in bijection with $(2, n)$ -partition trees, that is, pairs of unordered partitions of $[n]$ whose intersection graph is a tree. These pairs of partitions were first studied and called *essential complementary partitions* in [Che69, CG71, KUC82]. Specializing Proposition 3.3, we now explain how to order these pairs of partitions to get the facets of Δ^{LA} and Δ^{SU} .

Theorem 5.17. *Let (σ, τ) be a pair of ordered partitions of $[n]$ whose underlying intersection graph is a $(2, n)$ -partition tree. The pair (σ, τ) is a facet of the LA (resp. SU) diagonal if and only if the minimum (resp. maximum) of every directed path between two consecutive blocks of σ or τ is oriented from σ to τ (resp. from τ to σ).*

Proof. We specialize Proposition 3.3 to the LA diagonal, the proof for the SU diagonal is similar. Let \mathbf{v} be a vector inducing the LA diagonal as in Definition 5.3. Without loss of generality, we place the first copy of the braid arrangement centered at 0, and the second copy centered at \mathbf{v} . From Definition 1.12 and Remark 4.18, we get that $A_{1,s,t} = 0$ and $A_{2,s,t} = v_s - v_t$ for any edges s, t . We treat the case of two consecutive blocks A and B of σ , the analysis for τ is similar. The directed path between A and B is a sequence of edges r_0, r_1, \dots, r_q . Let us denote by $I := \{r_0, r_2, \dots\}$ the set of edges directed from σ to τ , and by $J := \{r_1, r_3, \dots\}$ its complement. According to Proposition 3.3, the order between A and B is determined by the sign of $A_{1,r_0,r_q} - \sum_{p \in [q]} A_{i_p, r_{p-1}, r_p}$, where i_p is the copy of the block adjacent to both edges r_{p-1} and r_p . Thus, the order between A and B is determined by the sign of $\sum_{i \in I} v_i - \sum_{j \in J} v_j$, which according to the definition of Δ^{LA} is positive whenever $\min(I \cup J) \in I$. Thus, the pair $(\sigma, \tau) \in \Delta^{\text{LA}}$ if and only if the minimum of every directed path between two consecutive blocks of σ or τ is oriented from σ to τ . \square

In the rest of the paper, we shall represent ordered $(2, n)$ -partition trees (σ, τ) of facets by drawing σ on the left, and τ on the right, with their blocks from top to bottom. The conditions “oriented from σ to τ ” in the preceding Theorem then reads as “oriented from left to right”, an expression we shall adopt from now on.

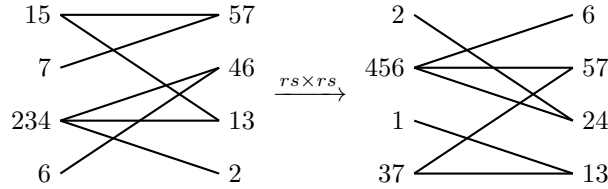
Example 5.18. Below are the two orderings of the $(2, 7)$ -partition tree $\{15, 234, 6, 7\} \times \{13, 2, 46, 57\}$ giving facets of the LA (left) and SU (right) diagonals, obtained via Theorem 5.17. Note that ordered partitions should be read from top to bottom.



In the LA facet (left), we have $7 < 234$, since in the path between the two vertices $7 \xrightarrow{7} 57 \xrightarrow{5} 15 \xrightarrow{1} 13 \xrightarrow{3} 234$, the minimum 1 is oriented from left to right. In this case, we have $(I, J) = (\{1, 7\}, \{3, 5\})$. Similarly, the path $57 \xrightarrow{5} 15 \xrightarrow{1} 13 \xrightarrow{3} 234 \xrightarrow{4} 46$ imposes that $57 < 46$, for $(I, J) = (\{1, 4\}, \{3, 5\})$.

Remark 5.19. Note that forgetting the order in a facet of Δ^{LA} , and then ordering again the $(2, n)$ -partition tree to obtain a facet of Δ^{SU} , provides a bijection between facets that was not considered in Section 5.3. However, this map is not defined on the other faces.

Example 5.20. The isomorphism $rs \times rs$ from Theorem 5.15 sends the LA facet from Example 5.18 (left) to the following SU facet (right).



Moreover, it sends the path $57 \xrightarrow{5} 15 \xrightarrow{1} 13 \xrightarrow{3} 234 \xrightarrow{4} 46$ to the path $24 \xrightarrow{4} 456 \xrightarrow{5} 57 \xrightarrow{7} 37 \xrightarrow{3} 13$, where the maximum 7 is oriented from right to left, witnessing the fact that $24 < 13$. The associated $(I, J) = (\{1, 4\}, \{3, 5\})$ becomes $(r(J), r(I)) = (\{3, 5\}, \{4, 7\})$.

5.5. Vertices of operadic diagonals. We are now interested in characterizing the vertices that occur in an operadic diagonal as pattern-avoiding pairs of partitions of $[n]$. These pairs form a strict subset of the weak order intervals. We first need the following Lemma, which follows directly from the definition of domination (Definition 4.15).

Lemma 5.21. *Let σ be an ordered partition of $[n]$ and let $I, J \subseteq [n]$ be such that I dominates J in σ . For an element i in I or J , we denote by $\sigma^{-1}(i)$ the index of the block containing it in σ . Then, for any $i \in I, j \in J$, we have $I \setminus i$ dominates $J \setminus j$ in σ if and only if*

- (1) either $\sigma^{-1}(j) < \sigma^{-1}(i)$ (meaning that j comes strictly before i in σ),
- (2) or for all k between $\sigma^{-1}(i)$ and $\sigma^{-1}(j)$, the first k blocks of σ contain strictly more elements of I than of J .

Definition 5.22. For $k \leq n$, a permutation τ of $[k]$ is a *pattern* of a permutation σ of $[n]$ if there exists a subset $I := \{i_1 < \dots < i_k\} \subset [n]$ so that the permutation τ gives the relative order of the entries of σ at positions in I , i.e. $\tau_u < \tau_v := \sigma_{i_u} < \sigma_{i_v}$. We say that σ *avoids* τ if τ is not a pattern of σ .

Example 5.23. The pairs of permutations (σ, τ) avoiding the patterns $(21, 12)$ are precisely the intervals of the weak order.

Theorem 5.24. *A pair of permutations of $[n]$ is a vertex of the LA (resp. SU) diagonal if and only if for any $k \geq 1$ and for any $(I, J) \in \text{LA}(k)$ (resp. $\text{SU}(k)$) of size $\#I = \#J = k$ it avoids the patterns*

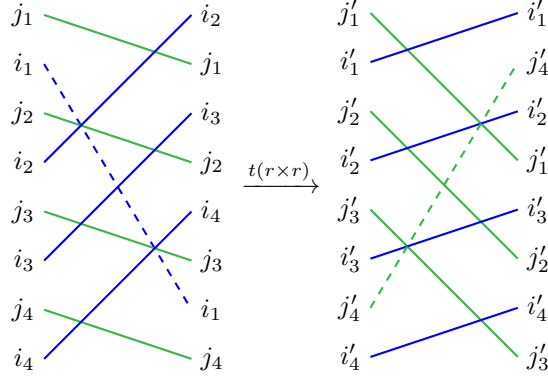
$$\begin{aligned} \text{(LA)} & \quad (j_1 i_1 j_2 i_2 \cdots j_k i_k, i_2 j_1 i_3 j_2 \cdots i_k j_{k-1} i_1 j_k), \\ \text{(SU)} & \quad \text{resp. } (j_1 i_1 j_2 i_2 \cdots j_k i_k, i_1 j_k i_2 j_1 \cdots i_{k-1} j_{k-2} i_k j_{k-1}), \end{aligned}$$

where $I = \{i_1, \dots, i_k\}$, $J = \{j_1, \dots, j_k\}$ and $i_1 = 1$ (resp. $j_k = 2k$).

Example 5.25. For each $k \geq 1$, there are $\binom{2k-1}{k-1}(k-1)!k!$ avoided standardized patterns. For $k = 1$, both diagonals avoid $(21, 12)$, so the vertices are intervals of the weak order. For $k = 2$,

- LA avoids $(3142, 2314), (4132, 2413), (2143, 3214), (4123, 3412), (2134, 4213), (3124, 4312)$.
- SU avoids $(1243, 2431), (1342, 3421), (2143, 1432), (2341, 3412), (3142, 1423), (3241, 2413)$.

As such, the vertices of LA and SU are a strict subset of all intervals of the weak order. Here is an illustration of the patterns avoided for $k = 4$. The LA pattern is drawn on the left, the SU pattern is drawn on the right, and they are in bijection under the isomorphism $t(r \times r)$ (Section 5.3), where the bijection between elements is $(i_1, i_2, i_3, i_4) \mapsto (j'_4, j'_1, j'_2, j'_3)$ and $(j_1, j_2, j_3, j_4) \mapsto (i'_1, i'_2, i'_3, i'_4)$.



The alternate isomorphism $t(s \times s)$, provides an alternate way to establish a bijection between these two patterns. The avoided patterns for higher k extend this crisscrossing shape.

Proof of Theorem 5.24. We give the proof for the LA diagonal, the one for the SU diagonal is similar, and can be obtained by applying either of the two isomorphisms of Section 5.3. According to Theorem 4.16, we have $(\sigma, \tau) \notin \Delta^{\text{LA}}$ if and only if there is an (I, J) such that J dominates I in σ and I dominates J in τ . It is clear that if a pair of permutations (σ, τ) contains a pattern of the form (LA), then the associated (I, J) satisfies the domination condition. Thus, we just need to show the reverse implication. We proceed by induction on the cardinality $\#I = \#J$. The case of cardinality 1 is clear. Now suppose that for all (I, J) of size $\#I = \#J \leq m - 1$, we have if J dominates I in σ and I dominates J in τ , then (σ, τ) contains a pattern of the form (LA).

We need to show that this is still true for the pairs (I, J) of size $\#I = \#J = m$. Firstly, we need only consider standardized I, J conditions, and pairs of permutations of $[2m]$. Indeed, if we define $(\sigma', \tau') := \text{std}(\sigma \cap (I \cup J), \tau \cap (I \cup J))$, and $(I', J') := \text{std}(I', J')$, then if (σ, τ) satisfies the (I, J) domination condition, this implies (σ', τ') satisfies (I', J') . Conversely, if (σ', τ') has a pattern, then this implies (σ, τ) has the same pattern, which yields the indicated simplification.

Let (σ, τ) be such a pair of permutations. Suppose the leftmost element i_1 of I in σ is not 1, and let us write j_1 for the leftmost element of J in τ . Consider the pair $(I', J') := (I \setminus \{i_1\}, J \setminus \{j_1\})$. Using both cases of Lemma 5.21, we have J' dominates I' in σ , and I' dominates J' in τ , and we can thus conclude by induction that (σ, τ) contains a smaller pattern.

So, we assume the leftmost element of I in σ is $i_1 = 1$, and for $n \geq 1$ we prove that,

- If $(\sigma, \tau) = (j_1 i_1 j_2 i_2 \dots j_{n-1} i_{n-1} w i_n w', i_2 j_1 i_3 j_2 \dots i_n j_{n-1} w'')$, and j_n is the leftmost element of $J \setminus \{j_1, \dots, j_{n-1}\}$ in τ , then either $w = j_n$, or it matches a smaller pattern.
- If $(\sigma, \tau) = (j_1 i_1 j_2 i_2 \dots j_{n-1} i_{n-1} w'', i_2 j_1 i_3 j_2 \dots i_{n-1} j_{n-2} w j_{n-1} w'')$, and i_n is the leftmost element of $I \setminus \{i_1, \dots, i_{n-1}\}$ in σ , then either $w = i_n$, or it matches a smaller pattern.

We prove (a), the proof of (b) proceeds similarly. Let j_n be the leftmost element of $J \setminus \{j_1, \dots, j_{n-1}\}$ in τ . If $w \neq j_n$, then either (i) w consists of multiple elements of J including j_n , or (ii) j_n comes after i_n in σ . Now consider the pair $(I', J') := (I \setminus \{i_n\}, J \setminus \{j_n\})$. As was the case for the proof that $i_1 = 1$, we have I' dominates J' in τ . To prove that J' dominates I' in σ , we split by the cases. In case (i), we may apply condition (2) of Lemma 5.21. In case (ii), either i_n comes before j_n , in which case we meet condition (1) of Lemma 5.21, or j_n comes before i_n . In this last situation, we have condition (2) of Lemma 5.21 holds as i_n is the leftmost element of $I \setminus \{i_1, \dots, i_{n-1}\}$ in σ . Thus, if $w \neq j_n$, by the inductive hypothesis, we match a smaller pattern.

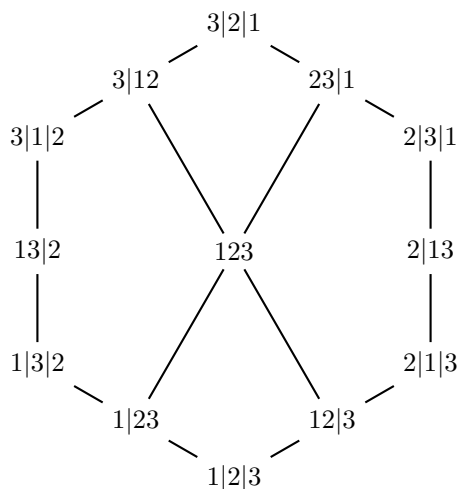


FIGURE 19. The Hasse diagram of the facial weak order for Perm(3).

Finally, using statements (a) and (b) above, we can inductively generate (σ, τ) , determining j_1 via (a), then i_2 via (b), then j_2 via (a), and so on. This inductive process fully generates σ , and places all elements of τ except i_1 , yielding $\tau = i_2 j_1 i_3 j_2 \cdots i_k j_{k-1} w j_k w''$. However, as j_k must be dominated by an element of I , this forces $w = i_1$ and $w'' = \emptyset$, completing the proof. \square

5.6. Relation to the facial weak order. There is a natural lattice structure on all ordered partitions of $[n]$ which extends the weak order on permutations of $[n]$. This lattice was introduced in [KLN⁺01], where it is called *pseudo-permutahedron* and defined on packed words rather than ordered partitions. It was later generalized to arbitrary finite Coxeter groups in [PR06, DHP18], where it is called *facial weak order* and expressed in more geometric terms. We now recall a definition of the facial weak order on ordered partitions, and use the vertex characterization of the preceding section to show all faces of the LA and SU diagonal are intervals of this order.

Definition 5.26 ([KLN⁺01, PR06, DHP18]). The *facial weak order* on ordered partitions is the transitive closure of the relations

- (4) $\sigma_1 | \dots | \sigma_k < \sigma_1 | \cdots | \sigma_i \sqcup \sigma_{i+1} | \cdots | \sigma_k$ for any $\sigma_1 | \dots | \sigma_k$ with $\max \sigma_i < \min \sigma_{i+1}$,
- (5) $\sigma_1 | \cdots | \sigma_i \sqcup \sigma_{i+1} | \cdots | \sigma_k < \sigma_1 | \dots | \sigma_k$ for any $\sigma_1 | \dots | \sigma_k$ with $\min \sigma_i > \max \sigma_{i+1}$.

The facial weak order recovers the weak order on permutations as illustrated in Figure 19.

Proposition 5.27. *If $(\sigma, \tau) \in \Delta^{\text{LA}}$, or $(\sigma, \tau) \in \Delta^{\text{SU}}$, then $\sigma \leq \tau$ under the facial weak order.*

Proof. By Proposition 4.8, the faces (σ, τ) satisfy $\max_{\mathbf{v}} \sigma \leq \min_{\mathbf{v}} \tau$ under the weak order. Thus, if we can show that $\sigma \leq \max_{\mathbf{v}} \sigma$ and $\min_{\mathbf{v}} \tau \leq \tau$ under the facial weak order, then the result immediately follows. If σ is a face of the permutahedra, then under both the LA, and SU orientation vectors, the vertex $\max_{\mathbf{v}} \sigma$ is given by writing out each block of σ in decreasing order, and the vertex $\min_{\mathbf{v}} \sigma$ is given by writing out each block of σ in increasing order. Then under the facial weak order $\sigma \leq \max_{\mathbf{v}} \sigma$, as repeated applications of Equation (5) shows that a block of elements is smaller than those same elements arranged in decreasing order. Similarly $\min_{\mathbf{v}} \sigma \leq \sigma$, as repeated applications of Equation (4) shows that a sequence of increasing elements is smaller than those same elements in a block. \square

Example 5.28. The facet $13|24|57|6 \times 3|17|456|2 \in \Delta^{\text{SU}}$, satisfies the inequality through the vertices

$$13|24|57|6 < 3|1|4|2|7|5|6 < 3|1|7|4|5|6|2 < 3|17|456|2.$$

6. SHIFT LATTICES

In this section, we prove that the geometric SU diagonal Δ^{SU} agrees at the cellular level with the original Sanedblidze-Umble diagonal defined in [SU04]. This involves some shift operations on facets of the diagonal, which are interesting on their own right, and lead to lattice and cubic structures. The proof is technical and proceeds in several steps: we introduce two additional combinatorial descriptions of the diagonal, that we call the 1-shift and m -shift SU diagonals, and show the sequence of equivalences

$$\text{original } \Delta^{\text{SU}} \xleftarrow{6.15} \text{1-shift } \Delta^{\text{SU}} \xleftarrow{6.14} \text{m-shift } \Delta^{\text{SU}} \xrightarrow{6.23} \text{geometric } \Delta^{\text{SU}}.$$

Throughout this section, we borrow notation from [SU22].

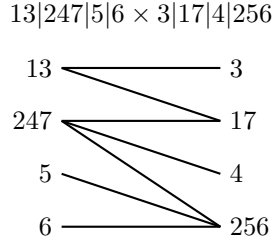
6.1. Topological enhancement of the original SU diagonal. We proceed to introduce different versions of the SU diagonal, and to prove that all these notions coincide.

6.1.1. *Strong complementary pairs.* We start by the following definition.

Definition 6.1. A *strong complementary pair*, or **SCP** for short, is a pair (σ, τ) of ordered partitions of $[n]$ where σ is obtained from a permutation of $[n]$ by merging the adjacent elements which are decreasing, and τ is obtained from the same permutation by merging the adjacent elements which are increasing.

We denote by $\text{SCP}(n)$ the set of SCPs of $[n]$, which is in bijection with the set of permutations of $[n]$. As is clear from the definition, the intersection graph of a SCP is a $(2, n)$ -partition tree.

Example 6.2. The SCP associated to the permutation $3|1|7|4|2|5|6$ is



Observe that the permutation can be read off the intersection graph of the SCP by a vertical down slice through the edges.

Notation 6.3. For a $(2, n)$ -partition tree (σ, τ) , we denote by $\sigma_{i,j}$ (resp. $\tau_{i,j}$) the unique oriented path between blocks σ_i and σ_j (resp. τ_i and τ_j). Note that we make a slight abuse in notation, as the path $\sigma_{i,j}$ also depends on τ .

We can immediately characterize the paths between adjacent blocks in SCPs.

Proposition 6.4. For any SCP (σ, τ) , we have

- (1) $\sigma_{i,i+1} = (\min \sigma_i, \max \sigma_{i+1})$ and $\min \sigma_i < \max \sigma_{i+1}$, and
- (2) $\tau_{i,i+1} = (\max \tau_i, \min \tau_{i+1})$ and $\min \tau_{i+1} < \max \tau_i$.

As a consequence, all SCPs are in both Δ^{LA} and Δ^{SU} , and constitute precisely the set of facets (σ, τ) of these diagonals such that $\max_{\mathbf{v}}(\sigma) = \min_{\mathbf{v}}(\tau)$.

Proof. First, the path description of (σ, τ) is a straightforward observation. Second, since the minima of these paths are traversed from left to right, and the maxima from right to left, Theorem 5.17 implies that SCPs are in both geometric operadic diagonals Δ^{LA} and Δ^{SU} . Third, the fact that these constitute the facets $(\sigma, \tau) \in \Delta^{\text{LA}}$ or Δ^{SU} satisfying $\max_{\mathbf{v}}(\sigma) = \min_{\mathbf{v}}(\tau)$ can be seen as follows. The maximal (resp. minimal) vertex of a face σ of the permutahedron with respect to the weak order, is obtained by ordering the elements of each block of σ in decreasing (resp. increasing) order. Thus, it is clear that the original permutation giving rise to a SCP (σ, τ) is the permutation $\max_{\mathbf{v}}(\sigma) = \min_{\mathbf{v}}(\tau)$, for any vector \mathbf{v} inducing the weak order. Since both diagonals agree with this order on the vertices, we have that SCPs are indeed facets of Δ^{LA} and

Δ^{SU} with the desired property. The fact that these are *all* the facets with this property follows from the bijection between $\text{SCP}(n)$ and the permutations of $[n]$. \square

6.1.2. *Shifts and the SU diagonals.* We recall the definition of the original SU diagonal of [SU04], based on the exposition given in [SU22]. We then introduce two variants of this definition, the 1-shift and m -shift SU diagonals, which will be shown to be equivalent to the original one.

Definition 6.5. Let $\sigma = \sigma_1 | \cdots | \sigma_k$ be an ordered partition, and let $M \subsetneq \sigma_i$ be a non-empty subset of the block σ_i . For $m \geq 1$, the *right m -shift* R_M , moves the subset M , m blocks to the right, *i.e.*

$$R_M(\sigma) := \sigma_1 | \cdots | \sigma_i \setminus M | \cdots | \sigma_{i+m} \cup M | \cdots | \sigma_k$$

while the *left m -shift* L_M , moves the subset M , m blocks to the left, *i.e.*

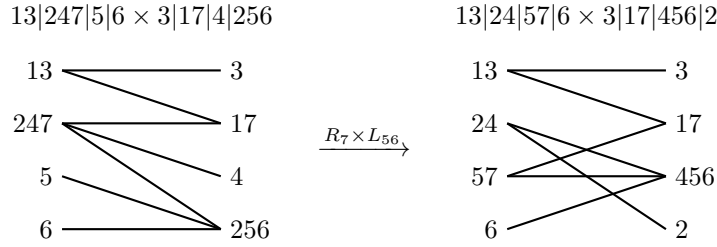
$$L_M(\sigma) := \sigma_1 | \cdots | \sigma_{i-m} \cup M | \cdots | \sigma_i \setminus M | \cdots | \sigma_k.$$

Definition 6.6. Let σ denote either one of the two ordered partitions of $[n]$ in an ordered $(2, n)$ -partition tree, and let $M \subsetneq \sigma_i$. The right m -shift R_M (resp. the left m -shift L_M) is

- (1) *block-admissible* if $\min \sigma_i \notin M$ and $\min M > \max \sigma_{i+m}$ (resp. $\min M > \max \sigma_{i-m}$),
- (2) *path-admissible* if $\min M > \max \sigma_{i,i+m}$ (resp. $\min M > \max \sigma_{i,i-m}$).

Remark 6.7. Observe that for a given subset M , an inverse to the right m -shift R_M (resp. left m -shift L_M) is given by the left m -shift L_M (resp. right m -shift R_M). Moreover, one m -shift is path-admissible if and only if its inverse is.

Example 6.8. Performing the 1-shifts R_7 and L_{56} (they are both block and path admissible) of the SCP (σ, τ) of Example 6.2, one obtains the pair $R_7(\sigma) \times L_{56}(\tau)$, as illustrated below.



We shall concentrate on three families of shifts: block-admissible 1-shifts of subsets of various sizes, path-admissible 1-shifts of singletons, and path-admissible m -shifts of singletons, for various $m \geq 1$, and show that specific sequences generate the same diagonal.

Definition 6.9. Let σ denote either one of the two ordered partitions of $[n]$ in an ordered $(2, n)$ -partition tree, and let $\mathbf{M} = (M_1, \dots, M_p)$ with $M_1 \subsetneq \sigma_{i_1}, \dots, M_p \subsetneq \sigma_{i_p}$ for some $p \geq 1$. Then the sequence of right shifts $R_{\mathbf{M}}(\sigma) := R_{M_p} \dots R_{M_1}(\sigma)$ is

- (1) *block-admissible* if we have $1 \leq i_1 < i_2 < \cdots < i_p \leq k - 1$, and each R_{M_j} is a block-admissible 1-shift,
- (2) *path-admissible* if each R_{M_j} is a path-admissible m_j -shift, for some $m_j \geq 1$.

Admissible sequences of left shifts are defined similarly and are denoted by $L_{\mathbf{M}}(\tau)$.

By convention, we declare the empty sequence of shift operators to be admissible, and to act by the identity, *i.e.* we have $R_{\emptyset}(\sigma) := \sigma$ and $L_{\emptyset}(\tau) := \tau$.

Definition 6.10. The facets of the *original SU diagonal*, the *1-shift SU diagonal* and the *m -shift SU diagonal* are defined by the formula

$$\Delta^{\text{SU}}([n]) = \bigcup_{(\sigma, \tau)} \bigcup_{\mathbf{M}, \mathbf{N}} R_{\mathbf{M}}(\sigma) \times L_{\mathbf{N}}(\tau)$$

where the unions are taken over all SCPs (σ, τ) of $[n]$, and respectively over all block-admissible sequences of subset 1-shifts \mathbf{M}, \mathbf{N} , over all path-admissible sequences of singleton 1-shifts, and over all path-admissible sequences of singleton m_j -shifts, for various $m_j \geq 1$.

Remark 6.11. Observe that the left (resp. right) shifts acts on the right (resp. left) ordered partition. In the analogous description for the LA diagonal Δ^{LA} obtained at in Section 6.2, left and right shifts act on the left and right ordered partitions, respectively.

6.1.3. *First isomorphism between SU diagonals.* We start by analyzing the original SU diagonal.

Proposition 6.12. *Block-admissible sequences of subset 1-shifts, defining the original SU diagonal, conserve*

- (1) *the maximal element of any path between two blocks of the same ordered partition,*
- (2) *the direction in which this element is traversed.*

In particular, for a pair of ordered partitions $(R_{\mathbf{M}}(\sigma), L_{\mathbf{N}}(\tau))$ obtained via a block-admissible sequence of 1-shifts from a SCP (σ, τ) , we have

$$(P) \quad \max R_{\mathbf{M}}(\sigma)_{i,j} = \max \sigma_{i,j} \quad \text{and} \quad \max L_{\mathbf{N}}(\tau)_{i,j} = \max \tau_{i,j}$$

and consequently

$$(B) \quad \max R_{\mathbf{M}}(\sigma)_{i,i+1} = \max \sigma_{i+1} \quad \text{and} \quad \max L_{\mathbf{N}}(\tau)_{i,i+1} = \max \tau_i.$$

Note that in Equation (P), the maxima $\max \sigma_{i,j}$ and $\max \tau_{i,j}$ are maxima of *paths*, while in Equation (B) the maxima $\max \sigma_{i+1}$ and $\max \tau_i$ are maxima of *blocks*.

Proof. We consider the right shift operator; the left shift operator proceeds similarly. Let us start with Point (1). As SCPs trivially meet the above conditions, we will prove the result inductively by assuming that the result holds for $(R_{\mathbf{M}}(\sigma), L_{\mathbf{N}}(\tau))$, and then showing that applying a block-admissible operator R_{M_k} , for $M_k \subsetneq \sigma_k$, conserves the maximal elements of paths. By the inductive hypothesis, we know that $\max R_{\mathbf{M}}(\sigma)_{k,k+1} = \max \sigma_{k+1}$. As R_{M_k} is an admissible operator, we know two things: firstly that $\min M_k > \max R_{\mathbf{M}}(\sigma)_{k+1}$, and secondly that $\max \sigma_{k+1} = \max R_{\mathbf{M}}(\sigma)_{k+1}$, as k is greater than the maximal index used by \mathbf{M} . So combining these, we know that

$$(W) \quad \min M_k > \max R_{\mathbf{M}}(\sigma)_{k+1} = \max \sigma_{k+1} = \max R_{\mathbf{M}}(\sigma)_{k,k+1}.$$

A key consequence of this inequality is that the intersection graph of $(R_{M_k} R_{\mathbf{M}}(\sigma), L_{\mathbf{N}}(\tau))$ is a bipartite tree conditional on $(R_{\mathbf{M}}(\sigma), L_{\mathbf{N}}(\tau))$ being a bipartite tree: the shift will not disconnect the graph as none of the shifted elements are in the path $R_{\mathbf{M}}(\sigma)_{k,k+1}$. So, it is legitimate to speak of unique paths between blocks.

We now explicitly explore how the shift operator R_{M_k} alters paths. Throughout the rest of this proof, we use the following shorthand: we denote by $\delta_{k,k+1} := R_{\mathbf{M}}(\sigma)_{k,k+1}$ the path between the k^{th} and $(k+1)^{\text{st}}$ blocks in $(R_{\mathbf{M}}(\sigma), L_{\mathbf{N}}(\tau))$, and by $\delta_{k+1,k}$ the same path reversed. Let γ be any path between two blocks of $(R_{\mathbf{M}}(\sigma), L_{\mathbf{N}}(\tau))$, and let γ' be the path between the same blocks, by indices, in $(R_{M_k} R_{\mathbf{M}}(\sigma), L_{\mathbf{N}}(\tau))$. There are four cases to consider.

- i) the path γ does not contain an element of M_k . In this case, it is unaffected by the shift, so $\gamma' = \gamma$. We note that in light of Equation (W), the path $\delta_{k,k+1}$ meets this case.
- ii) the path γ contains one element $m \in M_k$, *i.e.* it is of the form $\gamma = \alpha m \beta$, with α or β possibly empty. We assume that m is incoming to $R_{\mathbf{M}}(\sigma)_k$, the case when it is outgoing is similar. We must have $\alpha \cap \delta_{k,k+1} = \emptyset$, since otherwise there would be an oriented loop from $R_{\mathbf{M}}(\sigma)_k$ to itself. For the same reason, $\beta \cap \delta_{k,k+1}$ must be connected and starting at $R_{\mathbf{M}}(\sigma)_k$. Then there are two cases to consider:
 - (a) the path β does not use any steps of $\delta_{k,k+1}$, in which case $\gamma' = \alpha m \delta_{k+1,k} \beta$. This is a path in the tree of $(R_{M_k} R_{\mathbf{M}}(\sigma), L_{\mathbf{N}}(\tau))$ with no repeated steps, as such it must be the unique minimal path.
 - (b) the path β uses steps of $\delta_{k,k+1}$, in which case $\gamma' = \alpha m (\delta_{k+1,k} \setminus \beta) (\beta \setminus \delta_{k+1,k})$. This follows, as we know that β must follow the path $\delta_{k,k+1}$ for some time before diverging (β could also be a subset of $\delta_{k,k+1}$, in which case it will never diverge). As such, the path $(\delta_{k+1,k} \setminus \beta)$ reaches the point of divergence from $R_{\mathbf{M}}(\sigma)_{k+1}$ instead of $R_{\mathbf{M}}(\sigma)_k$, and the path $(\beta \setminus \delta_{k+1,k})$ completes the rest of the route unchanged.

- iii) the path γ contains two elements of M_k . In this case we still have $\gamma' = \gamma$ (in path elements) but γ' will step through the $(k+1)^{\text{st}}$ block instead of γ stepping through the k^{th} block.
- iv) the path γ contains more than two elements of M_k . This is impossible, as γ would not be a minimal path on a tree.

Observe that all (non-trivial or non-contradictory) paths γ' contain $m \geq \min M_k$ and either some addition or deletion by $\delta_{k,k+1}$. It thus follows from Equation (W) that $\max \gamma' = \max \gamma$, since in each case, the maximal element will either be m , or in α , or in β . This finishes the proof of Point (1).

For Point (2), we need to see that the maximal element $\max \gamma = \max \gamma'$ is traversed in the same direction. It is immediate for cases (i), (ii.a) and (iii); the condition is empty in the case (iv). For the case (ii.b) it follows from the observation that the number of steps of $\beta \cap \delta_{k,k+1}$ and $\delta_{k,k+1} \setminus \beta$ have the same parity: since $\delta_{k,k+1}$ has an even number of steps, either they both have an even number of steps, or an odd number, which completes the proof. \square

Corollary 6.13. *Path-admissible sequences of singleton 1-shifts, defining the 1-shift SU diagonal, conserve*

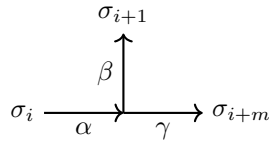
- (1) the maximal element of any path between two blocks of the same ordered partition,
- (2) the direction in which this element is traversed.

Proof. By the definition of path-admissible 1-shifts (Definition 6.9), the outer inequality of Equation (W) holds by assumption. As such, can run the proof of Proposition 6.12 *mutatis mutandis*. \square

We are now in position to show that the 1-shift and m -shift descriptions are equivalent.

Proposition 6.14. *The 1-shift and m -shift SU diagonals coincide.*

Proof. It is clear that any path-admissible sequence of 1-shifts is a path-admissible sequence of m -shifts, and thus that the facets of the 1-shift SU diagonal are facets of the m -shift SU diagonal. For the reverse inclusion, we need to show that any m -shift can be re-expressed as a path-admissible sequence of 1-shifts. We proceed by induction, and consider only the case of right shifts, the case of left shifts is similar. For right 1-shifts, there is nothing to prove. Let (σ, τ) be a pair of ordered partitions which has been generated only by k -shifts, for $k < m$. We wish to show that any path-admissible right m -shift R_ρ^m on σ can be decomposed as a path-admissible 1-shift R_ρ^1 followed by a path-admissible $(m-1)$ -shift R_ρ^{m-1} , which yields the result by induction. As R_ρ^m is path-admissible, we know that $\rho > \max \sigma_{i,i+m}$, and we want to show that $\rho > \max \sigma_{i,i+m} \geq \max \sigma_{i,i+1}, \max R_\rho^1(\sigma)_{i+1,i+m}$.



We define the oriented paths $\alpha := \sigma_{i,i+1} \setminus \sigma_{i+1,i+m}$, $\beta := \sigma_{i,i+1} \setminus \sigma_{i,i+m}$ and $\gamma := \sigma_{i,i+m} \setminus \sigma_{i,i+1}$, as illustrated above. Suppose that β is not empty, and moreover that $\max \sigma_{i+1,i+m} > \max \sigma_{i,i+m}$ or $\max \sigma_{i,i+1} > \max \sigma_{i,i+m}$. Then we must have that $\max \beta > \max \alpha, \max \gamma$. However, $\max \beta$ cannot be the maximum of both $\sigma_{i,i+1}$ and $\sigma_{i+1,i+m}$. Indeed, in this case, it would be traversed in two opposite directions, which is impossible since by the induction hypothesis (σ, τ) can be generated by 1-shifts, and by Corollary 6.13 these conserve the maximal elements of paths and their direction. We thus have $\max \sigma_{i,i+m} \geq \max \sigma_{i,i+1}, \max \sigma_{i+1,i+m}$, and applying Corollary 6.13 again yields $\max \sigma_{i,i+m} \geq \max R_\rho^1(\sigma)_{i+1,i+m}$ as required. \square

We stress that Equation (W) holds for m -shifts without us needing to perform shifts in increasing order, or requiring $\min M_k > \max R_M(\sigma)_{k+1}$. We are now ready to prove that the m -shift description is equivalent to the original one.

Theorem 6.15. *The original and m -shift SU diagonals coincide.*

Proof. Since m -shift and 1-shift diagonals are equivalent (Proposition 6.14), it suffices to show that the 1-shift and original SU diagonals coincide. We analyze the right shift operator, the case of the left shift is similar. First, we observe that any block-admissible right shift $R_M(\sigma)$, for $M \subsetneq \sigma_k$, can be decomposed into a series of singleton right 1-shifts; since $\min M > \max \sigma_{k,k+1}$ by the proof of Proposition 6.12, we can shift the elements of M to the right, one after the other (in any order!). This shows that any facet of the original SU diagonal is also a facet in the 1-shift SU diagonal.

For the reverse inclusion, we proceed by induction. We are required to show that if we apply a right 1-shift to $(R_{\mathbf{M}}(\sigma), L_{\mathbf{N}}(\tau))$, say $(R_{\rho}R_{\mathbf{M}}(\sigma), L_{\mathbf{N}}(\tau))$, then this can be re-expressed as a well-defined subset shift operation $(R_{M'}(\sigma), L_{\mathbf{N}}(\tau))$. Suppose that prior to the 1-shift, the element ρ lives in block ℓ , then we must have

$$1 \leq i_1 < \cdots < i_j \leq \ell < i_{j+1} < \cdots < i_p \leq k-1$$

for some j . If $i_j < \ell$, then we have $R_{\rho}R_{\mathbf{M}}(\sigma) = R_{M_p} \cdots R_{\{\rho\}}R_{M_j} \cdots R_{M_1}(\sigma)$, and we are done. Otherwise, if $i_j = \ell$, we set $M'_j := M_j \cup \{\rho\}$. It is clear that $R_{\rho}R_{\mathbf{M}}(\sigma) = R_{M_p} \cdots R_{M'_j} \cdots R_{M_1}(\sigma)$, however, we need to check that $R_{M'_j}$ is block-admissible, *i.e.* that $\min M'_j > \max(R_{M_{j-1}} \cdots R_{M_1}(\sigma))_{i_j+1}$. If we have $\rho > \min M_j$, then we are done since in this case $\min M'_j = \min M_j$ and R_{M_j} is block-admissible. Otherwise, we have $\rho = \min M'_j$. Since by definition block-admissible shift operators do not move the minimal element of a block, we have $\rho > \min R_{\mathbf{M}}(\sigma)_{i_j} = \min(R_{M_{j-1}} \cdots R_{M_1}(\sigma))_{i_j}$. Then, by induction, Proposition 6.12 shows that $\rho > \max \sigma_{i_j+1} = \max(R_{M_{j-1}} \cdots R_{M_1}(\sigma))_{i_j+1}$, where the equality follows as $i_1 < \cdots < i_j$. This proves that $R_{M'_j}$ is block-admissible, completing the inductive proof. \square

6.1.4. *Inversions.* Our next goal is to prove the equivalence between the m -shift and geometric SU diagonals (Theorem 6.23). As a tool for this proof, we now study *inversions*, or crossings in the partition trees of the geometric SU diagonal.

Definition 6.16. Let σ be an ordered partition.

- The *inversions* of an ordered partition are $I(\sigma) := \{(i, j) : i < j \wedge \sigma^{-1}(j) < \sigma^{-1}(i)\}$.
- The *anti-inversions* of an ordered partition are $J(\sigma) := \{(i, j) : i < j \wedge \sigma^{-1}(i) < \sigma^{-1}(j)\}$.

We then define the *inversions of an ordered partition pair* $I((\sigma, \tau)) := I(\tau) \cap J(\sigma)$.

In words, the inversions of an ordered partition pair are those $i < j$ pairs in which j comes in an earlier block than i in τ , and i comes in an earlier block than j in σ .

Proposition 6.17. *The set of inversions of a facet of the geometric SU diagonal is in bijection with its set of edge crossings. Moreover, under this bijection, strong complementary pairs correspond to facets with no crossings.*

Proof. For the first part of the statement, we note that crossings are clearly produced by both $I(\tau) \cap J(\sigma)$ and $I(\sigma) \cap J(\tau)$ (*i.e.* in the second case j appears before i in σ and i before j in τ). However, the later cannot occur in a facet of the geometric Δ^{SU} ; this follows immediately from the (I, J) -conditions for $\#I = \#J = 1$. The second part of the statement follows from the fact that facets of the diagonal Δ^{SU} with no crossings are in bijection with permutations. By definition (Definition 6.1), from a partition one obtains a SCP, which is in the geometric Δ^{SU} (Proposition 6.4). In the other way around, given a SCP, one can read-off the partition in the associated tree, which has no crossings, by a vertical down-slice of edges (Example 6.2). \square

See Figure 20 for an example of this bijection.

Definition 6.18. We say that an edge crossing is an *adjacent crossing* if the two crossing elements are in adjacent blocks of the partition tree (*i.e.* they are in blocks of the form $\sigma_i|\sigma_{i+1}$ or $\tau_i|\tau_{i+1}$).

Lemma 6.19. *A facet (σ, τ) of the geometric SU diagonal has a crossing if and only if it has an adjacent crossing.*

Proof. An adjacent crossing is clearly a crossing. In the other direction, suppose there is a crossing between an element of σ_i and an element of σ_j . If σ_i and σ_j are not adjacent, then the “triangle” produced by the crossing elements encloses another σ_k such that $i < k < j$, and this produces other crossings. We may repeat this process until an adjacent crossing is found. \square

6.1.5. *Second isomorphism between SU diagonals.* We now aim at showing that the m -shift and the geometric SU diagonal coincide (Theorem 5.13). Recall from Remark 6.7 that left and right path-admissible m -shifts are inverses to one another.

Proposition 6.20. *Let (σ, τ) be a facet of the geometric SU diagonal Δ^{SU} . Then, any pair of ordered partitions obtained by applying a path-admissible m -shift to (σ, τ) is also in the geometric SU diagonal.*

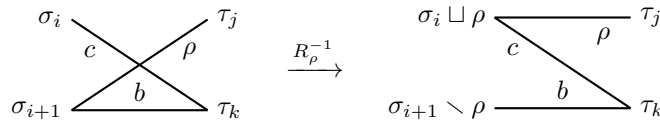
Proof. We consider a right path-admissible shift R_ρ , the left shift and dual result proceeds similarly. Combining Corollary 6.13 and Proposition 6.14, we have that the maxima of paths between consecutive vertices in $(R_\rho(\sigma), \tau)$ are the same as the ones in (σ, τ) , and are moreover traversed in the same direction. Thus, all maxima of paths in $(R_\rho(\sigma), \tau)$ are traversed from right to left, and hence by Theorem 5.17, we have that $(R_\rho(\sigma), \tau)$ is in the geometric SU diagonal. \square

Lemma 6.21. *Any facet (σ, τ) of the geometric SU diagonal Δ^{SU} is mapped to a SCP by a path-admissible sequence of inverse m -shifts.*

Proof. We show that any facet (σ, τ) which has a crossing, and is hence not a SCP, admits an inverse shift operation. This shows that a finite number of inverse shift operations converts any facet to a SCP (if σ is an ordered partition of n with k blocks, then clearly less than n^k inverse shifts are possible). We consider the following partition of the set of facets with crossings, illustrated by example in Example 6.22.

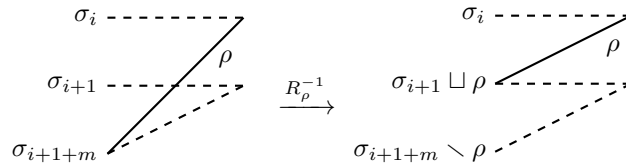
- (1) All adjacent blocks are connected by paths of length 2.
- (2) There exist adjacent blocks which are connected by a path of length $2k$ for $k > 1$.
 - (a) The maximal step of this path is not the last step.
 - (i) The τ block containing the maximal step is not the greatest block.
 - (ii) The τ block containing the maximal step is the greatest block.

In Case (1), as (σ, τ) has a crossing, it has an adjacent crossing by Lemma 6.19. This adjacent crossing is of the following form (we illustrate the case where the crossing happens on the left, the case when it happens on the right is similar):



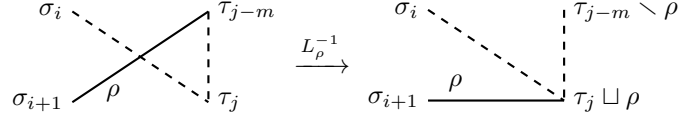
By the path characterization of the geometric SU diagonal (Theorem 5.17), the fact that $\tau_j < \tau_k$ implies that $\rho > b$, and the fact that $\sigma_i < \sigma_{i+1}$ implies that $b > c$. Thus, we have $\rho > \max \sigma_{i,i+1}$, which implies that a path-admissible left shift R_ρ^{-1} can be performed.

In Case (2.a), consider the two adjacent blocks say $\sigma_i | \sigma_{i+1}$ (the τ case is similar), let $\rho := \max \sigma_{i,i+1}$ denote the maximum of the path between them, and let $m \geq 1$ be such that ρ steps into σ_{i+1+m} . Since $\max \sigma_{i,i+1+m} = \max \sigma_{i,i+1} = \rho$ the definition of the geometric SU diagonal implies that the block σ_{i+1+m} comes after the block σ_i , and by assumption after the block σ_{i+1} . Thus, we know that $m > 1$, and using dashed lines to denote paths of length ≥ 1 we have the following picture

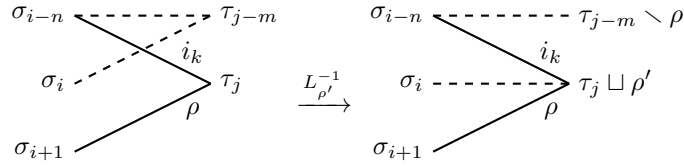


As we have $\rho = \max \sigma_{i,i+1} > \max \sigma_{i+1+m,i+1}$, an inverse m -shift operation can be performed.

In the Case (2.b.i), there exists $j, m > 0$ such that τ_{j-m} is the block of τ which contains the maximal element ρ , and τ_j is any greater block on the path from σ_i to σ_{i+1} . Then we may apply the following inverse m -shift operator.



There remains to be treated Case (2.b.ii). We consider the path $\sigma_{i,i+1} := (i_1, j_1, i_2, \dots, i_k, \rho)$ to be of length $2k$, $k > 1$. We denote by τ_j the block of τ containing the maximal step ρ of this path, which by hypothesis is the last block of τ . Let σ_{i-n} be the last block of σ which is attained by the path $\sigma_{i,i+1}$ before the block σ_{i+1} . We must have $n > 1$, since ρ is the last step and $\sigma_i | \sigma_{i+1}$ are adjacent blocks. The situation can be pictured as on the left.

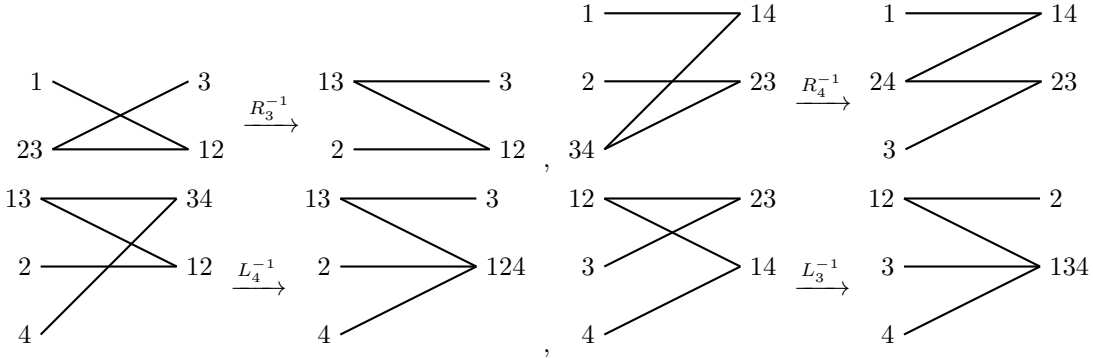


Now let $\rho' := \max \sigma_{i,i-n}$ be the maximum of the path $\sigma_{i,i-n} = (i_1, j_1, i_2, \dots, i_{k-1}, j_{k-1})$, and let τ_{j-m} , $m \geq 1$ be the block of τ containing ρ' . We want to show that an inverse left m -shift can bring ρ' back to τ_j , *i.e.* we need $\rho' > \max \tau_{j-m,j}$. As $\rho' := \max \sigma_{i,i-n}$, and apart from the step i_k we have $\tau_{j-m,j} \subset \sigma_{i,i-n}$, we just need to show that $\rho' > i_k$. To see that this is indeed the case, it suffices to look at the last steps

$$\tau_l \xrightarrow{j_{k-1}} \sigma_{i-n} \xrightarrow{i_k} \tau_j \xrightarrow{\rho} \sigma_{i+1}$$

of the path $\sigma_{i,i+1}$. By the definition of the geometric SU diagonal, the fact that $\tau_l < \tau_j$ implies that $j_{k-1} > i_k$, and thus that $\rho' > i_k$, which finishes the proof. \square

Example 6.22. Here are examples of each of the cases in the proof of Lemma 6.21. We display cases (1), (2.a), (2.b.i) and, (2.b.ii) respectively, reading the diagrams from top-left to bottom-right.



Note that, as we have chosen minimal illustrative examples, each inverse m -shift is an inverse 1-shift, and after each shift we obtain a SCP. This is not typically the case.

Theorem 6.23. *The m -shift and the geometric SU diagonals coincide.*

Proof. We first note that SCPs are known elements of both the m -shift and the geometric SU diagonals (Proposition 6.4). The proof that every facet of the m -shift Δ^{SU} is in geometric Δ^{SU} follows from the closure of Δ^{SU} under the shift operators (Proposition 6.20). The proof that every facet of geometric Δ^{SU} is in shift Δ^{SU} follows from the closure of Δ^{SU} under the inverse shift operator (Proposition 6.20) and the fact that every facet is sent to a SCP after a finite number of inverse shifts (Lemma 6.21). In particular, for any given facet in geometric Δ^{SU} , this provides a SCP and a sequence of shifts to form it, showing it is a facet of m -shift Δ^{SU} . \square

Combining Theorem 6.15 and Theorem 6.23, we obtain the desired equivalence between the original SU diagonal from [SU04] and the geometric SU diagonal from Definition 5.3.

Theorem 6.24. *The original and geometric SU diagonals coincide.*

6.2. Shifts under the face poset isomorphism. Having proven the equivalence of the original and geometric SU diagonals, we now use the face poset isomorphisms between the geometric LA and SU diagonals from Section 5.3 to translate results and combinatorial descriptions from one to the other. Under the isomorphism $t(r \times r) : \Delta^{\text{LA}} \rightarrow \Delta^{\text{SU}}$ from Remark 5.16, we get a straightforward analogue of Definition 6.9 for the LA diagonal. Firstly, the morphism $r \times r$ exchanges max and min, which yields the following “dual” notions of admissibility.

Definition 6.25. Let σ denote either one of the two ordered partitions of $[n]$ in a $(2, n)$ -partition tree, and let $M \subsetneq \sigma_i$. The right m -shift R_M (resp. the left m -shift L_M) is

- (1) *block-admissible* if $\max \sigma_i \notin M$ and $\max M < \min \sigma_{i+m}$ (resp. $\max M < \min \sigma_{i-m}$),
- (2) *path-admissible* if $\max M < \min \sigma_{i,i+m}$ (resp. $\max M < \min \sigma_{i,i-m}$).

Secondly, as the morphism t switches our ordered partitions, this means that the LA lefts shifts will act on the left ordered partition, and the LA right shifts will act on the right ordered partition. Consequently, admissible sequences of LA shifts are defined similarly to Definition 6.9 (simply replace σ with τ). Which provides an analogue of Definition 6.10 for the LA diagonal.

Definition 6.26. The facets of the *subset shift, 1-shift and m -shift LA diagonals* are given by the formula

$$\Delta^{\text{LA}}([n]) = \bigcup_{(\sigma, \tau)} \bigcup_{\mathbf{M}, \mathbf{N}} L_{\mathbf{M}}(\sigma) \times R_{\mathbf{N}}(\tau)$$

where the unions are taken over all SCPs (σ, τ) of $[n]$, and respectively over all block-admissible sequences of subset 1-shifts \mathbf{M}, \mathbf{N} , over all path-admissible sequences of singleton 1-shifts, and over all path-admissible sequences of singleton m_j -shifts, for various $m_j \geq 1$.

We now formally verify that the isomorphism $t(r \times r)$ relates these shift definitions as claimed.

Proposition 6.27. *Let (σ, τ) be a facet of Δ^{LA} . For each type of LA shift, let \mathbf{M}, \mathbf{N} be admissible sequences of this type, then*

$$t(r, r)(L_{\mathbf{N}}(\sigma), R_{\mathbf{M}}(\tau)) = (R_{r\mathbf{M}}(r\tau), L_{r\mathbf{N}}(r\sigma))$$

where $r\mathbf{M} := (rM_1, \dots, rM_p)$ and $r\mathbf{N}$ (defined similarly) are admissible sequences of SU shifts of the same type.

Proof. As reversing the elements then shifting them is the same as shifting the elements then reversing them, it is clear that the equality holds if $r\mathbf{M}, r\mathbf{N}$ are admissible sequences of SU shifts. As such, we must simply verify the admissibility, and given the equivalence of the various shift definitions, we just do this for path-admissibility of 1-shifts. Consider a right shift R_M , for $M \in \sigma_i$, which is path-admissible in the LA sense (Definition 6.25). Then, we have $\max M < \min \sigma_{i,i+1}$ which implies that $\min rM > \max r\sigma_{i,i+1}$, and thus the right shift R_{rM} is path-admissible in the SU sense (Definition 6.9). Here, $rM \in r\sigma_i$ is interpreted as being in a block of the right partition (τ in the notation of the definition). So, if $\mathbf{M} = (M_{i_1}, \dots, M_{i_p})$, define $r(\mathbf{M}) := (rM_1, \dots, rM_p)$, and from the prior it is clear this is a path-admissible sequence of SU shifts, finishing the proof. \square

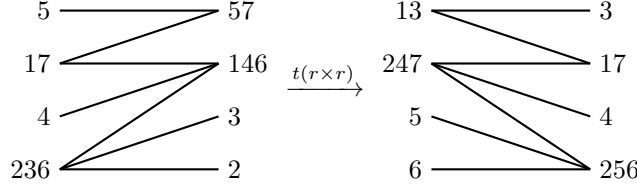
Thus, given $t(r \times r)$ is an isomorphism of the geometric diagonals (Remark 5.16), and the geometric SU diagonal coincides with the shift SU diagonals (Section 6.1.2), we immediately obtain the following statement.

Proposition 6.28. *The geometric LA diagonal and all shift LA diagonals coincide.*

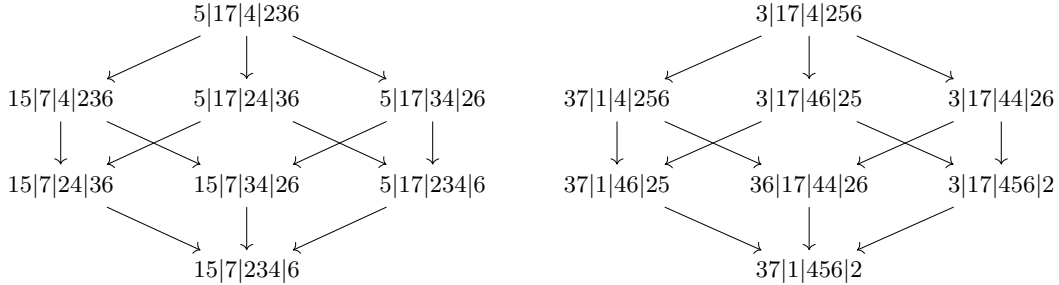
Remark 6.29. The isomorphism $rs \times rs : \Delta^{\text{LA}} \rightarrow \Delta^{\text{SU}}$, identified in Theorem 5.15, also sends shifts operators to shift operators, but it sends left shift operators to right shift operators and vice versa. The LA^{op} and SU^{op} diagonals also admit obvious dual shift descriptions.

We now explore in example how the isomorphism $t(r \times r)$ translates the shift operators.

Example 6.30. The isomorphism $t(r \times r)$ sends the SCP $(\sigma, \tau) := (5|17|4|236, 57|146|3|2)$ to the SCP $(\sigma', \tau') := (13|247|5|6, 3|17|4|256)$. The corresponding $(2, n)$ -partition trees present a clear symmetry



We now illustrate all possible path admissible LA 1-shifts of (σ, τ) and all possible path admissible SU 1-shifts of (σ', τ') . We first display how the LA left shifts act on σ , and the SU left shifts act on τ' . The LA shifts have been drawn so that the leftmost arrow shifts the smallest element, and the SU shifts have been drawn so that the leftmost arrow shifts the largest element. As such, the face poset isomorphism $t(r \times r)$ directly translates one diagram to the other. The specific element being shifted can be inferred by the source and target of the arrow.



We now illustrate all the possible LA right shifts acting on τ

$$\sigma \times 57|146|3|2 \xrightarrow{\rho=1} \sigma \times 57|46|13|2 \xrightarrow{\rho=1} \sigma \times 57|46|3|12$$

and all possible SU right shifts acting on σ'

$$13|247|5|6 \times \tau' \xrightarrow{\rho=7} 13|24|57|6 \times \tau' \xrightarrow{\rho=7} 13|24|5|67 \times \tau'.$$

No other shifts are possible; observe for instance that we cannot perform the LA left shift $15|7|234|6 \times 57|46|13|2 \xrightarrow{\rho=2} 15|27|34|6 \times 57|46|13|2$ as the minimal path connecting 234 and 7 contains 1, which is smaller than 2 (see Example 5.18). We shall see in Section 6.3, that these diagrams are the Hasse diagrams of lattices.

Example 6.31. It was observed in [LA22] that the LA and SU diagonals coincided up until $n = 3$, however due to their dual shift structure they generate the non-SCP pairs in a dual fashion. In particular, the two center faces of the subdivided hexagon of Figure 18 are generated by



and



where we have aligned each element, of each diagonal, vertically with its dual element.

6.3. Shift lattices. In this section, we show that the 1-shifts of the operadic diagonals Δ^{LA} and Δ^{SU} , define the covering relations of a lattice structure on the set of facets. More precisely, we show that each SCP is the minimal element of a lattice isomorphic to a product of chains, where the partial order is given by shifts. Given the bijection between SCPs and permutations, and our prior enumeration of the facets of the diagonal, this produces two new statistics on permutations. In addition, later in Section 6.4, we will use the lattice structure to relate the cubical and shift definitions of the Δ^{SU} diagonal.

Definition 6.32. The LA *shift poset* on the set of facets $(\sigma, \tau) \in \Delta^{\text{LA}}$ is defined to be the transitive closure of the relations $(\sigma, \tau) \prec (L_\rho \sigma, \tau)$ and $(\sigma, \tau) \prec (\sigma, R_\rho \tau)$, for all LA path-admissible 1-shifts L_ρ and R_ρ . The SU *shift poset* is defined similarly. Then, for each permutation v of $[n]$, we define the subposet $\tilde{\Sigma}_v^{\text{LA}}$ (resp. $\tilde{\Sigma}_v^{\text{SU}}$) to be the set of all admissible LA (resp. SU) shifts of the associated SCP.

Given the shift definitions of Δ^{SU} and Δ^{LA} (Definitions 6.10 and 6.26), the subposets $\tilde{\Sigma}_v^{\text{LA}}$ and $\tilde{\Sigma}_v^{\text{SU}}$ are clearly connected components of their posets, with a unique minimal element corresponding to the SCP. We now aim to prove they are also lattices (Proposition 6.37).

Lemma 6.33. *The m -shift operators defining the facets of an operadic diagonal commute. That is, whenever the successive composition of two m_1, m_2 -shifts is defined on a facet of the LA or SU diagonal, the reverse order of composition is also defined, and the two yield the same facet.*

Proof. A Δ^{SU} (resp. Δ^{LA}) m -shift is defined when ρ is greater (resp. smaller) than the maximal (resp. minimal) element of the connecting path. Combining Corollary 6.13 and Proposition 6.14, we know m -shifts conserve the maximal (minimal) elements of paths and their directions. As such, we can commute any two shift operators. \square

Definition 6.34. Let v be a permutation of $[n]$, and (σ, τ) the SCP corresponding to v . For $\rho \in [n]$, we define the LA *left height* and *right height* of ρ to be

$$\begin{aligned} \ell_v(\rho) &:= \max(\{0\} \cup \{m > 0 : L_\rho(\sigma) \text{ is a path admissible LA } m\text{-shift}\}), \\ r_v(\rho) &:= \max(\{0\} \cup \{m > 0 : R_\rho(\tau) \text{ is a path admissible LA } m\text{-shift}\}). \end{aligned}$$

The left and right heights for the SU diagonal are defined similarly.

The height of an element ρ in a SCP can be explicitly calculated as follows.

Lemma 6.35. *Let (σ, τ) be the SCP corresponding to a permutation v . Then, the right LA height $r_v(\rho)$ (resp. the left LA height $\ell_v(\rho)$) of $\rho \in [n]$ is given by the number of consecutive blocks of σ (resp. of τ) to the right (resp. left) of the one containing ρ whose minima are larger than ρ . The SU heights are obtained similarly by considering blocks whose maxima are smaller than ρ .*

Proof. We consider the right SU height, the other cases are similar. As (σ, τ) is a SCP, we have $\max \sigma_{k, k+1} = \max \sigma_{k+1}$ for all $k \geq 1$. Moreover, from the equivalence between 1-shifts and m -shifts (Proposition 6.14), there exists a m -shift of ρ from σ_i to σ_{i+m} if, and only if, there exists a sequence of m consecutive 1-shifts, each satisfying $\rho > \max \sigma_{j, j+1} = \max \sigma_{j+1}$. Thus, these iterated 1-shifts will be path-admissible until the first failure at $j = r_v(\rho) + 1$. \square

Remark 6.36. The height calculations can also be reformulated directly in terms of the permutation. For instance, for the SU diagonal $r_v(\rho)$ is the number of consecutive descending runs, to the right of the descending run containing ρ , whose maximal element is smaller than ρ .

Proposition 6.37. *The subposets $\tilde{\Sigma}_v^{\text{LA}}$ and $\tilde{\Sigma}_v^{\text{SU}}$, are lattices isomorphic to products of chains*

$$\tilde{\Sigma}_v^{\text{LA}} \cong \prod_{\rho \in [n]} [0, \ell_v(\rho)] \times \prod_{\rho \in [n]} [0, r_v(\rho)] \quad \text{and} \quad \tilde{\Sigma}_v^{\text{SU}} \cong \prod_{\rho \in [n]} [0, r_v(\rho)] \times \prod_{\rho \in [n]} [0, \ell_v(\rho)],$$

where $[0, k]$ is the chain lattice $0 < 1 < \dots < k$, for $k \geq 0$.

Proof. We denote by L_ρ^m (resp. R_ρ^m) a left (right) m -shift of ρ for $m > 0$, and we let it be the identity if $m = 0$. By the commutativity of m -shift operators (Lemma 6.33), and the existence of unique heights for each element (Lemma 6.35), every element of $\tilde{\Sigma}_v^{\text{LA}}$ admits a unique shift description $(L_n^{\ell_n} \dots L_1^{\ell_1}(\sigma), R_n^{r_n} \dots R_1^{r_1}(\tau))$, where $0 \leq \ell_\rho \leq \ell_v(\rho)$ and $0 \leq r_\rho \leq r_v(\rho)$. Thus, we identify it with the pair of tuples $(\ell_1, \dots, \ell_n) \times (r_1, \dots, r_n)$. This is clearly an isomorphism of lattices. \square

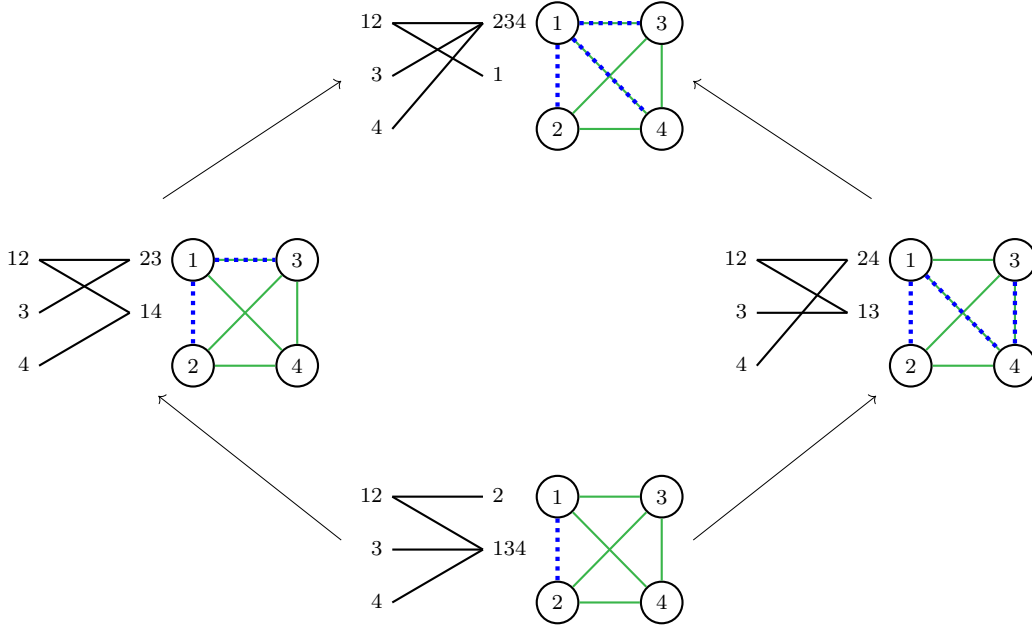


FIGURE 20. The shift lattice $\bar{\Sigma}_v^{\text{SU}}$ for $v = 4|3|1|2$. Each facet is drawn next to a graph encoding its inversions (Definition 6.16). If $(i, j) \in J(\sigma)$, then a green edge connects (i, j) , and if $(i, j) \in I(\tau)$, then a blue dotted edge connects (i, j) . Consequently, $I((\sigma, \tau))$ is encoded by the presence of both edges, and also the crossings, by Proposition 6.17.

Note that the maximal element of $\bar{\Sigma}_v$ (for either diagonal) is given by shifting each element of (σ, τ) by its maximal shift. The joins and meets of any two elements are also thus given by isomorphism to the product of chains. For instance, in the case of meets,

$$(\ell_1, \dots, \ell_n, r_1, \dots, r_n) \wedge (\ell'_1, \dots, \ell'_n, r'_1, \dots, r'_n) = (\min\{\ell_1, \ell'_1\}, \dots, \min\{\ell_n, \ell'_n\}, \min\{r_1, r'_1\}, \dots, \min\{r_n, r'_n\})$$

For clear examples of the Hasse diagrams corresponding to our lattices, we direct the reader to Example 6.30, and Figure 20. We note that Figure 20 also illustrates that there is no general relation between the shift lattice structure and inversions sets. In particular, the shift lattices are not sub-lattices of the facial weak order (discussed in Section 5.6), as $24|13$ and $234|1$ are incomparable.

Remark 6.38. As a consequence of Proposition 6.37, the facets of the operadic diagonals are disjoint unions of lattices. However, any lattice L on permutations (such as the weak order) induces a lattice on the facets as follows. For every $v \in L$, we can substitute the lattice $\bar{\Sigma}_v^{\text{LA}}$ (or $\bar{\Sigma}_v^{\text{SU}}$) into the permutation v . In particular, every element which was covered by v is now covered by the minimal element of $\bar{\Sigma}_v^{\text{LA}}$, and every element which was covering v now covers the maximal element of $\bar{\Sigma}_v^{\text{LA}}$.

Given our previously obtained formulae for the number of elements in the diagonal (Section 4.3), and the results of this section, we obtain the following statistics on permutations.

Corollary 6.39. *Using the heights of either diagonal,*

$$2(n+1)^{n-2} = \sum_{v \in \mathbb{S}_n} \prod_{\rho \in [n]} (\ell_v(\rho) + 1)(r_v(\rho) + 1)$$

Moreover, denoting by $\mathbb{S}_n^{k_1} \subseteq \mathbb{S}_n$ the set of permutations with k_1 ascending runs, and consequently $k_2 = n - 1 - k_1$ descending runs, we have

$$n \binom{n-1}{k_1} (n-k_1)^{k_1-1} (n-k_2)^{k_2-1} = \sum_{v \in \mathbb{S}_n^{k_1}} \prod_{\rho \in [n]} (\ell_v(\rho) + 1)(r_v(\rho) + 1).$$

Proof. This follows directly from Corollary 4.22, with the observation that shifts conserve the number of blocks, and hence the dimensions of the faces. \square

6.4. Cubical description. In this section, we recall the cubical definition of the SU diagonal from [SU22] and explicitly relate it to their shift description, using a new proof that exploits the lattice description of the diagonal (Section 6.3). Then we construct an analogous cubical definition of the LA diagonal, transferring the cubical formulae via isomorphism.

6.4.1. *The cubical SU diagonal.* We define inductively a subdivision $\square_{n-1}^{\text{SU}}$ of the $(n-1)$ -dimensional cube which is combinatorially isomorphic to the permutahedron $\text{Perm}(n)$ (Proposition 6.42).

Construction 6.40. Given a $(n-k)$ -dimensional face $\sigma = \sigma_1 | \cdots | \sigma_k$ of the $(n-1)$ -dimensional permutahedron $\text{Perm}(n)$, we set $n_j := \#\sigma_{k-j+1} \cup \cdots \cup \sigma_k$, and define a subdivision $I_\sigma := I_1 \cup \cdots \cup I_k$ of the interval $[0, 1]$ by the following formulas

$$I_j := \begin{cases} [0, 1 - 2^{-n_j}] & \text{if } j = 1, \\ [1 - 2^{-n_{j-1}}, 1 - 2^{-n_j}] & \text{if } 1 < j < k, \\ [1 - 2^{-n_{j-1}}, 1] & \text{if } j = k. \end{cases}$$

Let \square_0^{SU} be the 0-dimensional cube (a point), trivially subdivided by the sole element 1 of $\text{Perm}(1)$. Then, assuming we have constructed the subdivision $\square_{n-1}^{\text{SU}}$ of the $(n-1)$ -cube, we construct \square_n^{SU} as the subdivision of $\square_{n-1}^{\text{SU}} \times [0, 1]$ given, for each face σ of $\square_{n-1}^{\text{SU}}$, by the polytopal complex $\sigma \times I_\sigma$. We label the faces $\sigma \times I$ of the subdivided rectangular prism $\sigma \times I_\sigma$ by the following rule

$$(I) \quad \sigma \times I := \begin{cases} \sigma_1 | \cdots | \sigma_k | n+1 & \text{if } I = \{0\}, \\ \sigma_1 | \cdots | \sigma_j | n+1 | \sigma_{j+1} | \cdots | \sigma_k & \text{if } I = I_j \cap I_{j+1} \text{ with } 1 \leq j \leq k-1, \\ n+1 | \sigma_1 | \cdots | \sigma_k & \text{if } I = \{1\}, \\ \sigma_1 | \cdots | \sigma_j \cup \{n+1\} | \cdots | \sigma_k & \text{if } I = I_j \text{ with } 1 \leq j \leq k. \end{cases}$$

This defines a subdivision \square_n^{SU} of the n -cube.

Figure 21 illustrates this subdivision for the first few dimensions. We indicate, in bold, the embedding $\square_{n-1}^{\text{SU}} \hookrightarrow \square_n^{\text{SU}}$ induced by the natural embedding $\mathbb{R}^{n-1} \hookrightarrow \mathbb{R}^n$. Only the vertices of \square_3^{SU} are labelled, but its edges, facets and outer face are all identified with the expected elements of $\text{Perm}(4)$.

Remark 6.41. A consequence of the construction is that each edge of \square_n^{SU} is parallel to one of the canonical basis vectors e_i of \mathbb{R}^n , and corresponds to shifting the element $i+1$ of $[n+1] \setminus \{1\}$.

Proposition 6.42. The polytopal complex \square_n^{SU} is combinatorially isomorphic to the permutahedron $\text{Perm}(n+1)$.

Proof. By construction it is clear that the faces of \square_n^{SU} and $\text{Perm}(n+1)$ are in bijection, and that this bijection preserves the dimension. It remains to show that this bijection is a poset isomorphism. Let $\sigma_1 | \cdots | \sigma_i | \sigma_{i+1} | \cdots | \sigma_k \prec \sigma_1 | \cdots | \sigma_i \cup \sigma_{i+1} | \cdots | \sigma_k$ be a covering relation in the face poset of $\text{Perm}(n+1)$. We need to see that the corresponding faces F, G of \square_n^{SU} satisfy $F \prec G$. From Equation (I) this clearly holds for lines. Since any face of \square_n^{SU} is a product of lines, the result follows by induction on the dimension of the faces. \square

We now unpack how certain properties of $\text{Perm}(n)$ have been encoded in the cubical structure of \square_n^{SU} . This will later allow us to construct a cubical formula for the diagonal through maximal pairings of k -subdivision cubes of \square_n^{SU} , which we now introduce.

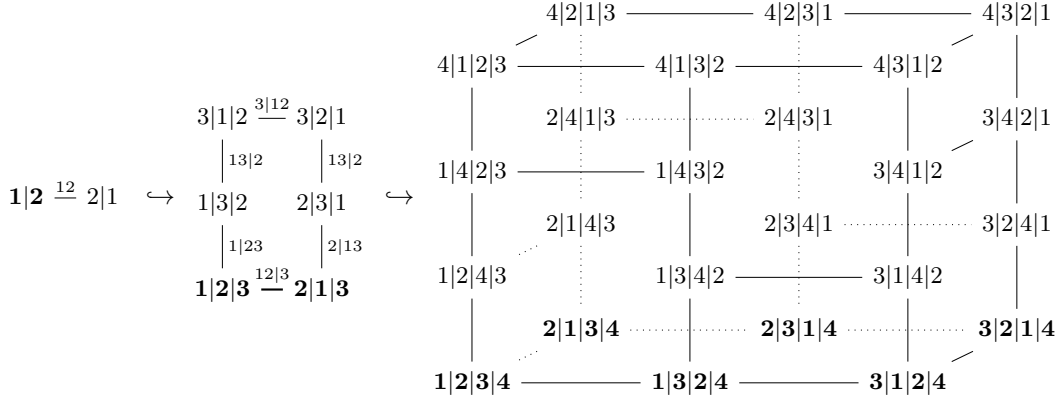


FIGURE 21. Cubical realizations \square_1^{SU} , \square_2^{SU} and \square_3^{SU} of the permutahedra $\text{Perm}(2)$, $\text{Perm}(3)$ and $\text{Perm}(4)$, respectively, from Construction 6.40.

Definition 6.43. For $k \geq 0$, a *k-subdivision cube* of \square_n^{SU} is a union of k -faces of \square_n^{SU} whose underlying set is a k -dimensional rectangular prism.

An important example of a k -subdivision cubes are the k -faces of \square_n^{SU} (other examples are provided in Example 6.48).

Lemma 6.44. A k -subdivision cube has a unique maximal (resp. minimal) vertex with respect to the weak order on permutations.

Proof. By construction, the edges of \square_n^{SU} are parallel to the basis vectors of \mathbb{R}^n (Remark 6.41), and correspond to inversions on permutations. Thus, the vector $\mathbf{v} := (1, \dots, 1)$ induces the weak order on the vertices of \square_n^{SU} . Since each k -subdivision cube is a rectangular prism whose edges are not perpendicular to \mathbf{v} , the scalar product with \mathbf{v} is maximized (resp. minimized) at a unique vertex. \square

Definition 6.45. The *maximal (resp. minimal) k-face* of a k -subdivision cube, with respect to the weak order, is the unique k -face in the subdivision cube which contains the maximal (resp. minimal) vertex.

Construction 6.46. For a k -dimensional face σ of the cubical permutahedron \square_n^{SU} , we construct the unique maximal k -subdivision cube, with respect to inclusion, whose maximal (resp. minimal) k -face with respect to the weak order is σ .

We only treat the case for the maximal k -face σ , the minimal face proceeds similarly. We build the maximal subdivision cubes inductively. Let σ be an edge of \square_n^{SU} , and let v be its maximal vertex. Let $\rho \in [n+1] \setminus \{1\}$ be the element shifted by this edge (Remark 6.41). Shifting this element to the right as far as possible (ρ will be shifted all the way to the right, or be blocked by a larger element), we get the desired 1-subdivision line.

Suppose that we have constructed maximal subdivision cubes up to dimension k , and let σ be a $(k+1)$ -face of \square_n^{SU} , with maximal vertex v . Consider the $k+1$ elements of $[n]$, which correspond to dimensions spanned by σ (Remark 6.41), and let ρ be the largest such element. Let σ_L be the 1-face, with maximal vertex v , whose only non-trivial dimension corresponds to ρ . From the initial step above, there is a unique maximal 1-subdivision line L with maximal 1-face σ_L . Let σ_C be the k -face, with maximal vertex v , spanned by the complement of ρ in $[n+1] \setminus \{1\}$. By induction, there is a maximal k -subdivision cube C with maximal k -face σ_C . Then, it is clear that the product $L \times C$ defines a $(k+1)$ -subdivision cube of \square_n^{SU} , with maximal vertex v . Indeed, as ρ is the maximal element corresponding to dimensions of $L \times C$, the faces of $L \times C$ are the

$(k + 1)$ -dimensional rectangular prisms resulting from shifting ρ through the k -faces of C , as in Equation (1).

Finally, $L \times C$ is maximal under inclusion. If there was a larger $(k + 1)$ -subdivision cube enveloping $L \times C$, then one of its projections would be a 1 or k -subdivision cube enveloping L or C , contradicting the assumption that they are maximal. This finishes the construction.

Definition 6.47. For a vertex v of \square_n^{SU} , the *hourglass* of \square_n^{SU} at v is the maximal pair of subdivision cubes $\tilde{\Sigma}_v^{\text{SU}}$, with respect to inclusion, within the set of all pairs (C, C') of subdivision cubes such that C has maximal vertex v , C' has minimal vertex v , and $\dim C + \dim C' = n$.



FIGURE 22. The hourglass $\tilde{\Sigma}_v^{\text{SU}}$ of \square_3^{SU} at $v = 4|3|1|2$.

The following examples are pictured in Figure 22.

Example 6.48. The sets of faces $\{1234\}$, $\{1|234\}$, $\{1|234, 14|23\}$, and $\{1|3|24, 1|34|2\}$ are all subdivision cubes of \square_3 . In contrast, the sets of faces $\{134|2, 14|23\}$, $\{1|234, 134|2, 14|23\}$, and $\{1|2|34, 1|23|4\}$ are not subdivision cubes of \square_3^{SU} . For $v = 4|3|1|2$, the only 1-subdivision cube with minimal vertex v is $4|3|12$, and the three 2-subdivision cubes with maximal vertex v are $\{134|2\}$, $\{13|24, 134|2\}$, $\{1|234, 13|24, 14|23, 134|2\}$. This defines the hourglass $\tilde{\Sigma}_v^{\text{SU}} = \{1|234, 13|24, 14|23, 134|2\} \times \{4|3|12\}$ of \square_3^{SU} at v .

Let us observe that the SCP corresponding to v is $(\sigma, \tau) := (134|2, 4|3|12)$. The ordered partition σ admits three distinct right shifts, $13|24$, $14|23$, $1|234$, and τ admits no left shifts. Theorem 6.49 shows that $\tilde{\Sigma}_v^{\text{SU}}$ is generated by all shifts of the SCP corresponding to v .

Theorem 6.49. Let v be a vertex of the cubical permutahedron \square_n^{SU} , and let (σ, τ) be its associated SCP. Then, we have

$$\tilde{\Sigma}_v^{\text{SU}} = \bigcup_{M, N} R_M(\sigma) \times L_N(\tau),$$

where the union is taken over all block-admissible sequences of SU shifts M, N .

Proof. We prove the result inductively from lines, and consider the case of σ , τ proceeds similarly. Combining Construction 6.46 with Lemma 6.35, we have that if L is a maximal 1-subdivision cube with maximal 1-face σ , then its faces are generated by the right 1-shifts R_ρ^i , for i between 0 and its maximal right height r_ρ (Definition 6.34).

Now consider the unique maximal $(k + 1)$ -subdivision cube of \square_n^{SU} with maximal $(k + 1)$ -face σ . By Construction 6.46, this subdivision cube is given by the product $L \times C$ of a line corresponding to the maximal element ρ being shifted, and a k -cube C corresponding to all other elements. By induction hypothesis, both the line L and the cube C are generated by all block-admissible right shifts from their unique maximal faces σ_L and σ_C . Moreover, if ρ is in the i th block of σ_C , then σ is obtained from σ_C by merging the i^{th} and $(i + 1)^{\text{st}}$ blocks.

On the one hand, the right height of any element being shifted in C is the same as its right height in $L \times C$. This follows from the inductive description of \square_n^{SU} (Equation (I)): every k -face in C has ρ in a singleton block, and as ρ is larger than all other elements it blocks all other shifts.

On the other hand, we know from Construction 6.46 that the $(k+1)$ -faces of $L \times C$ are obtained by weaving ρ through the k -faces of C . Indeed, every k -face in C has ρ in a fixed singleton set, and every k -face on the opposite side of $L \times C$ has ρ in another fixed singleton set; given Equation (I), this final singleton block in any k -face of C is either the last block, or is followed by a block containing an element larger than ρ . If we translate this observation back to the $(k+1)$ -faces of $L \times C$ that are adjacent to the boundary of L , then this corresponds to an equivalent calculation of the right height of ρ in σ .

Given the lattice description of the diagonal (Proposition 6.37), we thus have that $L \times C$ is generated by all block-admissible sequences of right shifts of σ , which concludes the proof. \square

This recovers the formulas [SU22, Form. (1) & (3)].

6.4.2. *LA cubical description.* The LA diagonal also admits a similar cubical description, which we may quickly induce by isomorphism. We first define inductively a subdivision $\square_{n-1}^{\text{LA}}$ of the $(n-1)$ -dimensional cube which is combinatorially isomorphic to the permutahedron $\text{Perm}(n)$, analogous to the one from the preceding sections.

Construction 6.50. *Given a $(n-k)$ -dimensional face $\sigma = \sigma_1 | \dots | \sigma_k$ of the $(n-1)$ -dimensional permutahedron $\text{Perm}(n)$, we set $n_j := \#\sigma_{k-j+1} \cup \dots \cup \sigma_k$, and define a subdivision $I_\sigma := I_1 \cup \dots \cup I_k$ of the interval $[0, 1]$ by the same formulas as in Construction 6.40.*

Let \square_0^{LA} be the 0-dimensional cube (a point), trivially subdivided by the sole element 1 of $\text{Perm}(1)$. Then, assuming we have constructed the subdivision $\square_{n-1}^{\text{LA}}$ of the $(n-1)$ -cube, we construct \square_n^{LA} as the subdivision of $\square_{n-1}^{\text{LA}} \times [0, 1]$ given, for each face σ of $\square_{n-1}^{\text{LA}}$, by the polytopal complex $\sigma \times I_\sigma$. We label the faces $\sigma \times I$ of the subdivided rectangular prism $\sigma \times I_\sigma$ by the following rule

$$\sigma \times I := \begin{cases} \sigma'_1 | \dots | \sigma'_k | 1 & \text{if } I = \{0\}, \\ \sigma'_1 | \dots | \sigma'_j | 1 | \sigma'_{j+1} | \dots | \sigma'_k & \text{if } I = I_j \cap I_{j+1} \text{ with } 1 \leq j \leq k-1, \\ 1 | \sigma'_1 | \dots | \sigma'_k & \text{if } I = \{1\}, \\ \sigma'_1 | \dots | \sigma'_j \cup \{1\} | \dots | \sigma'_k & \text{if } I = I_j \text{ with } 1 \leq j \leq k, \end{cases}$$

where each block of σ has been renumbered as $\sigma'_i := \{p+1 \mid p \in \sigma_i\}$ for all $1 \leq i \leq k$. We obtain a subdivision \square_n^{LA} of the n -cube isomorphic to the permutahedron $\text{Perm}(n+1)$.

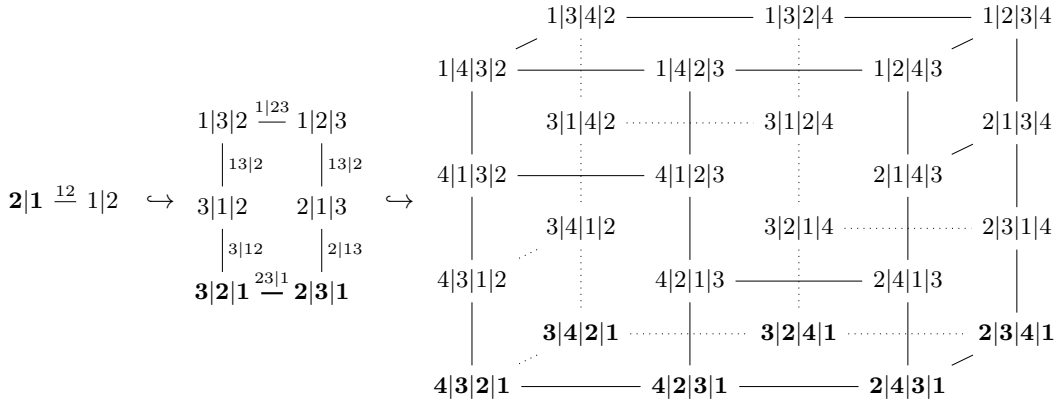


FIGURE 23. Cubical realizations of the permutahedra $\text{Perm}(2)$, $\text{Perm}(3)$ and $\text{Perm}(4)$ from Construction 6.50.

Figure 23 illustrates \square_n^{LA} in dimensions 1 to 3. We have indicated in bold the embedding $\square_{n-1}^{\text{LA}} \hookrightarrow \square_n^{\text{LA}}$ induced by the natural inclusions $\mathbb{R}^n \hookrightarrow \mathbb{R}^{n+1}$.

The appropriate base definitions for the LA diagonal of k -subdivision cubes (Definition 6.43) and hourglasses Σ_v (Definition 6.47) are the same as in the SU case. The proof that Σ_v^{LA} is indeed combinatorially isomorphic to $\text{Perm}(n+1)$ proceeds similarly to Proposition 6.42.

Recall from Section 5.3 the face poset isomorphism of the permutahedra which acts on $A_1 | \cdots | A_k$, by replacing each block A_j by the block $r(A_j) := \{n-i+1 \mid i \in A_j\}$. We have the analogue of Theorem 6.49 for the LA diagonal.

Theorem 6.51. *Let v be a vertex of the cubical permutahedron \square_n , and let (σ, τ) be its associated SCP. Then, we have*

$$\Sigma_v^{\text{LA}} = \bigcup_{M, N} L_M(\sigma) \times R_N(\tau),$$

where the union is taken over all block-admissible sequences of LA shifts M, N .

Proof. It is straightforward to see that the involution r induces a k -subdivision cube isomorphism $r : \square_n^{\text{SU}} \rightarrow \square_n^{\text{LA}}$ between the cubical subdivisions of Construction 6.40 and Construction 6.50, which sends the hourglass Σ_v^{SU} to the hourglass $\Sigma_{r(v)}^{\text{LA}}$. By Theorem 6.49, we know that Σ_v^{SU} is generated by SU shifts; we want to deduce that $\Sigma_{r(v)}^{\text{LA}}$ is generated by LA shifts. First, we observe that the diagram

$$\begin{array}{ccc} \text{SCP} & \xleftarrow{t(r \times r)} & \text{SCP} \\ \updownarrow & & \updownarrow \\ \mathbb{S}_n & \xleftarrow{r} & \mathbb{S}_n, \end{array}$$

where t is the permutation of the two factors, and the vertical arrows are the bijection between SCPs and permutations (Definition 6.1), is commutative. Thus, if we start from a SCP and consider its associated SU hourglass Σ_v^{SU} , applying the subdivision cube isomorphism r or applying the map $t(r \times r)$ both give the LA hourglass $\Sigma_{r(v)}^{\text{LA}}$. Combining this with the fact that the map $t(r \times r) : \Delta^{\text{LA}} \rightarrow \Delta^{\text{SU}}$ is an isomorphism between the LA and SU diagonal (Remark 5.16) which preserves left and right shifts (Proposition 6.27), we obtain the desired result. \square

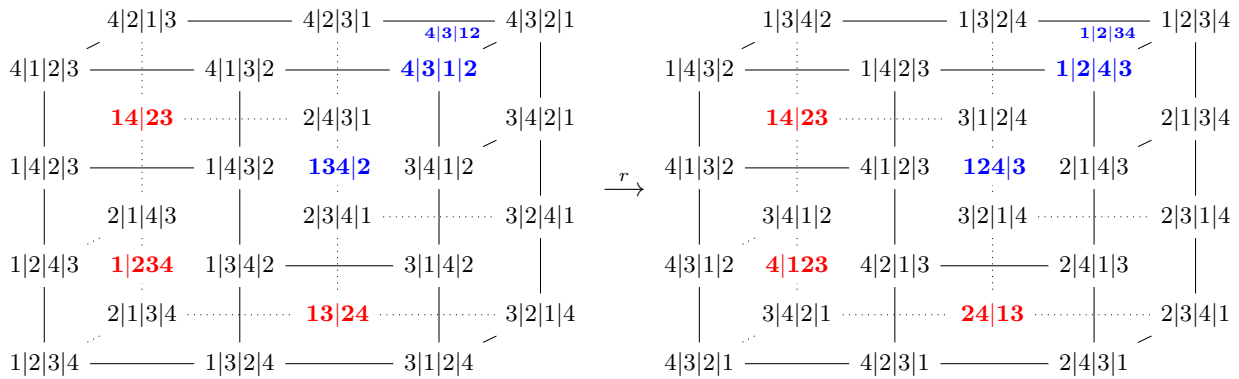


FIGURE 24. The isomorphism r applied to the SU cubical subdivision from Figure 22.

Example 6.52. Applying the isomorphism r to Example 6.48 yields the illustration of Figure 24. As r is an isomorphism of k -subdivision cubes, the maximal pair of SU subdivision cubes has been mapped to a maximal pair of LA subdivision cubes. Note that the maximal SU 2-subdivision cube with maximal vertex $4|3|1|2$ was generated by SU right shifts. Its image under r is the maximal LA 2-subdivision cube with minimal vertex $1|2|4|3$, and it is generated by LA right shifts.

6.5. Matrix description. For completeness, we recall from [SU04] the matrix description of facets of the SU diagonal. We previously saw that SCPs and permutations are in bijection (Definition 6.1). There is also a third equivalent way to encode this data, the *step matrices* of [SU04, Def. 6]. Given a permutation, one defines its associated step matrix by starting in the bottom left corner, writing increasing sequences vertically and decreasing sequences horizontally one after the other, leaving all other entries 0. See Figure 25.

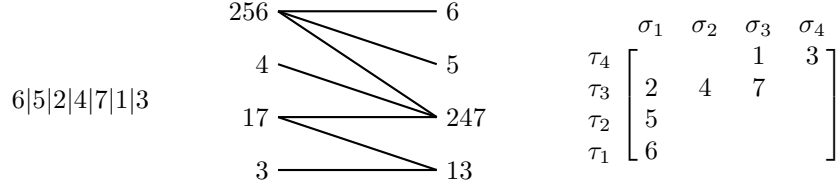


FIGURE 25. A permutation, its associated SCP, and their step matrix.

Given a matrix A whose only non-zero entries are the elements $[n]$, let $\sigma_i(A)$ denote the non-zero entries of the i^{th} column, and $\tau_j(A)$ the non-zero entries of the $(r - j + 1)^{\text{st}}$ row, where r is the number of rows of A . See the labelling in Figure 25. With this identification, the definitions of the shift operators can be translated directly: the right shift operator R_M shifts the elements of a subset $M \subset \sigma_i(A)$ one column to the right, or one row up, replacing only elements of value 0, and leaving 0 elements in their wake, while the left shift operator L_M shifts the elements of M to the left, or down one row.

The fact that the shifts avoid collisions with other elements is a consequence of their admissibility. Recall from Definition 6.6, that a right SU 1-shift R_M is *block-admissible* if $\min \sigma_i \notin M$ and $\min M > \max \sigma_{i+1}$, and that admissible sequence of right shifts proceed in increasing order (Definition 6.9).

Proposition 6.53. *Admissible sequences of matrix shift operators are well-defined.*

Proof. We verify the claim that the admissible sequences of matrix shift operators never replace non-zero elements. It is straightforward to show that this is true when a shift operator is applied to a SCP (σ, τ) . From here we proceed inductively. We assume that all prior shift operators have been well-defined, and we then check that applying another admissible shift operator is also well-defined. Suppose that an admissible right shift R_M is not well-defined, as it tries to move a value m into a non-zero matrix entry n . Then, n must have been placed into that column by a prior left shift operator L_{N_j} , and consequently $n > \min N_j > \max \tau_{j-1} > m$. However, $n \in \sigma_{i+1}$ so $\max \sigma_{i+1} > n > m > \min M_i$ implies that M is not block-admissible, a contradiction. \square

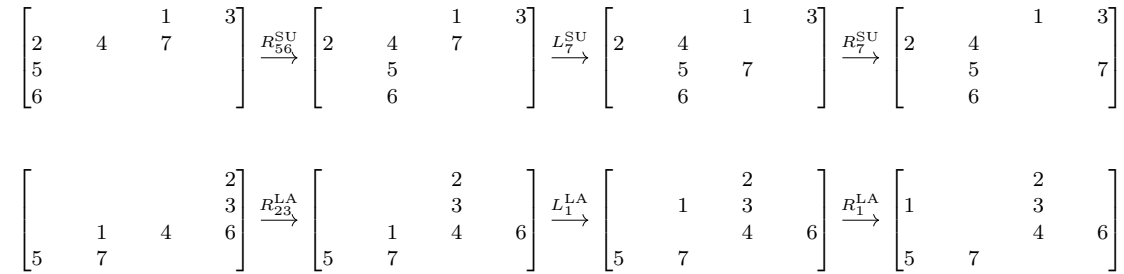


FIGURE 26. Matrix shifts under the isomorphism $t(r \times r)$ between the LA and SU diagonals.

Configuration matrices [SU04, Def. 7] are the matrices corresponding to SCPs and those generated by admissible sequences of shifts. Consequently, they are in bijection with the facets of

the SU diagonal. The translation of these results for the LA diagonal is clear. One can use the isomorphism $t(r \times r)$ as in the following example.

Example 6.54. The first row of Figure 26 contains a sequence of admissible SU subset shifts applied to the matrix encoding of the SCP $256|4|17|3 \times 6|5|147|13$. The second row is the image of these shifts under the isomorphism $t(r \times r)$. Note that the shifts of this example are also isomorphic to those of Example 6.30, under the isomorphism $(rs \times rs)$.

Part III. Higher algebraic structures

In this third part, we derive some higher algebraic consequences of the results obtained in Part II. We first prove in Section 7.1 that there are exactly two topological operad structures on the family of operahedra (resp. multiplihedra) which are compatible with the generalized Tamari order, and thus two geometric universal tensor products of (non-symmetric non-unital) homotopy operads (resp. A_∞ -morphisms). Then, we show that these topological operad structures are isomorphic (Section 7.2). However, these isomorphisms do not commute with the diagonal maps (Examples 7.14 and 7.17). Finally, we show that contrary to the case of permutahedra, the faces of the LA and SU diagonals of the operahedra (resp. multiplihedra) are in general not in bijection (Section 7.3). However, from a homotopical point of view, the two tensor products of homotopy operads (resp. A_∞ -morphisms) that they define are ∞ -isomorphic (Theorems 7.18 and 7.22).

7. HIGHER TENSOR PRODUCTS

7.1. Topological operadic structures. The permutahedra are part of a more general family of polytopes called Loday realizations of the *operahedra* [LA22, Def. 2.9], which encodes the notion of homotopy operad [LA22, Def. 4.11] (we consider here only *non-symmetric non-unital* homotopy operads). Let PT_n be the set of planar trees with n internal edges, which are labelled by $[n]$ using the infix order. For every planar tree t , there is a corresponding operahedron P_t whose codimension k faces are in bijection with nestings of t with k non-trivial nests.

Definition 7.1 ([LA22, Def. 2.1 & 2.22]). A *nest* of $t \in \text{PT}_n$ is a subset of internal edges which induce a subtree, and a *nesting* of t is a family of nests which are either included in one another, or disjoint. See Figure 27.

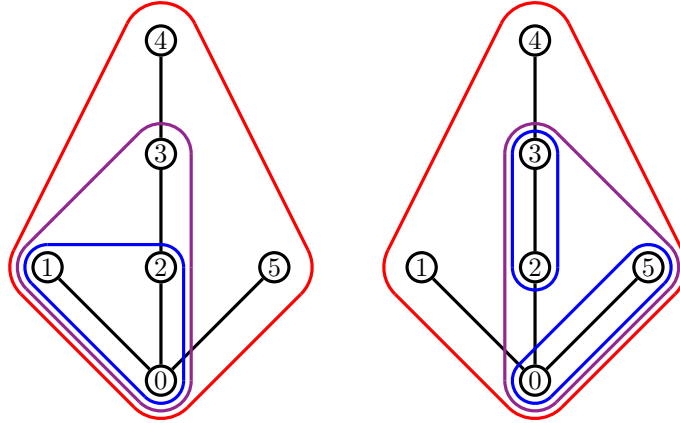


FIGURE 27. Two nestings of a tree with 5 internal edges. These nestings, Definition 7.1, are also 2-colored, Definition 7.6.

Since the operahedra are generalized permutahedra [LA22, Coro. 2.16], a choice of diagonal for the permutahedra induces a choice of diagonal for every operahedron [LA22, Coro. 1.31]. Every face of an operahedron is isomorphic to a product of lower-dimensional operahedra, via an isomorphism Θ which generalizes the one from Section 5.2, see Point (5) of [LA22, Prop. 2.3].

Definition 7.2. An *operadic diagonal* for the operahedra is a choice of diagonal Δ_t for each Loday operahedron P_t , such that $\Delta := \{\Delta_t\}$ commutes with the map Θ , *i.e.* it satisfies [LA22, Prop. 4.14].

An operadic diagonal gives rise to topological operad structure on the set of Loday operahedra [LA22, Thm 4.18], and via the functor of cellular chains, to a universal tensor product of homotopy operads [LA22, Prop. 4.27]. Here, by *universal*, we mean a formula that applies uniformly to *any*

pair of homotopy operads. Since such an operad structure and tensor product are induced by a geometric diagonal, we shall call them *geometric*.

Theorem 7.3. *There are exactly*

- (1) *two geometric operadic diagonals of the Loday operahedra, the LA and SU diagonals,*
- (2) *two geometric colored topological cellular operad structures on the Loday operahedra,*
- (3) *two geometric universal tensor products of homotopy operads,*

which agree with the generalized Tamari order on fully nested trees.

Proof. Let us first examine Point (1). By Theorem 5.13, we know that if one of the two choices Δ^{LA} or Δ^{SU} is made on an operahedron P_t , one has to make the same choice on every lower-dimensional operahedron appearing in the decomposition $P_{t_1} \times \cdots \times P_{t_k} \cong F \subset P_t$ of a face F of P_t . Now suppose that one makes two distinct choices for two operahedra P_t and $P_{t'}$. It is easy to find a bigger tree t'' , of which both t and t' are subtrees. Therefore, P_t and $P_{t'}$ appear as facets of $P_{t''}$ and by the preceding remark, any choice of diagonal for $P_{t''}$ will then contradict our initial two choices. Thus, these had to be the same from the start, which concludes the proof.

Point (2) then follows from the fact that a choice of diagonal for the Loday realizations of the operahedra *forces* a unique topological cellular colored operad structure on them, see [LA22, Thm. 4.18]. Since universal tensor products of homotopy operads are induced by a colored operad structure on the operahedra [LA22, Coro. 4.24], we obtain Point (3). Finally, since only vectors with strictly decreasing coordinates induce the generalized Tamari order on the skeleton of the operahedra [LA22, Prop. 3.11], we get the last part of the statement. \square

This answers a question raised in [LA22, Rem. 3.14].

Example 7.4. The Loday associahedra correspond to the Loday operahedra associated with linear trees [LA22, Sect. 2.2], and define a suboperad. The restriction of the two operad structures of Theorem 7.3 coincide in this case, and both the LA and SU diagonals induce the *magical formula* of [MS06, MTTV21, SU22] defining a universal tensor product of A_∞ -algebras.

Example 7.5. The restriction of Theorem 7.3 to the permutahedra associated with 2-leveled trees gives two distinct universal tensor products of permutadic A_∞ -algebras, as studied in [LR13, Mar20].

Two other important families of operadic polytopes are the *Loday associahedra* and *Forcey multiplihedra*, which encode respectively A_∞ -algebras and A_∞ -morphisms [LAM23, Prop. 4.9], as well as A_∞ -categories and A_∞ -functors [LAM23, Sect. 4.3]. For every linear tree $t \in \text{PT}_n$, there is a corresponding Loday associahedron K_n , whose faces are in bijection with nestings of t , and a Forcey multiplihedron J_n whose faces are in bijection with 2-colored nestings of t .

Definition 7.6 ([LAM23, Def. 3.2]). A *2-colored nesting* is a nesting where each nest N is either blue, red, or blue and red (purple), and which satisfies that if N is blue or purple (resp. red or purple), then all nests contained in N are blue (resp. all nests that contain N are red). See Figure 27.

The Loday associahedra are faces of the Forcey multiplihedra: they correspond to 2-colored nestings where all the nests are of the same color (either blue or red).

Forcey realizations of the multiplihedra are not generalized permutahedra, but they are projections of the Ardila–Doker realizations, which are [LAM23, Prop. 1.16]. A choice of diagonal for the permutahedra thus induces a choice of diagonal for every Ardila–Doker multiplihedron, and a subset of these choices (the ones which satisfy [LAM23, Prop. 2.7 & 2.8]) further induce a choice of diagonal for the Forcey multiplihedra. Every face of a Forcey multiplihedron is isomorphic to a product of a Loday associahedron and possibly many lower-dimensional Forcey multiplihedra, via an isomorphism Θ similar to the one from Section 5.2, see Point (4) of [LAM23, Prop. 1.10].

Definition 7.7. An *operadic diagonal* for the multiplihedra is a choice of diagonal Δ_n for each multiplihedron J_n , such that $\Delta := \{\Delta_n\}$ commutes with the map Θ .

An operadic diagonal endows the Loday associahedra with a topological operad structure [MTTV21, Thm. 1], and the Forcey multiplihedra with a topological operadic bimodule structure over the operad of Loday associahedra [LAM23, Thm. 1]. Via the functor of cellular chains, it defines universal tensor products of A_∞ -algebras and A_∞ -morphisms [LAM23, Sec. 4.2.1]. Here again, by *universal* we mean a formula that applies uniformly to any pair of A_∞ -algebras or A_∞ -morphisms. We shall call such geometrically defined operadic structures and tensor products *geometric*.

Theorem 7.8. *There are exactly*

- (1) *two geometric operadic diagonals of the Forcey multiplihedra, the LA and SU diagonals,*
- (2) *two geometric topological cellular operadic bimodule structures (over the Loday associahedra) on the Forcey multiplihedra,*
- (3) *two compatible geometric universal tensor products of A_∞ -algebras and A_∞ -morphisms,*

which agree with the Tamari-type order on atomic 2-colored nested linear trees.

Proof. Let us first examine Point (1). Consider the vectors $\mathbf{v}_{\text{LA}} := (1, 2^{-1}, 2^{-2}, \dots, 2^{-n+1})$ and $\mathbf{v}_{\text{SU}} := (2^n - 1, 2^n - 2, 2^n - 2^2, \dots, 2^n - 2^{n-1})$ in \mathbb{R}^n . As previously observed, they induce the LA and SU diagonals on the permutahedra (Definition 5.3). One checks directly that both vectors satisfy [LAM23, Prop. 2.7 & 2.8], and thus define diagonals of the Forcey multiplihedron J_n which agree with the Tamari-type order [LAM23, Prop. 2.10]. Moreover, these diagonals commute with the map Θ for the Forcey multiplihedra [LAM23, Prop. 2.14]; this is because after deleting the last coordinate of \mathbf{v}_{LA} or \mathbf{v}_{SU} , and then applying Θ^{-1} , we still have vectors which induce the LA or SU diagonal, respectively.

By Theorem 5.13, we know that if one of the two choices Δ^{LA} or Δ^{SU} is made on a multiplihedron J_n , one has to make the same choice on every lower-dimensional multiplihedra and associahedra appearing in the product decomposition of any face of J_n . Now suppose that one makes two distinct choices for two multiplihedra J_n and $J_{n'}$. It is easy to find a bigger multiplihedron $J_{n''}$, for which J_n and $J_{n'}$ appear in the product decomposition of a face of $J_{n''}$ and by the preceding remark, any choice of diagonal for $J_{n''}$ will then contradict our initial two choices. Thus, these had to be the same from the start, which conclude the proof of Point (1).

Point (2) then follows from the fact that a choice of diagonal for the Loday associahedra and the Forcey multiplihedra *forces* a unique topological cellular colored operad and operadic bimodule structure on them, see [MTTV21, Thm. 1] and [LAM23, Thm. 1]. Since a universal tensor products of A_∞ -algebras, and a compatible universal tensor products of A_∞ -morphisms are induced by an operad and operadic bimodule structures on the associahedra and multiplihedra respectively [LAM23, Sec. 4.2.3], we obtain Point (3). Finally, since only vectors with strictly decreasing coordinates induce the Tamari-type order on the skeleton of the Loday multiplihedra [LAM23, Prop. 2.10], we get the last part of the statement. \square

This answers a question raised in [LAM23, Rem. 3.9].

Remark 7.9. Note that in the case of the Loday associahedra, there is only one geometric operadic diagonal which induces the Tamari order atomic 2-colored nested planar trees (equivalently, binary trees, see [LAM23, Fig. 6]). Therefore, there is only one geometric topological operad structure, and only one geometric universal tensor product. This is because any vector with strictly decreasing coordinates lives in the same chamber of the fundamental hyperplane arrangement of the Loday associahedra (see [LA22, Ex. 1.21]).

Remark 7.10. Considering all 2-colored nested trees instead of only linear trees, one should obtain similar results for tensor products of ∞ -morphisms of homotopy operads.

We shall see now that the two operad (resp. operadic bimodule) structures on the operahedra (resp. multiplihedra) are related to one another in the strongest possible sense: they are isomorphic as topological cellular colored operads (resp. topological operadic bimodule structure over the associahedra).

7.2. Relating operadic structures. Recall that the topological cellular operad structure on the operahedra [LA22, Def. 4.17] is given by a family of partial composition maps

$$\circ_i^{\text{LA}} : P_{t'} \times P_{t''} \xrightarrow{\text{tr} \times \text{id}} P_{(t', \omega)} \times P_{t''} \xrightarrow{\ominus} P_t.$$

Here, the map tr is the *unique* topological cellular map which commutes with the diagonal Δ^{LA} , see [MTTV21, Prop. 7]. This partial composition \circ_i^{LA} is an isomorphism in the category Poly [LA22, Def. 4.13] between the product $P_{t'} \times P_{t''}$ and the facet $t' \circ_i t''$ of P_t . At the level of trees, the composition operation \circ_i is given by *substitution* [LA22, Fig. 14]. Using the SU diagonal Δ^{SU} , one can define similarly a topological operad structure via the same formula, but with a different transition map tr , which commutes with Δ^{SU} .

Recall that a face F of P_t is represented by a nested tree (t, \mathcal{N}) , which can be written uniquely as a sequence of substitution of trivially nested trees $(t, \mathcal{N}) = ((\dots((t_1 \circ_{i_1} t_2) \circ_{i_2} t_3) \dots) \circ_{i_k} t_{k+1})$. Here we use the increasing order on nestings [LA22, Def. 4.5], and observe that any choice of sequence of \circ_i operations yield the same nested tree, since these form an operad [LA22, Def. 4.7]. At the geometric level, we have an isomorphism

$$((\dots((\circ_{i_1}^{\text{LA}}) \circ_{i_2}^{\text{LA}}) \dots) \circ_{i_k}^{\text{LA}}) : P_{t_1} \times P_{t_2} \times \dots \times P_{t_{k+1}} \xrightarrow{\cong} F \subset P_t$$

between a uniquely determined product of lower dimensional operahedra, and the face $F = (t, \mathcal{N})$ of P_t . Note that any choice of sequence of \circ_i^{LA} operations yield the same isomorphism, since they form an operad [LA22, Thm. 4.18]. The same holds when taking the \circ_i^{SU} operations instead of the \circ_i^{LA} .

Construction 7.11. For any operahedron P_t , we define a map $\Psi_t : P_t \rightarrow P_t$

- on the interior of the top face by the identity $\text{id} : \mathring{P}_t \rightarrow \mathring{P}_t$, and
- on the interior of the face $F = ((\dots((t_1 \circ_{i_1} t_2) \circ_{i_2} t_3) \dots) \circ_{i_k} t_{k+1})$ of P_t by the composition of the two isomorphisms

$$((\dots((\circ_{i_1}^{\text{SU}}) \circ_{i_2}^{\text{SU}}) \dots) \circ_{i_k}^{\text{SU}}) ((\dots((\circ_{i_1}^{\text{LA}}) \circ_{i_2}^{\text{LA}}) \dots) \circ_{i_k}^{\text{LA}})^{-1} : F \rightarrow F.$$

Theorem 7.12. The map $\Psi := \{\Psi_t\}$ is an isomorphism of topological cellular symmetric colored operad between the LA and SU operad structures on the operahedra, in the category Poly .

Proof. By definition, we have that Ψ is an isomorphism in the category Poly . It remains to show that it preserves the operad structures, *i.e.* that the following diagram commutes

$$\begin{array}{ccc} P_{t'} \times P_{t''} & \xrightarrow{\circ_i^{\text{LA}}} & P_t \\ \Psi_{t'} \times \Psi_{t''} \downarrow & & \downarrow \Psi_t \\ P_{t'} \times P_{t''} & \xrightarrow{\circ_i^{\text{SU}}} & P_t \end{array}$$

For two interior points $(x, y) \in \mathring{P}_{t'} \times \mathring{P}_{t''}$, the diagram clearly commutes by definition, since $\Psi_{t'}$ and $\Psi_{t''}$ are the identity in that case. If x is in a face $F = ((\dots((t_1 \circ_{i_1} t_2) \circ_{i_2} t_3) \dots) \circ_{i_k} t_{k+1})$ of the boundary of $P_{t'}$, then the lower composite is equal to $\circ_i^{\text{SU}}(\circ_{i_1}^{\text{SU}} \circ_{i_2}^{\text{SU}} \dots \circ_{i_k}^{\text{SU}} \times \text{id})(\circ_{i_1}^{\text{LA}} \circ_{i_2}^{\text{LA}} \dots \circ_{i_k}^{\text{LA}} \times \text{id})^{-1}$, and so is the upper composite since Ψ_t starts with the inverse $(\circ_i^{\text{LA}})^{-1}$ and the decomposition of F into $P_{t_1} \times \dots \times P_{t_{k+1}} \times P_{t''}$ is unique. The case when y is in the boundary of $P_{t''}$ is similar. Finally, the compatibility of Ψ with units and the symmetric group actions are straightforward to check, see [LA22, Def. 4.17 & Thm. 4.18]. \square

Remark 7.13. Construction 7.11 and Theorem 7.12 do not depend on a specific choice of operadic diagonal. In this case, however, we do not lose any generality by using specifically the LA and SU operad structures.

Example 7.14. Note that Ψ is *not* a morphism of ‘‘Hopf’’ operads, *i.e.* it does not commute with the respective diagonals Δ^{LA} and Δ^{SU} . Consider the two square faces $F := 12|34$ and $G := 24|13$ of the 3-dimensional permutahedron $\text{Perm}(4)$, and choose a point $z \in (\mathring{F} + \mathring{G})/2$. Then, $\Delta^{\text{LA}}(z)$

and $\Delta^{\text{SU}}(z)$ are two different pair of points on the 1-skeleton of $\text{Perm}(4)$. Since \circ_i^{LA} and \circ_i^{SU} are the identity both on the interior of $\text{Perm}(4)$ (by Construction 7.11) and on the 1-skeleton of $\text{Perm}(4)$ (see the proof of [MTTV21, Prop. 7]), we directly obtain that

$$\Delta^{\text{LA}}(z) = (\Psi \times \Psi)\Delta^{\text{LA}}(z) \neq \Delta^{\text{SU}}\Psi(z) = \Delta^{\text{SU}}(z).$$

Recall that the topological cellular operadic bimodule structure on the Forcey multiplihedra is given by a family of action-composition maps [LAM23, Def. 2.13]

$$\begin{aligned} \circ_{p+1}^{\text{LA}} &: \mathbb{J}_{p+1+r} \times \mathbb{K}_q \xrightarrow{\text{tr} \times \text{id}} \mathbb{J}_{(1, \dots, q, \dots, 1)} \times \mathbb{K}_q \xrightarrow{\Theta_{p,q,r}} \mathbb{J}_n \quad \text{and} \\ \gamma_{i_1, \dots, i_k}^{\text{LA}} &: \mathbb{K}_k \times \mathbb{J}_{i_1} \times \dots \times \mathbb{J}_{i_k} \xrightarrow{\text{tr} \times \text{id}} \mathbb{K}_{(i_1, \dots, i_k)} \times \mathbb{J}_{i_1} \times \dots \times \mathbb{J}_{i_k} \xrightarrow{\Theta^{i_1, \dots, i_k}} \mathbb{J}_{i_1 + \dots + i_k}. \end{aligned}$$

Here, the map tr is the *unique* topological cellular map which commutes with the diagonal Δ^{LA} , see [MTTV21, Prop. 7]. These action-composition maps \circ_{p+1}^{LA} and $\gamma_{i_1, \dots, i_k}^{\text{LA}}$ are isomorphisms in the category Poly [LAM23, Sec. 2.1] between the products $\mathbb{J}_{p+1+r} \times \mathbb{K}_q$ and $\mathbb{K}_k \times \mathbb{J}_{i_1} \times \dots \times \mathbb{J}_{i_k}$, and corresponding facets of \mathbb{J}_n and $\mathbb{J}_{i_1 + \dots + i_k}$, respectively. Using the SU diagonal Δ^{SU} , one defines similarly a topological operadic bimodule structure via the same formula, but with a different transition map tr , which commutes with Δ^{SU} .

There is a bijection between 2-colored planar trees and 2-colored nested linear trees [LAM23, Lem. 3.4 & Fig. 6], which translate grafting of planar trees into substitution at a vertex of nested linear trees. The indices of the \circ_{p+1} and γ_{i_1, \dots, i_k} operations above refer to grafting. Equivalently, a face of \mathbb{J}_n is represented by a 2-colored nested tree (t, \mathcal{N}) , which can be written uniquely as a sequence of substitution of trivially nested 2-colored trees $(t, \mathcal{N}) = ((\dots((t_1 \circ_{i_1} t_2) \circ_{i_2} t_3) \dots) \circ_{i_k} t_{k+1})$. Here we use the left-levelwise order on nestings [LAM23, Def. 4.12], and translate tree grafting operations \circ_{p+1} and γ_{i_1, \dots, i_k} into nested tree substitution \circ_{i_j} . Note that any choice of substitutions yield the same 2-colored nested tree, since these form an operadic bimodule.

At the geometric level, we have an isomorphism $((\dots((\circ_{i_1}^{\text{LA}}) \circ_{i_2}^{\text{LA}}) \dots) \circ_{i_k}^{\text{LA}})$ between a uniquely determined product of lower dimensional associahedra and multiplihedra, and the face (t, \mathcal{N}) . Note that any choice of \circ_i^{LA} operations (*i.e.* the \circ_{p+1}^{LA} and $\gamma_{i_1, \dots, i_k}^{\text{LA}}$ action-composition operations) yield the same isomorphism, since they form an operadic bimodule [LAM23, Thm. 1]. The same holds when taking the \circ_i^{SU} (*i.e.* the \circ_{p+1}^{SU} and $\gamma_{i_1, \dots, i_k}^{\text{SU}}$ action-composition) operations instead.

Construction 7.15. For any Forcey multiplihedron \mathbb{J}_n , we define a map $\Psi_n : \mathbb{J}_n \rightarrow \mathbb{J}_n$

- on the interior of the top face by the identity $\text{id} : \overset{\circ}{\mathbb{J}}_n \rightarrow \overset{\circ}{\mathbb{J}}_n$, and
- on the interior of the face $F = ((\dots((t_1 \circ_{i_1} t_2) \circ_{i_2} t_3) \dots) \circ_{i_k} t_{k+1})$ of \mathbb{J}_n by the composition of the two isomorphisms

$$((\dots((\circ_{i_1}^{\text{SU}}) \circ_{i_2}^{\text{SU}}) \dots) \circ_{i_k}^{\text{SU}}) ((\dots((\circ_{i_1}^{\text{LA}}) \circ_{i_2}^{\text{LA}}) \dots) \circ_{i_k}^{\text{LA}})^{-1} : F \rightarrow F.$$

Theorem 7.16. The map $\Psi := \{\Psi_n\}$ is an isomorphism of topological cellular operadic bimodule structure over the Loday associahedra between the LA and SU operadic bimodule structures on the Forcey multiplihedra, in the category Poly .

Proof. The proof is the same as the one of Theorem 7.12, with the multiplihedra \circ_i^{LA} and \circ_i^{SU} operations (that is, the action-composition maps \circ_{p+1}^{LA} and $\gamma_{i_1, \dots, i_k}^{\text{LA}}$, and \circ_{p+1}^{SU} and $\gamma_{i_1, \dots, i_k}^{\text{SU}}$) in place of the operahedra operations. \square

Example 7.17. Note that Ψ does not commute with the respective diagonals Δ^{LA} and Δ^{SU} . Consider the two square faces $F := [(\bullet \bullet \bullet) \bullet]$ and $G := (\bullet [\bullet \bullet] \bullet)$ of the 3-dimensional Forcey multiplihedron \mathbb{J}_4 , and choose a point $z \in (\overset{\circ}{F} + \overset{\circ}{G})/2$. Then, $\Delta^{\text{LA}}(z)$ and $\Delta^{\text{SU}}(z)$ are two different pair of points on the 1-skeleton of \mathbb{J}_4 (see [LAM23, Ex. 3.7 & Fig. 9]). Since the LA and SU action-composition maps are the identity both on the interior of \mathbb{J}_4 (by Construction 7.15) and on the 1-skeleton of \mathbb{J}_4 (see the proof of [MTTV21, Prop. 7]), we directly obtain that

$$\Delta^{\text{LA}}(z) = (\Psi \times \Psi)\Delta^{\text{LA}}(z) \neq \Delta^{\text{SU}}\Psi(z) = \Delta^{\text{SU}}(z).$$

7.3. Tensor products. Recall that a homotopy operad \mathcal{P} is a family of vector spaces $\{\mathcal{P}(n)\}_{n \geq 1}$ together with a family of operations $\{\mu_t\}$ indexed by planar trees t [LA22, Def. 4.11]. One can consider the category of homotopy operads with strict morphisms, that is morphisms of the underlying vector spaces which commute strictly with all the higher operations μ_t , or with their ∞ -morphisms, made of a tower of homotopies controlling the lack of commutativity of their first component with the higher operations [LV12, Sec. 10.5.2].

Theorem 7.18. *For any pair of homotopy operads, the two universal tensor products defined by the LA and SU diagonals are not isomorphic in the category of homotopy operads and strict morphisms. However, they are isomorphic in the category of homotopy operads and their ∞ -morphisms.*

Proof. Since the two morphisms of topological operads Δ^{LA} and Δ^{SU} do not have the same cellular image, the tensor products that they define are not strictly isomorphic. However, they are both homotopic to the usual thin diagonal. Recall that homotopy operads are algebras over the colored operad \mathcal{O}_∞ , which is the minimal model of the operad \mathcal{O} encoding (non-symmetric non-unital) operads [LA22, Prop. 4.9]. Using the universal property of the minimal model \mathcal{O}_∞ , one can show that the algebraic diagonals $\Delta^{\text{LA}}, \Delta^{\text{SU}} : \mathcal{O}_\infty \rightarrow \mathcal{O}_\infty \otimes \mathcal{O}_\infty$ are homotopic, in the sense of [MSS02, Sec. 3.10], see [MSS02, Prop. 3.136]. Then, by [DSV16, Cor. 2] there is an ∞ -isotopy, that is an ∞ -isomorphism whose first component is the identity, between the two homotopy operad structures on the tensor product. \square

Remark 7.19. Neither of the two diagonals Δ^{LA} or Δ^{SU} are cocommutative, or coassociative, as they are special cases of A_∞ -algebras [MS06, Thm. 13].

Note that restricting to linear trees, the two tensor products of A_∞ -algebras induced by the LA and SU diagonals coincide (and are thus strictly isomorphic). Restricting to 2-leveled trees, we obtain two tensor product of permutadic A_∞ -algebras whose terms are in bijection. For the operahedra in general, such a bijection does not exist, as the following example demonstrates.

Example 7.20. The LA and SU diagonals of the operahedra associated with trees that have less than 4 internal edges have the same number of facets. However, there are 24 planar trees with 5 internal edges, such that the number of facets of the LA and SU diagonals are distinct, displayed in Figure 28. To compute these numbers, we first computed the facets of the LA and SU diagonals of the permutahedra, and then used the projection from the permutahedra to the operahedra described in [LA22, Prop. 3.20].

Remark 7.21. The lack of symmetry in the trees in Figure 28 arises from the lack of symmetry inherent in the infix order, and in how the LA and SU diagonal treat maximal and minimal elements. A sufficient condition for the diagonals of a tree t to have the same number of facets is to satisfy, N is a nesting of t if and only if rN is a nesting of t . For a tree satisfying this condition, relabelling its edges via the function $r : [n] \rightarrow [n]$ defined by $r(i) := n - i + 1$ exchanges the number of facets between the LA and SU diagonals.

We have an analogous result for universal tensor products of A_∞ -morphisms. Let A_∞^2 denote the 2-colored operad whose algebras are pairs of A_∞ -algebras together with an A_∞ -morphism between them [LAM23, Sec. 4.4.1]. The datum of a diagonal of the operad A_∞ encoding A_∞ -algebras and a diagonal of the operadic bimodule M_∞ encoding A_∞ -morphisms is equivalent to the datum of a morphism of 2-colored operads $A_\infty^2 \rightarrow A_\infty^2 \otimes A_\infty^2$.

Theorem 7.22. *For any pair of A_∞ -morphisms, the two universal tensor products defined by the LA and SU diagonals are not isomorphic in the category of A_∞^2 -algebras and strict morphisms. However, they are isomorphic in the category of A_∞^2 -algebras and their ∞ -morphisms.*

Proof. Since the two morphisms of topological operadic bimodules on the multiplihedra Δ^{LA} and Δ^{SU} do not have the same cellular image, the tensor products that they define are not strictly isomorphic. However, they are both homotopic to the usual thin diagonal. Recall that the operad A_∞^2 is the minimal model of the operad As^2 , whose algebras are pairs of associative algebras together with a morphism between them [LA22, Prop. 4.9]. Using the universal property of the

minimal model A_∞^2 , one can show that the algebraic diagonals $\Delta^{\text{LA}}, \Delta^{\text{SU}} : A_\infty^2 \rightarrow A_\infty^2 \otimes A_\infty^2$ are homotopic, in the sense of [MSS02, Sec. 3.10]. Then, by [DSV16, Cor. 2] there is an ∞ -isotopy, that is an ∞ -isomorphism whose first component is the identity, between the two tensor products of A_∞ -morphisms. \square

Remark 7.23. As studied in [LAM23, Sec. 4.4], the above tensor products of A_∞ -morphisms are not coassociative, nor cocommutative. Moreover, there *does not exist* a universal tensor product of A_∞ -morphisms which is compatible with composition [LAM23, Prop. 4.23].

Example 7.24. The LA and SU diagonals of the multiplihedra associated with trees that have less than 4 edges have the same number of facets. However, for linear trees with 5 and 6 internal edges, the number of facets of the LA and SU diagonals differ, as displayed in Figure 29. To compute these numbers, we first computed the facets of the LA and SU diagonals of the permutahedra, and then used the projection from the permutahedra to the multiplihedra described in the proof of [Dok11, Thm. 3.3.6].

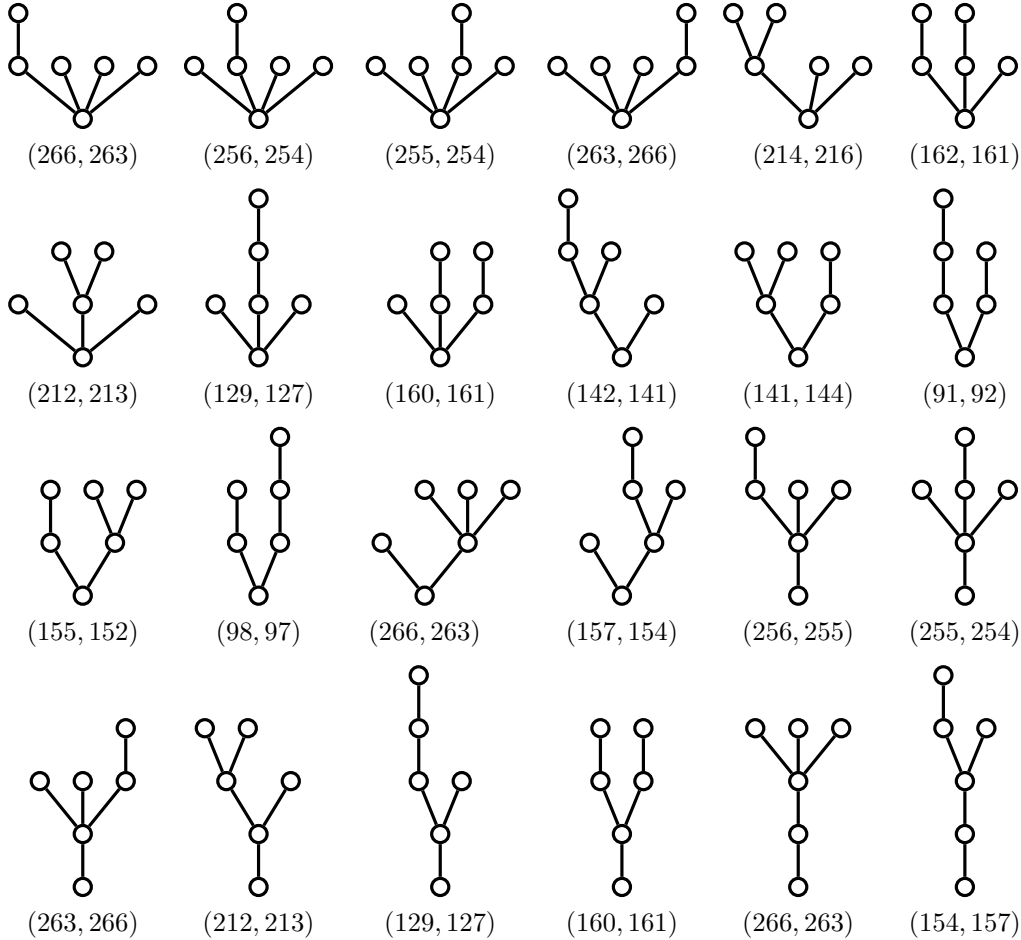


FIGURE 28. The 24 planar trees t with 5 internal edges for which the number of facets in the LA diagonal (left) and the SU diagonal (right) differ.

Internal edges	LA diagonal	LA only	Shared	SU only	SU diagonal
$n = 1$	2	0	2	0	2
$n = 2$	8	0	8	0	8
$n = 3$	42	5	37	5	42
$n = 4$	254	72	182	72	254
$n = 5$	1678	759	919	757	1676
$n = 6$	11790	7076	4714	7024	11738

TABLE 8. Number of facets in the LA and SU diagonals of the multiplihedra, indexed by linear trees with n internal edges.

REFERENCES

- [Bau80] Hans J. Baues. Geometry of loop spaces and the cobar construction. *Mem. Amer. Math. Soc.*, 25(230):ix+171, 1980.
- [BB97] Margaret M. Bayer and Keith A. Brandt. Discriminantal arrangements, fiber polytopes and formality. *J. Algebraic Combin.*, 6(3):229–246, 1997.
- [BCP23] Alin Bostan, Frédéric Chyzak, and Vincent Pilaud. Refined product formulas for Tamari intervals. Preprint, [arXiv:2303.10986](https://arxiv.org/abs/2303.10986), 2023.
- [Ber18] Olivier Bernardi. Deformations of the braid arrangement and trees. *Adv. Math.*, 335:466–518, 2018.
- [Bir95] Garrett Birkhoff. Lattices and their applications. In *Lattice theory and its applications (Darmstadt, 1991)*, volume 23 of *Res. Exp. Math.*, pages 7–25. Heldermann, Lemgo, 1995.
- [BM14] Jonas Bergström and Satoshi Minabe. On the cohomology of the Losev-Manin moduli space. *Manuscripta Math.*, 144(1-2):241–252, 2014.
- [BS92] Louis J. Billera and Bernd Sturmfels. Fiber polytopes. *Ann. of Math. (2)*, 135(3):527–549, 1992.
- [CG71] Wai-Kai Chen and I Goyal. Tables of essential complementary partitions. *IEEE Trans. Circuits and Systems*, 18(5):562–563, 1971.
- [Che69] Wai-kai Chen. Computer generation of trees and co-trees in a cascade of multiterminal networks. *IEEE Trans. Circuit Theory*, CT-16:518–526, 1969.
- [DHP18] Aram Dermenjian, Christophe Hohlweg, and Vincent Pilaud. The facial weak order and its lattice quotients. *Trans. Amer. Math. Soc.*, 370(2):1469–1507, 2018.
- [DKL22] Vladimir Dotsenko, Adam Keilthy, and Denis Lyskov. Reconnectads. Preprint, [arXiv:2211.15754](https://arxiv.org/abs/2211.15754), 2022.
- [Dok11] Jeffrey Samuel Doker. *Geometry of Generalized Permutohedra*. PhD thesis, University of California, Berkeley, 2011.
- [DSV16] Vladimir Dotsenko, Sergey Shadrin, and Bruno Vallette. Pre-Lie deformation theory. *Mosc. Math. J.*, 16(3):505–543, 2016.
- [EM54] Samuel Eilenberg and Saunders MacLane. On the groups $H(\Pi, n)$. III. *Ann. of Math. (2)*, 60:513–557, 1954.
- [FS97] William Fulton and Bernd Sturmfels. Intersection theory on toric varieties. *Topology*, 36(2):335–353, 1997.
- [HP91] Peter Hilton and Jean Pedersen. Catalan numbers, their generalization, and their uses. *Math. Intelligencer*, 13(2):64–75, 1991.
- [Kla70] David A. Klarner. Correspondences between plane trees and binary sequences. *J. Combinatorial Theory*, 9:401–411, 1970.
- [KLN⁺01] Daniel Krob, Matthieu Latapy, Jean-Christophe Novelli, Ha-Duong Phan, and Sylviane Schwer. Pseudo-Permutations I: First Combinatorial and Lattice Properties. 13th International Conference on Formal Power Series and Algebraic Combinatorics (FPSAC 2001), 2001.
- [KUC82] Yoji Kajitani, S. Ueno, and Wai Kai Chen. On the number of essential complementary partitions. *IEEE Trans. Circuits and Systems*, 29(8):572–574, 1982.
- [LA22] Guillaume Laplante-Anfossi. The diagonal of the operahedra. *Adv. Math.*, 405:Paper No. 108494, 50, 2022.
- [LAM23] Guillaume Laplante-Anfossi and Thibaut Mazuir. The diagonal of the multiplihedra and the tensor product of A_∞ -morphisms. *J. Éc. polytech. Math.*, 10:405–446, 2023.
- [Lew99] Richard P. Lewis. The number of spanning trees of a complete multipartite graph. volume 197/198, pages 537–541. 1999. 16th British Combinatorial Conference (London, 1997).
- [Lin16] Matthew Lin. *Graph Cohomology*. PhD thesis, Harvey Mudd College, 2016.
- [LM00] Andrei S. Losev and Yurii I. Manin. New moduli spaces of pointed curves and pencils of flat connections. volume 48, pages 443–472. 2000. Dedicated to William Fulton on the occasion of his 60th birthday.
- [Lod11] Jean-Louis Loday. The diagonal of the Stasheff polytope. In *Higher structures in geometry and physics*, volume 287 of *Progr. Math.*, pages 269–292. Birkhäuser/Springer, New York, 2011.
- [LR13] Jean-Louis Loday and María Ronco. Permutads. *J. Combin. Theory Ser. A*, 120(2):340–365, 2013.
- [LV12] Jean-Louis Loday and Bruno Vallette. *Algebraic operads*, volume 346 of *Grundlehren der mathematischen Wissenschaften [Fundamental Principles of Mathematical Sciences]*. Springer, Heidelberg, 2012.
- [Mar20] Martin Markl. Permutads via operadic categories, and the hidden associahedron. *J. Combin. Theory Ser. A*, 175:105277, 40, 2020.
- [MS89] Yurii I. Manin and V. V. Schechtman. Arrangements of hyperplanes, higher braid groups and higher Bruhat orders. In *Algebraic number theory*, volume 17 of *Adv. Stud. Pure Math.*, pages 289–308. Academic Press, Boston, MA, 1989.
- [MS06] Martin Markl and Steve Shnider. Associahedra, cellular W -construction and products of A_∞ -algebras. *Trans. Amer. Math. Soc.*, 358(6):2353–2372, 2006.
- [MSS02] Martin Markl, Steve Shnider, and Jim Stasheff. *Operads in algebra, topology and physics*, volume 96 of *Mathematical Surveys and Monographs*. American Mathematical Society, Providence, RI, 2002.
- [MTTV21] Naruki Masuda, Hugh Thomas, Andy Tonks, and Bruno Vallette. The diagonal of the associahedra. *J. Éc. polytech. Math.*, 8:121–146, 2021.
- [OEI10] The On-Line Encyclopedia of Integer Sequences. Published electronically at <http://oeis.org>, 2010.

- [Pos09] Alexander Postnikov. Permutohedra, associahedra, and beyond. *Int. Math. Res. Not. IMRN*, (6):1026–1106, 2009.
- [PR06] Patricia Palacios and María O. Ronco. Weak Bruhat order on the set of faces of the permutohedron and the associahedron. *J. Algebra*, 299(2):648–678, 2006.
- [Pro11] Alain Prouté. A_∞ -structures. Modèles minimaux de Baues-Lemaire et Kadeishvili et homologie des fibrations. *Repr. Theory Appl. Categ.*, (21):1–99, 2011. Reprint of the 1986 original, with a preface to the reprint by Jean-Louis Loday.
- [PS00] Alexander Postnikov and Richard P. Stanley. Deformations of Coxeter hyperplane arrangements. volume 91, pages 544–597. 2000. In memory of Gian-Carlo Rota.
- [Rad52] Richard Rado. An inequality. *J. London Math. Soc.*, 27:1–6, 1952.
- [Rot64] Gian-Carlo Rota. On the foundations of combinatorial theory. I. Theory of Möbius functions. *Z. Wahrscheinlichkeitstheorie und Verw. Gebiete*, 2:340–368 (1964), 1964.
- [RS18] Manuel Rivera and Samson Sanedlidze. A combinatorial model for the free loop fibration. *Bull. Lond. Math. Soc.*, 50(6):1085–1101, 2018.
- [San09] Samson Sanedlidze. The bitwisted Cartesian model for the free loop fibration. *Topology Appl.*, 156(5):897–910, 2009.
- [Sch11] Pieter Hendrik Schoute. *Analytical treatment of the polytopes regularly derived from the regular polytopes. Section I: The simplex.*, volume 11. 1911.
- [Ser51] Jean-Pierre Serre. Homologie singulière des espaces fibrés. Applications. *Ann. of Math. (2)*, 54:425–505, 1951.
- [Shi86] Jian Yi Shi. *The Kazhdan-Lusztig cells in certain affine Weyl groups*, volume 1179 of *Lecture Notes in Mathematics*. Springer-Verlag, Berlin, 1986.
- [Shi87] Jian Yi Shi. Sign types corresponding to an affine Weyl group. *J. London Math. Soc. (2)*, 35(1):56–74, 1987.
- [SU04] Samson Sanedlidze and Ronald Umble. Diagonals on the permutahedra, multiplihedra and associahedra. *Homology Homotopy Appl.*, 6(1):363–411, 2004.
- [SU22] Samson Sanedlidze and Ronald Umble. Comparing diagonals on the associahedra. Preprint, [arXiv:2207.08543](https://arxiv.org/abs/2207.08543), 2022.
- [Vej07] Mikael Vejdemo-Johansson. Enumerating the Sanedlidze-Umble diagonal terms. Preprint, [arXiv:0707.4399](https://arxiv.org/abs/0707.4399), 2007.
- [Zas75] Thomas Zaslavsky. Facing up to arrangements: face-count formulas for partitions of space by hyperplanes. *Mem. Amer. Math. Soc.*, 1(issue 1, 154):vii+102, 1975.
- [Zie98] Günter M. Ziegler. *Lectures on Polytopes*, volume 152 of *Graduate texts in Mathematics*. Springer-Verlag, New York, 1998.

(Bérénice Delcroix-Oger) INSTITUT MONTPELLIÉRAIN ALEXANDER GROTHENDIECK, UNIVERSITÉ DE MONTPELLIER, FRANCE

Email address: berenice.delcroix-oger@umontpellier.fr

URL: <https://oger.perso.math.cnrs.fr/>

(Guillaume Laplante-Anfossi) SCHOOL OF MATHEMATICS AND STATISTICS, THE UNIVERSITY OF MELBOURNE, VICTORIA, AUSTRALIA

Email address: guillaume.laplanteanfossi@unimelb.edu.au

URL: <https://guillaumelaplante-anfossi.github.io/>

(Vincent Pilaud) CNRS & LIX, ÉCOLE POLYTECHNIQUE, PALAISEAU, FRANCE

Email address: vincent.pilaud@lix.polytechnique.fr

URL: <http://www.lix.polytechnique.fr/~pilaud/>

(Kurt Stoeckl) SCHOOL OF MATHEMATICS AND STATISTICS, THE UNIVERSITY OF MELBOURNE, VICTORIA, AUSTRALIA

Email address: kstoeckl@student.unimelb.edu.au

URL: <https://kstoeckl.github.io/>